PNNL-14109

Pacific Northwest National Laboratory
Operated by Battelle for the U.S. Department of Energy

Estimating Field-Scale Hydraulic Parameters of Heterogeneous Soils Using a Combination of Parameter Scaling and Inverse Methods

Z. F. Zhang
A. L. Ward
G. W. Gee

December 2002

Prepared for the U.S. Department of Energy
under Contract DE-AC06-76RL01830

PACIFIC NORTHWEST NATIONAL LABORATORY
operated by
BATTELLE MEMORIAL INSTITUTE
for the
UNITED STATES DEPARTMENT OF ENERGY
under Contract DE-AC06-76RL1830

Printed in the United States of America

Available to DOE and DOE contractors from the

Office of Scientific and Technical Information, P.O. Box 62, Oak Ridge, TN 37831;

prices available from (865) 576-8401.

Available to the public from the National Technical Information Service,

U.S. Department of Commerce, 5285 Port Royal Rd., Springfield, VA 22161

PNNL-14109

Estimating Field-Scale Hydraulic Parameters of Heterogeneous Soils Using A Combination of Parameter Scaling and Inverse Methods

Z. F. Zhang
A. L. Ward
G. W. Gee

December 2002

Prepared for the U.S. Department of Energy
under Contract DE-AC06-76RL1830

Pacific Northwest National Laboratory
Richland, Washington 99352

Executive Summary

As the Hanford Site transitions into remediation of contaminated soil waste sites and tank farm closure, more information is needed about the transport of contaminants as they move through the vadose zone to the underlying water table. The hydraulic properties must be characterized for accurate simulation of flow and transport. This characterization includes the determination of soil texture types, their three-dimensional distribution, and the parameterization of each soil texture. This document describes a method to estimate the soil hydraulic parameter using the parameter scaling concept (Zhang et al. 2002) and inverse techniques. To this end, the Groundwater Protection Program Science and Technology Project funded vadose zone transport field studies, including an analysis of the results to estimate field-scale hydraulic parameters for modeling.

Parameter scaling is a new method to scale hydraulic parameters. The method relates the hydraulic-parameter values measured at different spatial scales for different soil textures. Parameter scaling factors relevant to a reference texture are determined using these local-scale parameter values, e.g., those measured in the lab using small soil cores. After parameter scaling is applied, the total number of unknown variables in hydraulic parameters is reduced by a factor equal to the number of soil textures. The field-scale values of the unknown variables can then be estimated using inverse techniques and a well-designed field experiment. Finally, parameters for individual textures are obtained through inverse scaling of the reference values using an a priori relationship between reference parameter values and the specific values for each texture.

Inverse methods have the benefits of 1) calculating parameter values that produce the best-fit between observed and simulated values, 2) quantifying the confidence limits in parameter estimates and the predictions, 3) providing diagnostic statistics that quantify the quality of calibration and data shortcomings and needs, and 4) not restricting the initial and boundary-flow conditions, the constitutive relationships, or the treatment of heterogeneity.

As part of the Vadose Zone Transport Field Study (VZTFS), inverse modeling was performed using a combination of two computer models, one for forward flow modeling and the other for nonlinear regression. The forward model used to simulate water flow was the Subsurface Transport Over Multiple Phases (STOMP) numerical simulator (White and Oostrom 2000). STOMP was designed to solve a variety of nonlinear, multiple-phase, flow and transport problems for unsaturated porous media. The Universal CODE (UCODE) model (Poeter and Hill 1998) was used to perform inverse modeling posed as a parameter-estimation problem using nonlinear regression. Inverse techniques were applied to two cases of one-dimensional flow in layered soils and one case of three-dimensional flow in a heterogeneous soil. The results show that the simulation errors were significantly reduced after applying parameter scaling and inverse modeling. When compared to the use of local-scale parameters, parameter scaling reduced the sum of squared weighted residual by 93 to 96% for the relatively smaller scale (~2 m [~6.6 ft]) one-dimensional flow and 59% for the more complex Sisson and Lu site, which has the spatial scale of about 18 m (60 ft). This parameter estimation method will be applied to analyze the first 2 two years of field experiments completed at the Sisson and Lu site.

References

Poeter EP, and MC Hill. 1998. *Documentation of UCODE, a computer code for universal inverse modeling,* U.S. Geological survey, water-resources investigations report 98-4080.

White MD, and M Oostrom. 2000. *User's guide of STOMP - Subsurface transport over multiple phases,* PNNL-12034 UC-2010, Pacific Northwest National Laboratory, Richland, WA.

Zhang ZF, AL Ward, and GW Gee. 2002. "A parameter scaling concept for estimating field-scale hydraulic functions of layered soils." In: *Findikakis A.N. (ed.), "Bridging the Gap between Measurement and Modeling in Heterogeneous Media", Proceedings of the International Groundwater Symposium*, March 25-28, Berkeley, CA, pp. 103-107, published by IAHR, Madrid, Spain.

Glossary

1-D	One-Dimensional
3-D	Three-Dimensional
CSS	Composite Scaled Sensitivities
DOE	U.S. Department of Energy
FS	Field Scale
LS	Local Scale
LCI	Linear Confidence Interval
PNNL	Pacific Northwest National Laboratory
RPP	River Protection Project
STOMP	Subsurface Transport Over Multiple Phases
UCODE	Universal CODE
VZTFS	Vadose Zone Transport Field Study

Acknowledgments

We thank Mark White for his help in implementing the modifications to STOMP and Eileen Poeter of the Colorado School of Mines for assisting us with the application of UCODE to the unsaturated flow problems. Pacific Northwest National Laboratory is operated for the U.S. Department of Energy by Battelle under Contract DE-AC06-76RL01830.

Contents

Executive Summary ... iii

Glossary ... v

1.0 Introduction ... 1.1

2.0 Parameter Scaling and Inverse Procedure ... 2.1

2.1 Calculation of Scaling Factors ... 2.1

2.2 Estimating Field-Scale Parameters of the Reference Texture ... 2.2

3.0 Computer Models ... 3.1

3.1 UCODE – the Inverse Model ... 3.1

3.2 Revised STOMP ... 3.2

3.3 Inverse Modeling Using STOMP/UCODE Combination ... 3.3
3.3.1 New Cards in the STOMP Input File ... 3.3
3.3.2 Construction of the UCODE Input Files ... 3.4
3.3.3 Procedures to Run UCODE/STOMP ... 3.4

4.0 One-Dimensional Flow in Layered Soil ... 4.1

4.1 Case 1: Hanford Grass Site ... 4.1
4.1.1 Experiment ... 4.1
4.1.2 Inverse Modeling ... 4.1
4.1.3 Results ... 4.3

4.2 Case 2: Andelfingen Site ... 4.5
4.2.1 Experiment ... 4.5
4.2.2 Inverse Modeling ... 4.5
4.2.3 Results ... 4.6

5.0 Flow From a Point Source ... 5.1

5.1 Experiments and Previous Simulations ... 5.1

5.2 The Power Function Fitting to the Calibration Data ... 5.3

5.3 Soil-Texture Classification ... 5.4

5.4 Inverse Modeling ... 5.7

5.5 Results ... 5.9

6.0 Conclusions 6.1

7.0 References 7.1

Appendix A: Input Files A.1

Figures

4.1. Comparison of the Observations and the Predictions of Water Content and Pressure Head of the Hanford Grass Site Soil Using (a) and (b), the Local-Scale Parameter Values, and (c) and (d), the Field-Scale Parameter Values 4.4

4.2. Comparison of the Observed and the Predicted Values of (a) Water Content and (b) Pressure Head of the Hanford Experiment: Lines = Predictions; Symbols = Observations 4.5

4.3. Comparison of the Observations and the Predictions of Water Content and Pressure Head of the Andelfingen Soil Using (a) and (b), the Local-Scale Parameter Values, and (c) and (d), the Field-Scale Parameter Values 4.8

4.4. Comparison of the Observed and the Predicted Water Contents of the Andelfingen Experiment 4.9

4.5. Comparison of the Observed and the Predicted Pressure Heads of the Andelfingen Experiment. 4.9

5.1. Plane View of the Layout of the Injection Well (empty circle at the center) and the Observation Wells (filled circles) at the Sisson and Lu Site 5.2

5.2. Comparison of the Linear, Shifted Linear, and Power Function Calibration Curves of Neutron Probe #4 (H33115140) 5.4

5.3. A Comparison of Calculated Water Content Calculated Using Different Calibration Curves for Probe 1 (H38092510): A) Polynomial Curve (Equation 9); (B) Linear Curve (Equation 10); and C) Power Function Curve (Combination of Equations 14 and 15) 5.4

5.4. The Distribution of Steady-State Water Content of the Sisson and Lu Site 5.5

5.5. The Distribution of Soil Porosity of the Sisson and Lu Site 5.6

5.6. A Scatter Plot Between the Porosity and the Steady-State Water Content of the Sisson and Lu Site 5.7

5.7. The Procedures to Estimate the Field-Scale Hydraulic Parameters Using the Combination of Parameter Scaling and Inverse Technique 5.8

5.8. Comparisons of the Simulates and Observed Water Contents of the Sisson and Lu Experiment Using the Local-Scale (Left Column) and Field-Scale (Right Column) Values of the Hydraulic Parameters 5.12

Tables

3.1. The Functions of each Phase of UCODE 3.1

3.2. UCODE Input files 3.2

4.1. The Values of the Hydraulic Parameters at Local Observation Scale and Calculated Scaling Factors Reference to the First Layer 4.2

4.2. The Inversely Determined Reference Values of the Hydraulic Parameters, their 95% Linear Confidence Intervals (LCI), and the Composite Scaled Sensitivities (CSS) of the Hanford Soil at Field Scale 4.3

4.3. The Mean Values of the Hydraulic Parameters of Individual Layers of the Hanford Soil 4.4

4.4. The Values of the Hydraulic Parameters at Local Observation Scale and Calculated Scaling Factors Reference to the First Layer 4.6

4.5. The Inversely Determined Reference Values of the Hydraulic Parameters, their 95% LCI and the CSS of the Andelfingen Soil at Field Scale 4.6

4.6. The Mean Values of the Hydraulic Parameters of Individual Layers of the Andelfingen Soil 4.7

5.1. Soil Classification of the Sisson and Lu Site Using Porosity 5.7

5.2. The Values of the Hydraulic Parameters at Local Observation Scale and Calculated Scaling Factors Reference to T4 .... 5.9

5.3. The Inversely Determined Field-Scale Reference Values of the Hydraulic Parameters, their 95% LCI of the Sisson and Lu Site 5.10

5.4. The Correlation Coefficient Between the Field-Scale Reference Values of the Hydraulic Parameters of the Sisson and Lu Site 5.10

5.5. The Effective Parameters of Individual Layers After an Inverse Scaling of the Inversely-Determined Parameters of the Reference Soil Material 5.10

1.0 Introduction

Approximately 200 million liters (53 million gallons) of highly radioactive wastes are stored in 177 large underground storage tanks at the Hanford Site in southeastern Washington State. Of these tanks, 149 are single-shell tanks containing liquid, sludges, and salt cake, i.e., crystallized salts. Over the years, much of the liquid stored in the single-shell tanks has been evaporated or pumped into double-shell tanks. In the past, some of these single-shell tanks have leaked, and other radioactive wastes were discharged into underground structures for waste disposal. These wastes have migrated into and through the vadose zone.

Accurate predictions of soil moisture and radionuclide transport at the Hanford Site are required to evaluate future waste site impacts to the groundwater and to design soil waste site remediation, including interim measures for leaked tank waste (e.g., RPP River Protection Project 2001). The currently accepted method for predicting moisture and contaminant distributions is to use computers to solve the soil moisture and convective-dispersion equations. Difficulties have been encountered when this method is used due to the spatially varying nature of soil, which creates uncertainty as to the number of values of each parameter that must be assigned throughout space. Wierenga et al. (1991) found that laboratory-determined parameters are usually not applicable to real field situations due to the effects of different observation scales. Therefore, to determine the overall accuracy of model predictions, field data must be compared directly to model predictions.

The Groundwater Protection Program, formerly the Groundwater/Vadose Zone Integration Project, initiated field studies to evaluate the processes controlling the transport of fluids and contaminants in the vadose zone and to develop a reliable database for testing vadose-zone transport models. The Vadose Zone Transport Field Study was initiated to conduct a series of field experiments involving *in situ* measurements of moisture and tracer distributions. The results of the field tests were to be analyzed and modeled to estimate field-scale parameters and develop parameter scaling factors, as described in Ward and Gee (2001, 2002) and Gee and Ward (2001).

A useful approach for estimating effective hydraulic parameters at the field scale is inverse modeling, which uses the nonlinear regression method to estimate the effective hydraulic parameters. This method minimizes the differences between field observations and the simulated values by analytical or numerical solutions that contain the set of parameters to be estimated. Inverse methods have the benefits of 1) calculating parameter values that produce the best-fit between observed and simulated values, 2) quantifying the confidence limits in parameter estimates and the predictions, 3) providing diagnostic statistics that quantify the quality of calibration and data needs, and 4) not restricting the initial and boundary-flow conditions, the constitutive relationships, or the treatment of heterogeneity. A number of laboratory and field applications (van Dam et al. 1992; Parkin et al., 1995; Simunek and van Genuchten 1996; Lehmann and Ackerer 1997; Abbaspour et al. 1997; Inoue et al. 2000; Zhang et al. 2000) have shown the potential of inverse techniques for improving the design and analysis of vadose-zone flow-and-transport experiments.

As more parameters are added to an inverse model, convergence becomes more difficult to attain and, in some cases, the system converges to a local minimum in the multi-dimensional parameter space. Zhang et al. (2002) proposed a parameter-scaling concept linking hydraulic properties to fewer parameters and applied it to estimate the hydraulic parameters in layered soils. When the parameters are to be estimated by an inverse procedure, the number of unknown variables is reduced by a factor of the number of textures. This is because the hydraulic parameters of all the textures are scaled to those of the reference and only the parameters of the reference texture are estimated using inverse modeling.

Hanford soils are composed of multiple soil textures. Assuming that each texture is nearly homogeneous, we can describe the hydraulic property of a texture by a set of effective parameters. To fully describe the hydraulic properties of the soil, usually a few tens of hydraulic parameters are needed. Therefore, the parameter scaling technique and inverse method can be useful tools to characterize the hydraulic properties of the soils at the Hanford Site with a minimum number of parameters.

Parameter scaling and the inverse method to characterize the hydraulic properties of heterogeneous soils are described in this report. The soil was categorized into different textures, each of which was assumed to have similar hydraulic properties. The hydraulic parameters of each texture at core-scale were determined using lab-measured data. These parameter values were then used to calculate the scaling factors associated with each texture. The scaling factor is simply the ratio of the parameter of a textural class divided by the reference texture parameter. After this, with the knowledge of the scaling factors, the field-scale parameter values of the reference texture were inversely estimated using the combination of Universal CODE/Subsurface Transport Over Multiple Phases (UCODE/STOMP).

Several example cases for applying the parameter estimation method are presented in this report. The methodology is being applied to field experiments at the Sisson and Lu Site described in Gee and Ward (2000) and field tests being conducted at a clastic dike site in FY 2002 (Ward and Gee 2002) and in FY 2003. These applications will be described in future updates on the VZTFS.

2.0 Parameter Scaling and Inverse Procedure

Soil hydraulic properties are commonly described by empirical functions to allow incorporation into numerical models (Brooks and Corey 1964; van Genuchten 1980). The concept of parameter scaling is different from traditional scaling in that we scale the soil hydraulic parameters of the hydraulic functions rather than the hydraulic properties. Assume a heterogeneous soil comprised of M different textures with each texture characterized by a set of hydraulic parameters β. A single texture is selected as the reference texture described by a set of parameters, $\tilde{\beta}$. The jth parameter of the ith texture, β_{ij}, is related to the reference parameters through a set of mutually independent linear scaling factors, γ_{ij}, for i = 1 to M textures, i.e.,

$$\beta_{ij} = \gamma_{ij}\,\tilde{\beta}_j \tag{1}$$

Similarly, a logarithmic scaling factor is defined as

$$\ln(\beta_{ij}) = \gamma_{ij}\ln(\tilde{\beta}_j) \tag{2}$$

Parameter scaling has the following characteristics: (1) it does not require the constitutional materials to be similar. As long the hydraulic properties of the soil materials can be described by a hydraulic function (e.g., Brooks and Corey 1964; van Genuchten 1980), parameter scaling is applicable. (2) Instead of scaling the hydraulic properties—i.e., the $\theta(\psi)$ and $K(\psi)$ relations, where θ is soil water content, ψ is soil water pressure head, and K is the unsaturated hydraulic conductivity—hydraulic parameters are scaled. As a result, the flow equation can always be expressed in real time and space rather than scaled time and space regardless of the soil heterogeneity. This has the potential to overcome the difficulty in estimating hydraulic parameters for heterogeneous systems using inverse procedures. (3) After scaling, the values of the hydraulic parameters of all the soil textures perfectly reduce to the reference values. No scaling error is introduced, and hence the application of an inverse scaling will return the original parameter values. (4) The spatial variability of each hydraulic parameter can be expressed by the scaling factors. Different parameters may have different variability structures within the same soil domain. (5) When the parameters are to be estimated by an inverse procedure, the number of unknown variables is reduced by a factor of M.

2.1 Calculation of Scaling Factors

Although the parameter values at the local scale are often different from those at the field scale, we assume that local-scale scaling factors (γ_{ij}) are equal to those at the field-scale, i.e.,

$$(\gamma_{ij})_{LS} = (\gamma_{ij})_{FS} \tag{3}$$

where the subscript LS denotes local-scale and FS field-scale. In this context, local scale means the range represented by an individual observation, and field scale is the three-dimensional range of an experimental site. Equation 3 essentially means that the relationships between the parameters of different textures are scale invariant. For example, if, at the local-scale, the saturated hydraulic conductivity of the ith texture is $10\cdot\left(\tilde{K}_s\right)_{LS}$, we expect the field-scale value of the ith texture to be $10\cdot\left(\tilde{K}_s\right)_{FS}$, although the value of $(\widetilde{K}_s)_{FS}$ may be quite different from that of $(\widetilde{K}_s)_{LS}$. Thus, the scaling factors can be determined with Equation 1 or 2 using the parameter values measured at the local scale or in the laboratory and then applied to the field-scale.

2.2 Estimating Field-Scale Parameters of the Reference Texture

After determining the values of the scaling factors as discussed above, the field-scale parameter values of reference texture are estimated by fixing the values of the scaling factors and solving an inverse problem. Solving the inverse problem requires minimizing the objective function, $S(\widetilde{\beta})$, with respect to the soil hydraulic parameters. The objective function is a measure of the fit between simulated values and observations and is defined as

$$S(\widetilde{\beta}) = \sum_{k=1}^{N} w_k [y_k - \hat{y}_k(\widetilde{\beta})]^2 \tag{4}$$

where y_k = observations of any data type, e.g., θ or ψ

$\hat{y}_k(\widetilde{\beta})$ = corresponding simulated values

w_k = weights associated with each observation and are defined as the reverse of the variance of the measurement error

N = total number of observations.

After applying parameter scaling in a heterogeneous soil with M textures, the number of hydraulic parameters to be estimated using the inverse procedure is reduced by a factor of M. The only unknown variables are the parameters of the reference texture. The reduction of the number of parameters to be estimated greatly reduces the uncertainty of the estimates and accelerates the convergence during inverse modeling.

3.0 Computer Models

This section includes a discussion of the inverse model (UCODE), the application model (STOMP), and inverse modeling using the two computer programs.

3.1 UCODE – the Inverse Model

The inverse modeling program UCODE (Poeter and Hill 1998) was developed by the U.S. Geological Survey in collaboration with the U.S. Army Corps of Engineers Waterways Experiment Station and the International Ground Water Modeling Center of the Colorado School of Mines. Any application model or set of models can be used. Application models can include preprocessors and postprocessors as well as models related to the processes of interest. Prior information on estimated parameters can be included in the regression. Sensitivities needed for the method are calculated approximately by forward or central differences. Statistics are calculated for use in (1) diagnosing inadequate data or identifying parameters that probably cannot be estimated with the available data, (2) evaluating the uncertainty of the estimated parameter values, (3) evaluating the model representation of the actual processes, and (4) quantifying the uncertainty of model simulated values. A powerful aspect of using nonlinear regression is the useful statistics, which are generated by UCODE. The statistics presented can be used diagnostically to measure the amount of information provided by the data and to identify model error (bias), or to infer the uncertainty with which values are calculated.

UCODE performs different functions by specifying different PHASE values (Table 3.1) in the universal file (Table 3.2). It is useful to begin with PHASE = 1 and proceed to 2 and/or 22, and then 3. Runs with PHASE = 33, 44, and 45 generally are performed only using a satisfactorily calibrated model. Phase 11 produces values that can be used to create a sum-of-squared, weighted-residuals contour graph.

Table 3.1. The Functions of each Phase of UCODE

Phase	Functions
1	Forwarding modeling using the starting parameter values
11	Performs a forward model run and calculates the sum-of-squared, weighted residuals of the objective function
2	Sensitivities at starting parameter values
22	Sensitivities and parameter variances, covariances, and correlations at starting parameter values
3	Performs inverse procedure to find the best-fit parameter values
33	Calculates the modified Beale's measure of model linearity
44	Calculates predictions and their linear confidence and prediction intervals
55	Calculates differences and their linear confidence and prediction intervals

Table 3.2. UCODE Input files

File Name	Format	Functions	Notes
Universal File	fn[(a)].uni	Contains control parameters for regression and printing, and observation information.	Required
Prepare File	fn.pre	Names the template file(s) and the application model input file(s). Provides the starting parameter values. Defines prior information on the parameters.	Required
Extract File	fn.ext	Describes how to extract values from the output and defines how to calculate simulated equivalents of the observations.	Required
Template File(s)	*[(b)].tpl	A copy of application model input file, edited such that search strings replace values derived from the defined parameters.	Required
Function File	fn.fnc	Allows functions of the parameter values to be used as input to the application model.	Optional
Temp files	temp.xxx[(c)]	Needed to calculate prediction linear confidence and prediction intervals.	Required for PHASE 44, 45

(a) fn in the file name is to be replaced by a user-defined prefix. For the case of using modified STOMP, fn = out_uc1.
(b) The symbol * is to be replaced by the name of the input file for the application model. For the case using STOMP, * = input.
(c) xxx can be u44, p44, f44, e44, u45, p45, f45, and e45.

UCODE always needs one universal file, one prepare file, one extract file, and one or more template files (Table 3.2) as input files. The function file is optional, depending on the parameter substitution method. Four more additional input files are needed when PHASE = 44 or 45. These files are created automatically at PHASE 3, but the user needs to rename the files. For detailed descriptions of constructing the files, please refer to Poeter and Hill (1998).

3.2 Revised STOMP

The application model used to simulate water flow for the parameter estimation procedure is the STOMP numerical simulator (White and Oostrom 2000). STOMP is designed to solve a variety of nonlinear, multiple-phase, flow and transport problems for unsaturated porous media. STOMP requires one text input file. When working together with UCODE, it needs only one template file. This input file has a structured format composed of cards, which contain associated groups of input data. Depending on the operational mode, input cards may be required, optional, or unused. Required cards must be present in an input file. Cards may appear in any order within the input file. However, the data structure within a card is critical and must follow the formatting directives.

The modified STOMP requires two more cards, i.e., the *ucode control card* and the *observed data card*, in the input file. To have these functions take effect, at the first line of the *solution control card*, the phrase “w/inverse” is needed before the last comma. For better performance and easy coupling with UCODE, STOMP was modified to have such functions that two of the UCODE input files, i.e., the *out_uc1.uni* and *out_uc1.ext* files, can be constructed by running STOMP before the start of the inverse modeling. A new output file, *out_uc1.sto*, is produced after each run of STOMP. The *out_uc1.sto* file includes all the simulated values corresponding to the observations. Multi-dimensional linear interpolation was used to calculate the simulated values at the positions where the observations were taken.

Another new function of the modified STOMP is that it accepts parameter scaling (Zhang et al. 2002) by including a *scaling card* in the input file. To have this function take effect, at the first line of the *solution control card*, the phrase "w/scaling" is needed before the last comma. Note that this card is optional for inverse modeling.

3.3 Inverse Modeling Using STOMP/UCODE Combination

3.3.1 New Cards in the STOMP Input File

STOMP accepts three cards, the *scaling card*, *ucode control card,* and the *observed data card*, to facilitate the use of parameter scaling and coupling with UCODE. The information in the last two cards is used to construct the UCODE universal file and extract file.

The first line of the *scaling card* includes five comma-delimited words, each of which is either "linear" or "logarithmic." They are sequentially associated with the parameters K_s, θ_s, α, n, and S_r, respectively, if the van Genuchten (1980) model is used, where K_s is the saturated hydraulic conductivity, θ_s is the saturated water content, α and n are fitting parameters, and S_r is residual saturation. The following lines list the values of the scaling factors for all the soil types. In each line, the soil name is followed by five comma-delimited numbers, which are sequentially associated with the parameters K_s, θ_s, α, n, and S_r, respectively. If the Brooks and Corey (1964) model is used, parameters α and n are substituted by the air-entry parameter (ψ_e) and the pore size distribution parameter (λ), respectively.

The *ucode control card* includes five lines of comma-delimited data. The seven numbers in the first line sequentially correspond to the information at the top part of the universal file. The second line gives the path of the nonlinear regression program, MRDRIVE. The third line gives the counts of application models. The fourth line is the name of the batch file to run the application model. The last line includes four integers corresponding to the last four numbers in the universal file before the data.

The *observed data card* contains the observation data and associated information such as position and time. The first integer in the card is the count of observation positions. All the data associated with the same position make a data unit. The total count of data units is the same as the count of the observation positions. Each data unit contains the associated information followed by data. The observation position can be expressed in either node numbers or actual distances in the order of x, y, z for the Cartesian coordinate system. The data items in the first line are comma-delimited and in the following order: keyword ("reference" or "field"), data type, e.g., moisture content, data units, x, y, z, data statistical index, data statistics, time-weighting factor, and spacing-weighting factor. If the key word "reference" is used, the values of x, y, and z are the node numbers. If the key word "field" is used, the values of x, y, and z are the actual distances from the origin, each of which is followed by corresponding units. The second line of each data unit gives the total count of observations contained in this unit. The observations are listed from the third line in the following format: observation time, time unit, observation value, and observation units. Each data item must be followed by a comma.

3.3.2 Construction of the UCODE Input Files

The universal and extract files can be constructed by running STOMP once. If produced this way, the files will have the names of *out_uc1.uni* and *out_uc1.ext*, respectively. Note that STOMP does not overwrite any existing universal or extract files. Hence, the two files must be removed manually if they need to be re-constructed.

The prepare file, *out_uc1.pre*, and an optional function file, *out_uc1.fnc*, need to be constructed manually. The template file, *input.tpl*, is constructed manually by replacing the parameters to be estimated by corresponding substituting strings that appeared in the *our_uc1.pre* file.

3.3.3 Procedures to Run UCODE/STOMP

As an initial test, the UCODE/STOMP combination may be run by setting the phase value in the universal file at 1. In this case, UCODE will run STOMP once at the initial parameter values and calculate the sum of the weighted-squared residuals. One of the output files, *out_uc1._ot*, may be examined for any possible mistakes. If there is no problem, other tasks can be performed by setting different phase values.

When the phase value is 2 or 22, UCODE calculates the sensitivity of each parameter at the initial parameter values using the forward or central difference method. The parameters that have very low sensitivity values may be excluded from the list of parameters to be estimated.

When the phase value is 3, UCODE performs nonlinear regression to search for the optimized parameter values. The steps to estimate the hydraulic parameters are as follows: (1) UCODE sends commands to execute STOMP at the initial or updated parameter values, (2) UCODE extracts the model predictions from the STOMP outputs and calculates the sum of the weighted squared residuals, (3) UCODE perturbs each of the parameter values and calculates parameter sensitivity, (4) UCODE updates the parameter values using the modified Gauss-Newton method, (5) Steps 1 through 4 are repeated until the convergence criterion is met, (6) UCODE calculates parameter sensitivity at the optimized parameter values, and (7) UCODE calculates the statistics of the inverse procedure, e.g., variance and covariance, confidence interval, and correlation coefficients between parameters.

Applications of the inverse techniques to estimate field-scale values of hydraulic parameters using parameter scaling and stomp/UCODE combination are presented in the following chapters.

4.0 One-Dimensional Flow in Layered Soil

This section discusses experiments at the Hanford Grass Site (Case 1) and the Andelfingern Site (Case 2). These initial applications were done to test the methodology and prepare for application to the Vadose Zone Transport Field Study sites.

4.1 Case 1: Hanford Grass Site

4.1.1 Experiment

Rockhold et al. (1988) conducted this experiment at the Hanford Site in Richland, WA. Hereafter, we refer to this soil as the Hanford soil. A drainage experiment was conducted at a site of 2 × 2 m (6.56 × 6.56 ft) with a neutron-probe access tube in the center. Tensiometers were placed at 0.15- to 0.30-m (0.5- to 1-ft) depth increments, down to 1.8 m (5.9 ft). Ponding was facilitated by using planking installed in narrow trenches around which the soil was thoroughly compacted. Water contents were monitored with a model 503DR Hydro-probe (Campbell Pacific Nuclear Corp., Martinez, CA). Pressure heads (ψ) were measured with tensiometers and a Tensimeter (Soil Measurement Systems, Tucson, AZ) pressure transducer. Tensiometer and neutron-probe readings were taken every 10 to 15 min during the initial drainage phase of the experiment, and less frequently as time passed (Rockhold et al. 1988).

The soil water retention curves of the soil (Rockhold et al. 1988) show that the soil is better treated as a four-layer soil. The water content and pressure-head data of their Tables A.7 and A.8, respectively, were used in our modeling. The pressure-head observations at 15 and 180 cm (5.9 and 70.1 in.) were set as the upper and lower boundaries, respectively. Note that we intentionally did not use the zero flux as the upper boundary because the pressure-head measurements suggest that there be upward flow at the upper part of the soil profile.

4.1.2 Inverse Modeling

The soil was classified into four layers (Table 4.1) according the θ-ψ relationship measured in the field. The flow was simulated using a one-dimensional (1-D) model, and the modeling domain was from a depth of 0.15 to 1.80 m (0.5 to 5.9 ft). The uniform Cartesian coordinate system was used, and the node size was 0.01 m (0.03 ft). The Dirichlet-type boundary condition was used for both the top (depth 0.15 m [0.5 ft]) and bottom (depth 1.80 m [5.9 ft]) boundaries.

The local-scale parameter values of α, n, θ_s, and θ_r at each soil depth (Table 4.1) were obtained by fitting soil-water retention curves to measured ψ and θ. We arbitrarily selected the parameter values of the top soil layer as the reference from which to calculate the scaling factors of these four parameters.

The scaling factors of K_s were determined using the best-fits of the remaining four parameters, i.e., α, n, θ_s, and θ_r, for each layer and the steady-state observations of θ and ψ. In the Rockhold et al. (1988) experiment, steady state was reached before the drainage was started. The water flux through each layer was the same at steady state. With the unit gradient assumption, the flux equals the unsaturated hydraulic conductivity at the corresponding state:

$$q_0 = K(\psi) \tag{5}$$

where q_0 is the steady-state flux. Using Equation 5 and the van Genuchten $K(\theta)$ and $K(\psi)$ relationships and rearranging yield

$$K_{s\theta} = q_0 \cdot S_{e0}^{-0.5}\left[1-\left(1-S_{e0}^{1/m}\right)^m\right]^{-2}, \quad 0 \le S_e \le 1 \tag{6}$$

and

$$K_{s\psi} = \begin{cases} q_0 \cdot \dfrac{\left[1+(\alpha\,|\,\psi_0\,|)^n\right]^{0.5m}}{\left\{1-(\alpha\,|\,\psi_0\,|)^{n-1}\left[1+(\alpha\,|\,\psi_0\,|)^n\right]^{-m}\right\}^2} & \text{if} \quad \psi < 0 \\ q_0 & \text{if} \quad \psi \ge 0 \end{cases} \tag{7}$$

where the subscript zero denotes the observation at steady-state with a flux of q_0, $K_{s\theta}$ and $K_{s\psi}$, which are the estimated values of K_s using the observations of θ and ψ, respectively. The values of $K_{s\theta}$ and $K_{s\psi}$ at the same flow state for the same texture may not be the same because of experimental error. Using Equation 6 or 7, the scaling factors of K_s for the i^{th} texture were calculated as

$$\gamma_{Ks_i} = \frac{K_{si}}{K_{s1}}. \tag{8}$$

Applying Equations 6 and 7 to 8 produces two sets of scaling factors associated with K_s. We used the average of the corresponding values of the two sets of scaling factors in our model (Table 4.1). In Equation 8, the variable q_0 cancelled out.

Table 4.1. The Values of the Hydraulic Parameters at Local Observation Scale and Calculated Scaling Factors Reference to the First Layer

		Layer 1	**Layer 2**	**Layer 3**	**Layer 4**
Depth (m)		0 - 0.225	0.225-0.375	0.375-0.525	0.525-1.80
Parameter	K_s (m s^{-1})	1×10^{-5}	4.29×10^{-7}	2.56×10^{-7}	1.05×10^{-7}
Values	α (m^{-1})	8.41	7.85	12.72	13.13
	n (-)	1.232	1.236	1.355	2.054
	θ_s (m^3 m^{-3})	0.264	0.199	0.153	0.146
	θ_r (m^3 m^{-3})	0.043	0.022	0.017	0.031
	S_r[(a)] (-)	0.163	0.111	0.111	0.212
Scaling	γ_{Ks}	1	0.0429	0.0256	0.0105
Factors	γ_{α}	1	0.933	1.512	1.561
	γ_n	1	1.003	1.100	1.667
	$\gamma_{\theta s}$	1	0.754	0.580	0.553
	γ_{Sr}	1	0.681	0.681	1.301
(a) $S_r = \theta_r / \theta_s$					

For the purpose of comparison, the K_s value at the local scale for the top layer of the Hanford soil was determined from measurements using the Guelph Permeameter in this layer (Table 4.1). Note that STOMP requires the input of the residual saturation (S_r) rather than the residual water content (θ_r), and hence the values of γ_{Sr} were calculated (Table 4.1).

4.1.3 Results

Using the values of the scaling factors in Table 4.1, the field-scale reference hydraulic parameters were inversely estimated, and their corresponding 95% LCI are given in Table 4.2. Since parameters $\tilde{K}_s$, $\tilde{\alpha}$, and $\tilde{n}$ were log-transformed when they were estimated, their 95% LCIs are expressed as the mean values multiplied or divided (×/÷) by a factor that has the minimum value of unity. Using the values of the scaling factors in Table 4.1 and the estimates of the field-scale reference parameters in Table 4.2, we calculated the field-scale values of the hydraulic parameters for each soil layer (Table 4.3).

Comparisons between the observed and the simulated values using the local- and field-scale parameter values are shown in Figure 4.1. When the field-scale parameter estimates (Table 4.3) were used to simulate the flow, the simulation errors were significantly reduced. The sum of the squared-weighted residual decreased by 96% from 15,484 to 604.

Figure 4.1 shows the water content and pressure head profiles at selected times. The water contents at the soil below 60 cm have a larger simulation errors relative to those above 60 cm (a). This is attributed to the soil below 60 cm being treated as one layer while the soils above were treated as three layers with different properties. The heterogeneity existing in the soil below 60 cm may be slightly larger than that within the rest of the layers. However, this small heterogeneity does not adversely affect the simulations of pressure head in this layer except at 500 h after the start of the drainage experiment (b).

Table 4.2. The Inversely Determined Reference Values of the Hydraulic Parameters, their 95% Linear Confidence Intervals (LCI), and the Composite Scaled Sensitivities (CSS) of the Hanford Soil at Field Scale

Parameters	Mean with 95% LCI	CSS
$\tilde{K}_s$	2.787×/÷1.57 (10^{-3} m s^{-1})	8.25
$\tilde{\alpha}$	11.27×/÷1.18 (m^{-1})	9.19
$\tilde{n}$	1.214×/÷1.04	8.23
$\tilde{\theta}_s$	0.258±0.011 (m^3 m^{-3})	2.30
$\tilde{S}_r$	0.213±0.039	1.35
$\tilde{\theta}_r$	0.055[a] (m^3 m^{-3})	-
(a) $\theta_r = S_r\theta_s$.		

Table 4.3. The Mean Values of the Hydraulic Parameters of Individual Layers of the Hanford Soil

Soil Depth (m)	K_s (m s^{-1})	α (m^{-1})	n (-)	θ_s (m^3 m^{-3})	S_r (-)	θ_r[(a)] (m^3 m^{-3})
0 - 0.225	2.79×10^{-3}	11.3	1.214	0.258	0.213	0.055
0.225 - 0.375	1.20×10^{-4}	10.5	1.218	0.195	0.145	0.028
0.375 - 0.525	7.13×10^{-5}	17.0	1.336	0.150	0.145	0.022
0.525 - 1.800	2.93×10^{-5}	17.6	2.024	0.143	0.277	0.040
(a) Calculated by $\theta_r = S_r\theta_s$						

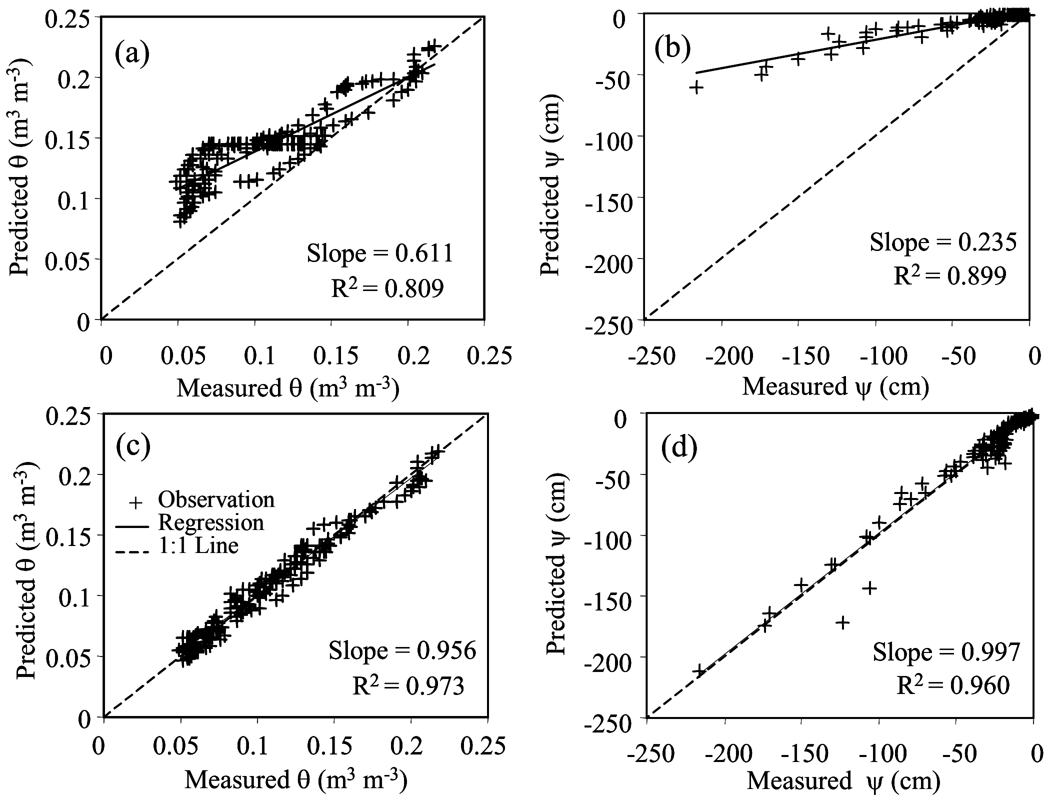

Figure 4.1. Comparison of the Observations and the Predictions of Water Content and Pressure Head of the Hanford Grass Site Soil Using (a) and (b), the Local-Scale Parameter Values, and (c) and (d), the Field-Scale Parameter Values

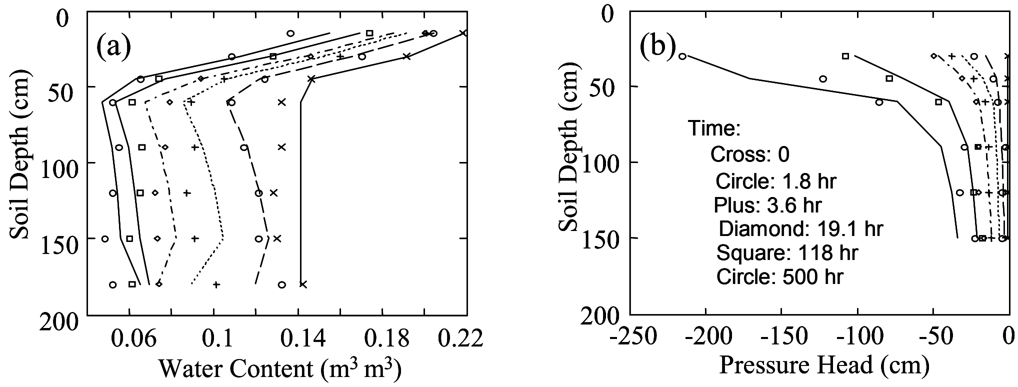

Figure 4.2. Comparison of the Observed and the Predicted Values of (a) Water Content and (b) Pressure Head of the Hanford Experiment: Lines = Predictions; Symbols = Observations

4.2 Case 2: Andelfingen Site

4.2.1 Experiment

Abbaspour et al. (2000) conducted this experiment at Andelfingen near Zurich, Switzerland. Hereafter, we will refer to this soil as the Andelfingen soil. Four texturally different layers were identified over a profile depth of 1.3 m (4.3 ft). The experimental plot (1.6 × 1.2 m [5.25 × 3.9 ft]) was covered with a greenhouse-type plastic tunnel to keep out natural precipitation. The experiment was carried out in two phases. First, the plot was irrigated at a constant rate of 2.61 ± 0.047 cm d^{-1} with an automated sprinkling device. The infiltration stage proceeded for about 27 days, leading to a quasi steady-state flow field in the soil, after which the soil was allowed to drain. Evaporation was measured directly during irrigation and averaged 0.23 cm d^{-1}. However, the evaporation rate was not measured during the drainage stage. The data points in Figures 6 and 7 of Abbaspour et al. (2000) were digitized as the inputs of the inverse parameter estimation model. The pressure-head observations at 20 and 95 cm (7.9 and 37.4 in.) were used as the upper and lower boundary conditions, respectively. The observations of both stages were used to estimate the hydraulic parameters in our inverse modeling. Hysteresis was neglected in the analysis.

4.2.2 Inverse Modeling

The soil was classified into four layers (Table 4.4) according the θ-ψ relationship measured in the field. The flow was simulated using a 1-D model, and the modeling domain was from a depth of 0.20 to 0.90 m (0.66 to 3 ft). The uniform Cartesian coordinate system was used, and the node size was 0.01 m (0.03 ft). The Dirichlet-type boundary condition was used for both the top (depth 0.20 m [0.66 ft]) and bottom (depth 0.90 m [2.9 ft]) boundaries.

The same as Case 1, the local-scale parameter values of α, n, θ_s, and θ_r at each soil depth (Table 4.4) were obtained by fitting soil-water retention curves to measured ψ and θ, and the top soil layer was selected as the reference from which to calculate the scaling factors of these four parameters. The method to determine the scaling factors of K_s is the same as that of Case 1.

Table 4.4. The Values of the Hydraulic Parameters at Local Observation Scale and Calculated Scaling Factors Reference to the First Layer

		Layer 1	Layer 2	Layer 3	Layer 4
Depth (m)		0-0.28	0.28-0.50	0.50-0.90	0.90-1.30
Parameter	K_s (m s^{-1})	3.858×10^{-7}	3.875×10^{-6}	2.268×10^{-4}	4.579×10^{-6}
Values	α (m^{-1})	0.383	1.56	6.62	0.733
	n (-)	1.331	1.435	1.594	1.368
	θ_s (m^3 m^{-3})	0.374	0.295	0.417	0.394
	θ_r (m^3 m^{-3})	0.093	0.062	0.000	0.090
	$S_r^{(a)}$(-)	0.249	0.210	0.000	0.228
Scaling	γ_{Ks}	1	10.053	587.9	11.87
Factors	γ_α	1	4.073	17.29	1.914
	γ_n	1	1.078	1.198	1.028
	$\gamma_{\theta s}$	1	0.789	1.115	1.053
	γ_{Sr}	1	0.845	0.000	0.919
(a) $S_r = \theta_r / \theta_s$					

4.2.3 Results

Using the values of the scaling factors in Table 4.4, the field-scale reference hydraulic parameters were inversely estimated and their corresponding 95% LCI are given in Table 4.5. The calculated values of the hydraulic parameters for each soil layer at field scale are listed in Table 4.6.

Table 4.5. The Inversely Determined Reference Values of the Hydraulic Parameters, their 95% LCI and the CSS of the Andelfingen Soil at Field Scale

Parameters	Mean with 95% LCI	CSS
$\tilde{K}_s$	3.59×/÷1.25 (10^{-8} m s^{-1})	48.0
$\tilde{\alpha}$	0.253×/÷1.09 (m^{-1})	24.4
$\tilde{n}$	1.43×/÷1.04	48.4
$\tilde{\theta}_s$	0.362±0.005 (m^3 m^{-3})	4.40
$\tilde{S}_r$	[0.249]	0.03
$\tilde{\theta}_r$	$0.090^{(a)}$ (m^3 m^{-3})	-
(a) $\theta_r = S_r\theta_s$. Square bracket: constant		

Table 4.6. The Mean Values of the Hydraulic Parameters of Individual Layers of the Andelfingen Soil

Soil Depth (m)	K_s (m s^{-1})	α (m^{-1})	n (-)	θ_s (m^3 m^{-3})	S_r (-)	θ_r [(a)] (m^3 m^{-3})
0 - 0.28	3.59×10^{-8}	0.25	1.43	0.362	0.249	0.090
0.28 - 0.50	3.61×10^{-7}	1.0	1.54	0.286	0.210	0.060
0.50 - 0.90	2.11×10^{-5}	4.4	1.71	0.404	0.000	0.000
0.90 - 1.30	4.26×10^{-7}	0.48	1.47	0.381	0.229	0.087
(a) Calculated by $\theta_r = S_r\theta_s$						

Comparisons between the observed and the simulated values using the local- and field-scale parameter values are shown in Figure 4.3. When the field-scale parameter estimates (Table 4.6) were used to simulate the flow, the simulation errors were significantly reduced. The sum of the squared weighted residual decreased by 93% from 13,517 to 907.

Figure 4.4 and Figure 4.5 show the time courses of θ and h at four observation depths for the Andelfingen experiment. Generally, both the water contents and pressure head were simulated very well. The simulations of θ of the drainage stage at 65 cm depth show larger error than those at other depths. This discrepancy could be due to an inadequate conceptual model. Mechanisms such as hysteresis and fingering were not considered.

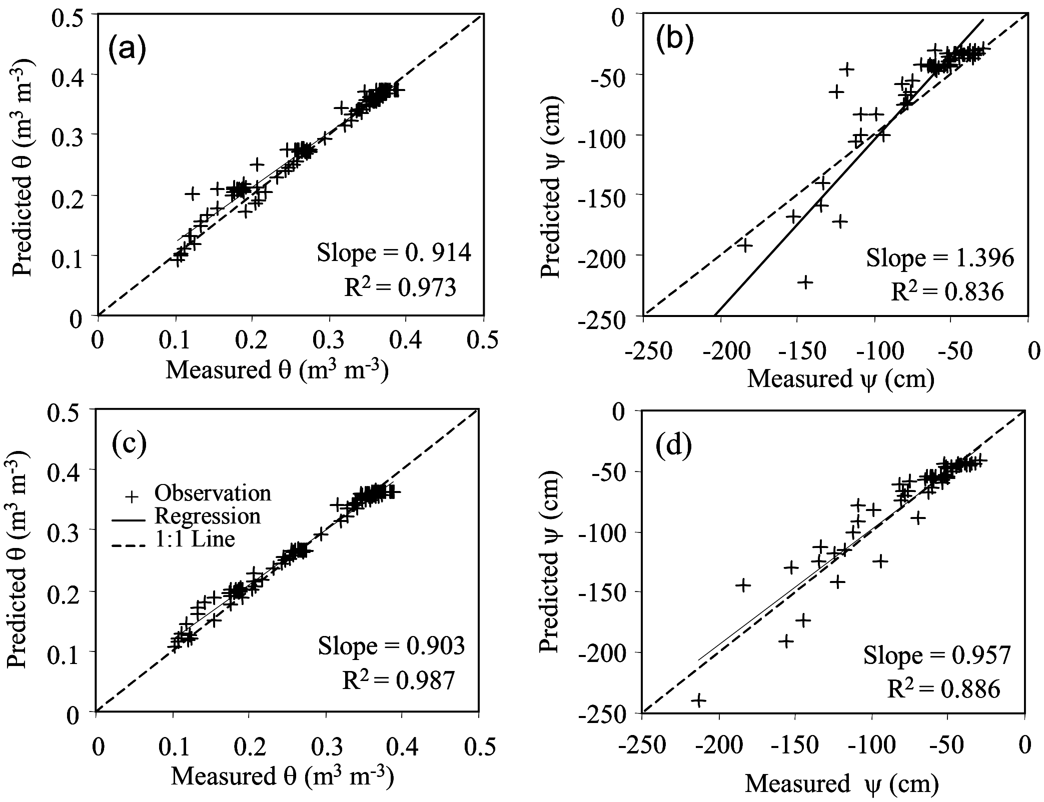

Figure 4.3. Comparison of the Observations and the Predictions of Water Content and Pressure Head of the Andelfingen Soil Using (a) and (b), the Local-Scale Parameter Values, and (c) and (d), the Field-Scale Parameter Values

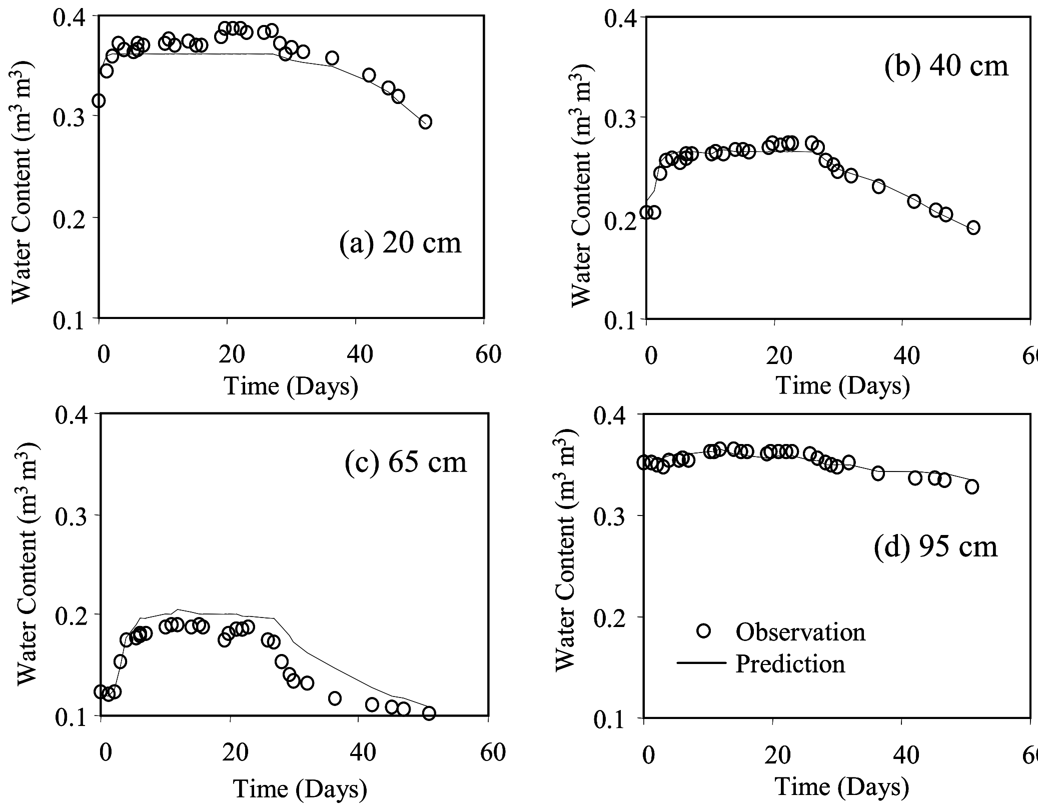

Figure 4.4. Comparison of the Observed and the Predicted Water Contents of the Andelfingen Experiment.

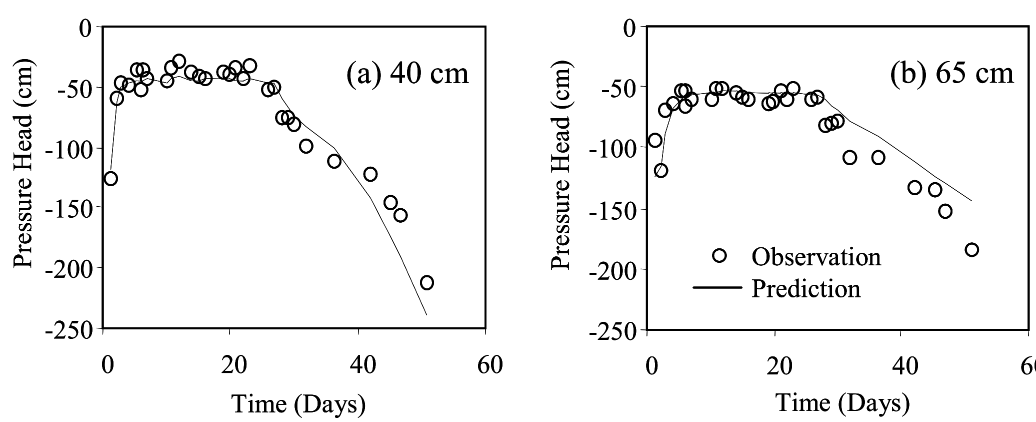

Figure 4.5. Comparison of the Observed and the Predicted Pressure Heads of the Andelfingen Experiment.

5.0 Flow From a Point Source

This section discusses injection experiments and previous simulations, recalibration of the neutron probes, the classification of soil textures, inverse modeling, and results.

5.1 Experiments and Previous Simulations

Fluid-injection experiments were conducted at the 200E Area of the Hanford Site during 1980 and 1981 (Sisson and Lu 1984). A plan view of the layout of the injection well and the 32 observation wells are shown in Figure 5.1. Each monitoring well was 18.3 m (60 ft) deep. The injection schedule consisted of 11 injections of approximately 4000 L (1056 gal) each. The injection well is located in the center of the observation-well network. The fluid was injected through a hole in a steel plate welded to the bottom of the injection well, which is about 4.57 m (15 ft) below the soil surface. Water-content measurements were made using three Campbell-Pacific Nuclear neutron probes at 0.3048 m (1 ft) vertical intervals. A more complete suite of 1920 points of measurements was taken before the first injection. Post-injection measurements included only wells within the radius of influence of the advancing water front. A general calibration curve of the three probes was given by Sisson and Lu (1984) as

$$\theta_v(\%) = c_0 + c_1 \cdot NC_{15} + c_2 \cdot NC_{15}^2 + c_3 \cdot NC_{15}^3 \quad (9)$$

where NC_{15} = 15-sec neutron counts
c_0 = -1.6641
c_1 = 9.37575×10^{-3}
c_2 = 9.13783×10^{-7}
c_3 = 2.62135×10^{-9}

Fayer et al. (1995) indicated some uncertainty with the calibration of the neutron probes reported by Sisson and Lu (1984). The neutron probes were re-calibrated by Fayer et al. (1995) as

Probe 1 (H38092510): $$\theta_v(\%) = 0.0182 \cdot NC_{15} - 3.82 \quad (10)$$

Probe 2 (D79102971): $$\theta_v(\%) = 0.0192 \cdot NC_{15} - 4.03 \quad (11)$$

Probe 3: $$\theta_v(\%) = 0.0202 \cdot NC_{15} - 6.39 \quad (12)$$

A fourth neutron probe was also calibrated, and the calibration curve is given as

Probe 4 (H33115140): $$\theta_v(\%) = 0.00559 \cdot NC_{16} - 6.98 \quad (13)$$

Note that there was a typing error in the calibration curve of Probe 4 in Table 3.4 of Fayer et al. (1995). The slope should be 0.00559 rather than 0.0059 since the slopes in their Table 3.4 should be the same as those in their Table 3.2.

Geophysical logging of the wells was also conducted with multiple tools in early 1995 to determine soil-water contents, bulk densities, and residual gamma emissions from the radioactive tracers (Fayer et al. 1995). The bulk-density data were collected at 0.1524-m (0.5-ft) vertical intervals and were used to calculate porosities.

Sisson and Lu (1984) conducted the preliminary simulation of the experiment. Lu and Khaleel (1993), Smoot and Lu (1994, pp. 1195-1213), Smoot (1995), and Rockhold et al. (1999, pp. 1391-1401) also attempted to test various models. The hydraulic parameter values used in these models were all based on laboratory measurements. A review of these simulations is presented in Fayer et al. (1995).

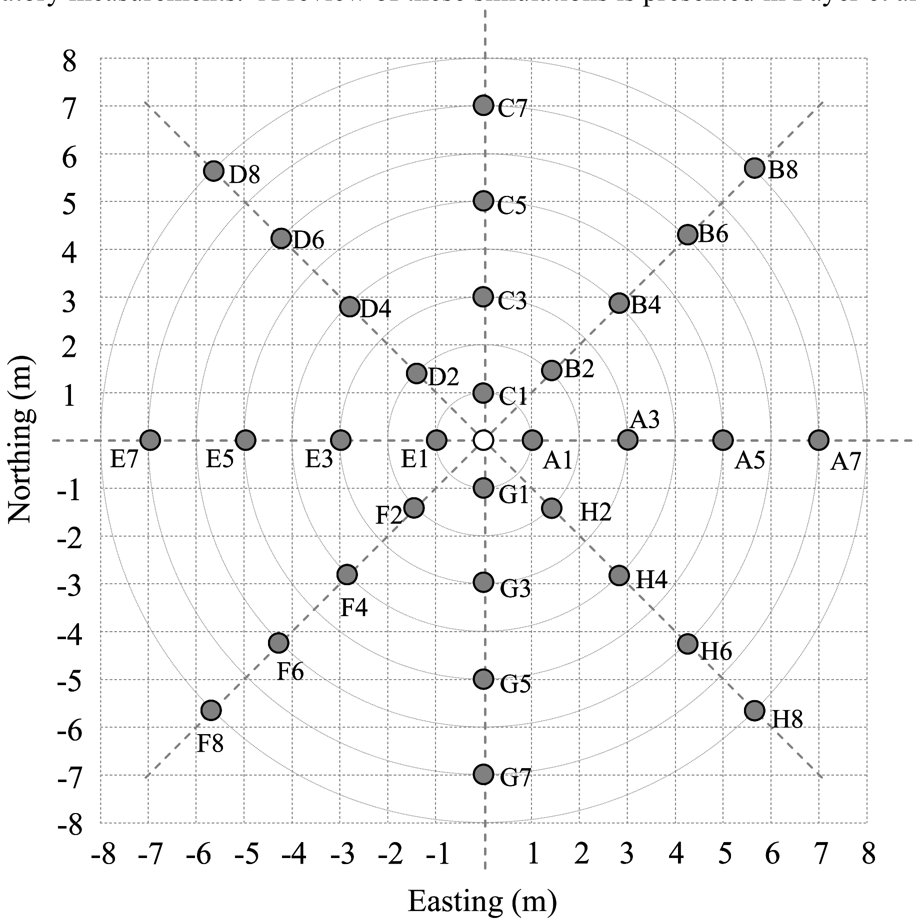

Figure 5.1. Plane View of the Layout of the Injection Well (empty circle at the center) and the Observation Wells (filled circles) at the Sisson and Lu Site

Sisson and Lu (1984) used 4 soil types and 13 horizontal layers with constant thicknesses in their simulation. They noted model bias when compared to the observations of individual wells. One of their recommendations was to use the natural pre-experiment water contents to predict the site lithology. They also recommended using a spatial interpolation procedure like kriging to transform point measurements of water content to the modeling grid.

Lu and Khaleel (1993) simulated the experiment in an attempt to understand the impact of layered sediments, saturation-dependent anisotropy, and hysteresis. Their results indicated that the integrated mass for the field-measured data was consistently higher by up to 35% compared to what was injected. They concluded that the structural layering in the geologic model and saturation-dependent anisotropy were significant processes and that hysteresis was not significant.

Smoot and Lu (1994, pp. 1195-1213) and Smoot (1995) simulated the experiment to demonstrate how multi-dimensional geologic information would impact flow-and-transport simulations. Model performances were examined by the differences between the simulated and interpolated measured water contents of the model cells. Smoot (1995) noted that the differences appeared to be invariant in time and that the model consistently over-predicted water contents by as much as 14% in the silt.

Rockhold et al. (1999, pp. 1391-1401) simulated the experiment using geostatistical-indicator simulation techniques for spatial interpolation of field-measured water contents and porosities and a conditional simulation method based on similar media scaling. The authors claimed that the overall shape of the simulated plume, as local variations within it, matched the characteristics of the actual plume reasonably well.

5.2 The Power Function Fitting to the Calibration Data

As Lu and Khaleel (1993) pointed out, the integrated mass for the field-measured data was consistently higher by up to 35% compared to what was injected. Fayer et al. (1995) recalculated the neutron probes and developed linear calibration curves. To match the water content of the Sisson and Lu site in January 1995, the original calibration curves (Table 2 of Fayer et al. 1995) were shifted upward by 6.0 to 6.9 percentage points (Figure 5.2). We fitted the calibration data of Fayer et al. (1995) using a power function, which describes the calibration curve better than a linear curve. The power function calibration is given as

Probe 4 (H33115140): $$\theta_v(\%) = 5.8293 \times 10^{-8} \times NC_{16p4}^{\ 2.2675} \qquad r^2 = 0.999 \tag{14}$$

where the subscript p4 represents Probe 4. A comparison of the linear and power function calibration curves of the neutron Probe 4 (H33115140) is shown in Figure 5.2.

To calculate the water content using the new calibration curve (Equation 14), the neutron probe counts of Probes 1, 2, and 3 need to be converted to the equivalent counts of neutron Probe 4. In 1995, cross calibrations were also carried out between Probes 1, 2, and 4. The equations used to convert the 15-sec neutron counts of the Probes 1 and 2 used in 1980 to the 16-sec neutron counts of Probe 4, respectively, were

$$NC_{16p4} = 3.3359 \cdot NC_{15p1} + 523.0 \tag{15}$$

$$NC_{16p4} = 3.1851 \cdot NC_{15p2} + 674.1 \tag{16}$$

where the subscripts p1and p2 represent Probes 1 and 2, respectively. Then, the soil-water contents were calculated using Equation 14 and the converted neutron probe counts. The conversion relation between Probes 3 and 4 was obtained by relating the equation (3.2) of Fayer et al. (1995) and Equation (16):

$$NC_{16p4} = 3.3507 \cdot NC_{15p3} + 544.8 \tag{17}$$

where the subscript p3 represents Probe 3.

A comparison of calculated water content using the calibration curves for Probe 1, i.e., Equations 9 and 10 and a combination of Equations 14 and 15, is shown in Figure 5.3. The power function calibration produces lower water content than the polynomial and linear curves.

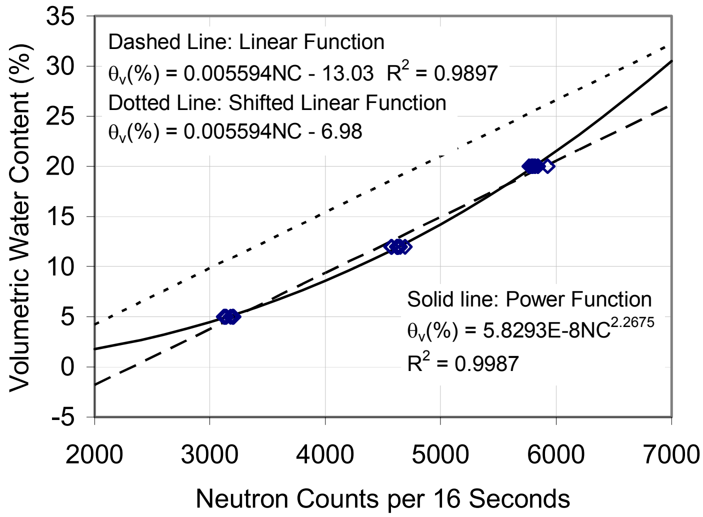

Figure 5.2. Comparison of the Linear, Shifted Linear, and Power Function Calibration Curves of Neutron Probe #4 (H33115140)

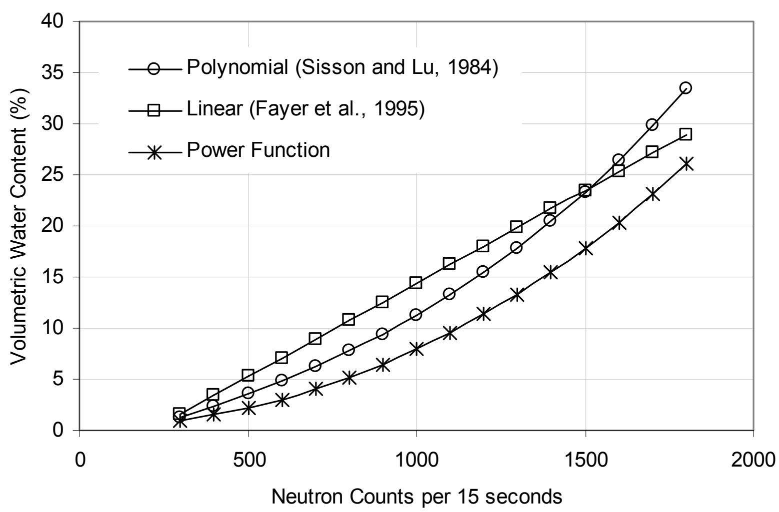

Figure 5.3. A Comparison of Calculated Water Content Calculated Using Different Calibration Curves for Probe 1 (H38092510): A) Polynomial Curve (Equation 9); (B) Linear Curve (Equation 10); and C) Power Function Curve (Combination of Equations 14 and 15)

5.3 Soil-Texture Classification

Fayer et al. (1995) also conducted geophysical logging of the wells with multiple tools to determine porosity (ϕ) and residual gamma emissions from the radioactive tracers at 2.5 cm (1.0 in) spacing. Some of the geophysical data may infer the lithology of the sediments. Sisson and Lu (1984) recommend that the natural pre-experiment (steady-state) water contents, θ_{ss}, be used to predict the site lithology. Since most observations of Sisson and Lu (1984) were taken at the depth between 3.05 m (10 ft) and 15.24 m (50 ft), we focused the soil domain within this range. To visually examine the correlations between the site lithology and θ_{ss} and ϕ, the observations were interpolated using a Kriging method. Three-dimensional distributions of θ_{ss} and ϕ were then plotted using TecPlot 9.0 (Amtec Engineering, Inc., Bellevue, WA).

Figure 5.4 shows the 3-D distribution of the steady-state water content. The θ_{ss} values vary from 1.8% to 10.1%. There are two layers, at the depths of about 7 and 12 m (23 and 39.4 ft), respectively, with higher θ_{ss} values than the adjacent soils. The thicknesses of the two layers vary from position to position and are between approximately 0.5 and 2 m (1.6 and 6.56 ft). However, many thin soil layers are not shown in Figure 5.4. This may be due to relatively large observation spacing of 0.30 m (1.0 ft). Figure 5.5 shows the spatial distribution of porosity, which ranges between 27.8% and 47.6%. More horizontal stratifications are shown in Figure 5.5 than in Figure 5.4.

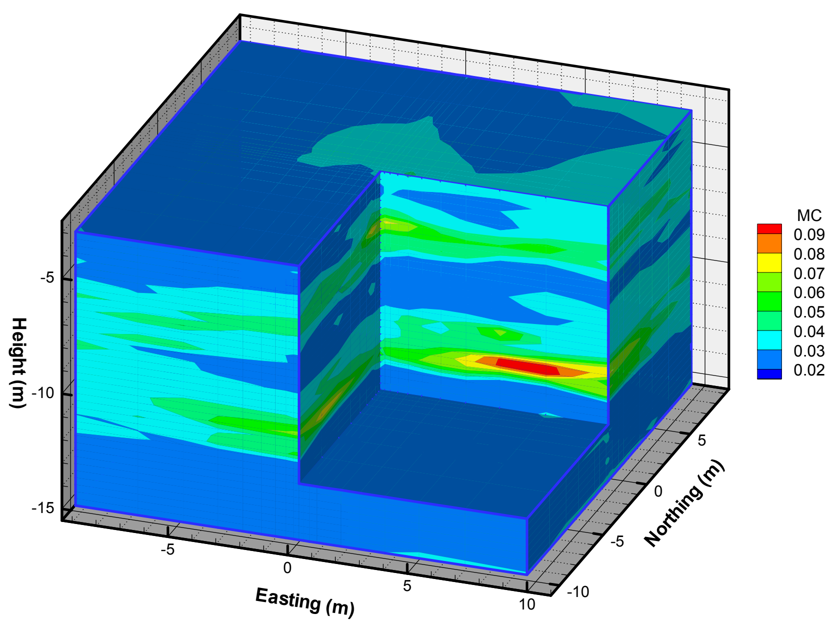

Figure 5.4. The Distribution of Steady-State Water Content of the Sisson and Lu Site

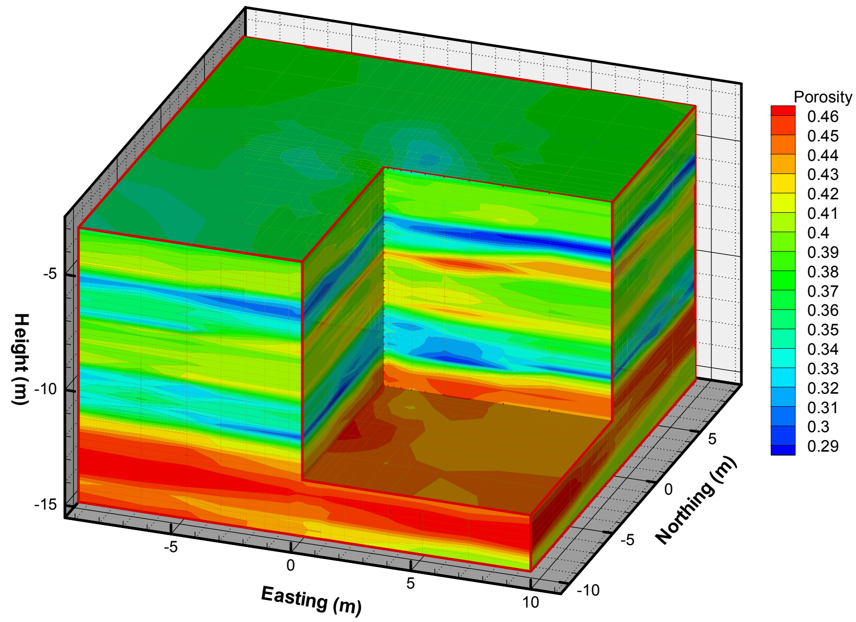

Figure 5.5. The Distribution of Soil Porosity of the Sisson and Lu Site

A scatter plot between θ_{ss} and ϕ is shown in Figure 5.6. There is an inverse correlation between θ_{ss} and ϕ. The lower θ_{ss} values generally correspond to the higher ϕ values, and the textures with these values are coarser generally and have higher permeability. However, ϕ varies from 0.28 to 0.47 while about 99% of θ_{ss} varies from 0.02 to 0.06. This means that a small change in θ_{ss} will cover soil materials with a quite large range of ϕ. Hence, the soil materials with quite different ϕ values will be categorized as a group, which is supposed to have the same hydraulic property. For example, if we categorize the soil materials with θ_{ss} from 0.035 to 0.040 $m^3\ m^{-3}$ as a group, then this group will include materials with ϕ ranging from 0.29 to 0.44 $m^3\ m^{-3}$. This suggests that ϕ is a better criterion for texture classification than θ_{ss}. Previous studies using soil coring data have found that the soil may be classified into seven textures (e.g., Smoot 1995). Last and Caldwell (2001) grouped the materials below 4.0 m (13.1 ft) of the Sisson and Lu site into seven general lithostratigraphic units. Thus, we also classified the soil into seven material types according to the values of ϕ (Table 5.1). The soil stratification in Figure 5.5 is consistent with Table 2 of Last and Caldwell (2001). For example, the two layers in the dark blue color in Figure 5.5 correspond to the two "sand to slightly silty sand" layers of Last and Caldwell (2001), respectively, at 4-6 m (13.1-19.7 ft) and 10-12 m (32.8-39.4 ft).

Table 5.1. Soil Classification of the Sisson and Lu Site Using Porosity

Material Types	Porosity (ϕ)
T1	≥ 0.450
T2	0.425 – 0.449
T3	0.400 – 0.424
T4	0.375 – 0.399
T5	0.350 – 0.374
T6	0.325 – 0.349
T7	< 0.325

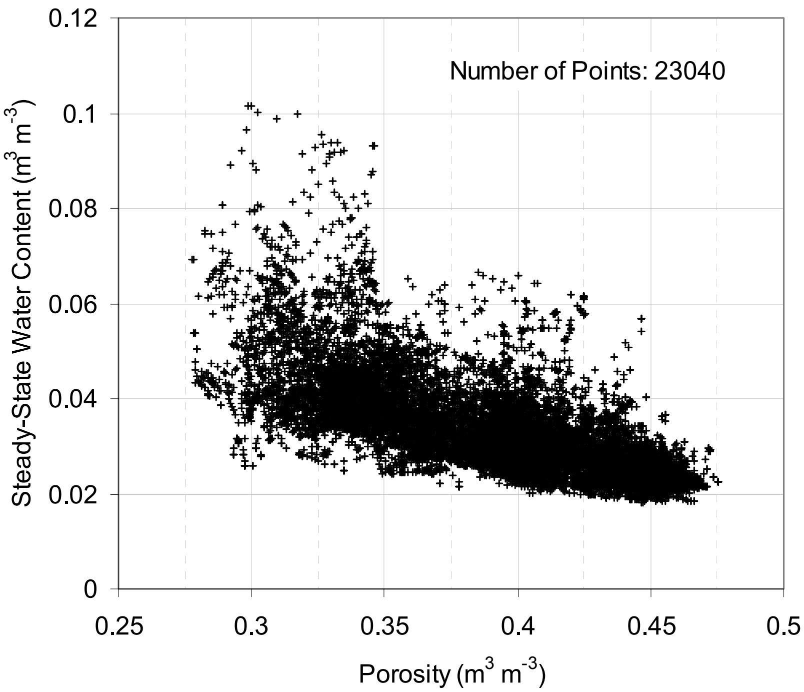

Figure 5.6. A Scatter Plot Between the Porosity and the Steady-State Water Content of the Sisson and Lu Site

5.4 Inverse Modeling

The flow was simulated using the STOMP simulator. A Cartesian coordinate system was used, and the origin was set at the lower southwest corner. Principle directions of anisotropy were assumed to be horizontal and vertical. Hysteresis was not considered. The size of the simulation domain was (x, y, z) = (40.7 m, 40.7 m, 12.2 m) (133.5 ft, 133.5 ft, 40 ft). The depth range of the simulation domain was from 3.048 m (10 ft) to 15.24 m (50 ft). The simulation domain was subdivided into a grid with a variable horizontal cell step (Δx and Δy) and a constant vertical cell step (Δz). The minimum values of Δx and Δy were 0.2 m, (0.66 ft), which were at the center of the domain. The values of Δx and Δy increased by a factor of 1.3 as the distance to the center of the domain increased. The value of Δz was 0.3048 m (1 ft). The source was placed at the center of the x-y plane and at the depth from 4.57 to 4.88 m (15 to 16 ft). The top boundary condition was zero-flux and the bottom unit gradient. The four sides had zero-flux boundary conditions. Note that the zero-flux side-boundary conditions were not true because of lateral flow movement. However, when the horizontal scale of the simulation domain is large enough, the zero-flux side-boundary conditions are still good approximations. The number of nodes at x, y, z direction were 24, 24, and 40, respectively. Totally, there were 23040 nodes. One forward simulation of flow for one week took about 2 h using a workstation with two 600 Mhz processors.

The seven soil textures of our classification were assumed to correspond to the seven textures of Smoot (1995) with Texture 1 being the coarsest and Texture 7 the finest (Table 5.1). Then, the local-scale values of parameters K_{sv}, α, and n were approximated using the parameter values of Smoot (1995), where K_{sv} is the K_s at vertical direction. The values of θ_s were approximated by 0.9ϕ (Pachepsky et al., 1999). The value of θ_r of a texture was approximated by the minimum value of the observed steady-state water content of this texture. In their simulation, Sisson and Lu (1984) used the soil anisotropy values of 8, 8, 5, and 2 for the four soil material types in their simulation. We hence assumed $K_{sh} = 5K_{sv}$, where K_{sh} is the K_s at horizontal direction. The local-scale values of the hydraulic parameter and their corresponding scaling factors are listed in Table 5.2.

The field-scale values of the hydraulic parameters were inversely estimated using the UCODE/STOMP combination and the parameter scaling method (Zhang et al. 2002). Considering the simulation time in the inverse modeling, 6241 observations of Injections #1, #5, and #9 were used, rather than the observations of all the 11 injections. The procedures to estimate the field-scale hydraulic parameters using the combination of parameter scaling and inverse technique are summarized in Figure 5.7.

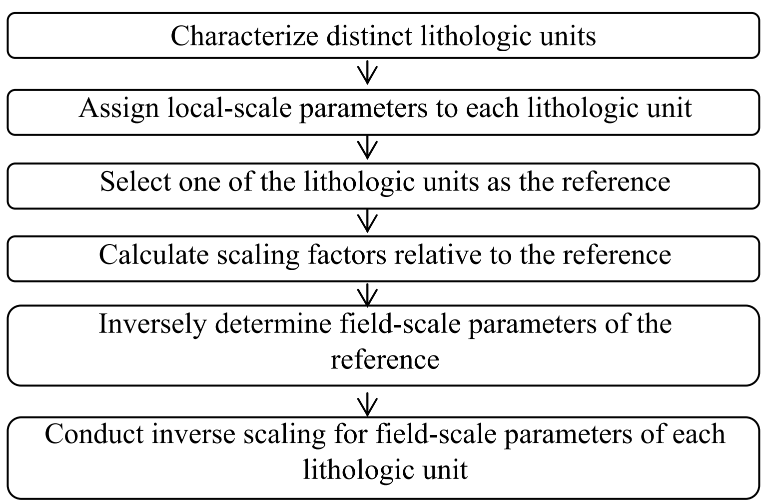

Figure 5.7. The Procedures to Estimate the Field-Scale Hydraulic Parameters Using the Combination of Parameter Scaling and Inverse Technique

Table 5.2. The Values of the Hydraulic Parameters at Local Observation Scale and Calculated Scaling Factors Reference to T4

	Material Type	θ_s (m^3 m^{-3})	K_{sh} (m s^{-1})	K_{sv} (m s^{-1})	α (m^{-1})	n (-)	θ_r(m^3 m^{-3})
Parameter Values	T1	0.416	3.27×10^{-3}	6.54×10^{-4}	12.6	1.55	0.01
	T2	0.394	1.09×10^{-3}	2.18×10^{-4}	2.4	1.65	0.01
	T3	0.371	6.55×10^{-4}	1.31×10^{-4}	8.9	1.48	0.01
	T4	0.349	3.03×10^{-4}	6.05×10^{-5}	4.1	1.94	0.015
	T5	0.326	1.62×10^{-5}	3.23×10^{-6}	0.7	2.80	0.015
	T6	0.304	1.62×10^{-5}	3.23×10^{-6}	0.7	2.80	0.015
	T7	0.270	6.95×10^{-6}	1.39×10^{-6}	1.4	1.55	0.02
Scaling Factors	T1	1.194	10.8	10.8	3.073	0.799	-
	T2	1.129	3.60	3.60	0.585	0.851	-
	T3	1.065	2.16	2.16	2.171	0.763	-
	T4	1.000	1.00	1.00	1.000	1.000	-
	T5	0.935	0.0534	0.0534	0.171	1.443	-
	T6	0.871	0.0534	0.0534	0.171	1.443	-
	T7	0.774	0.023	0.023	0.340	0.799	-

5.5 Results

There were seven textures in the experiment site, and the hydraulic property of each texture was described by six parameters (Table 5.2). This leads to a total of 42 parameters. An inversion of 42 parameters simultaneously was almost impossible due to the difficulty of convergence or the crash of the application model caused by some physically meaningless updated parameter values. Moreover, the extremely long inverse simulation time limits the inversion of so many parameters. After applying parameter scaling using the local-scale values of the hydraulic parameters and Equation 1, the number of parameters to be estimated reduced to 6 parameters of the reference texture. Sensitivity analysis showed that the flow was not very sensitive to parameters and $\tilde{\theta}_s$ and $\tilde{\theta}_r$; hence, the local-scale value of $\tilde{\theta}_s$, i.e., 0.349, with an assumed standard error of 0.1 was used as prior information. and parameter $\tilde{\theta}_r$ was not optimized during the inverse modeling.

The estimated field-scale values of the hydraulic parameters of the reference texture are listed in Table 5.3. The relative low-correlation coefficients (Table 5.4) indicate that these parameters were not significantly correlated. The converted hydraulic parameter values for the seven material types are listed in Table 5.5.

Table 5.3. The Inversely Determined Field-Scale Reference Values of the Hydraulic Parameters, their 95% LCI of the Sisson and Lu Site

Parameters	Mean with 95% LCI
$\tilde{\theta}_s$ ($m^3\ m^{-3}$)	0.333±0.005
$\tilde{K}_{sh}$ ($10^{-3} m\ s^{-1}$)	6.54×/÷1.13
$\tilde{K}_{sv}$ ($10^{-3} m\ s^{-1}$)	1.92×/÷1.09
$\tilde{\alpha}$ (m^{-1})	8.85×/÷1.08
$\tilde{n}$ (-)	2.33/÷1.02

Table 5.4. The Correlation Coefficient Between the Field-Scale Reference Values of the Hydraulic Parameters of the Sisson and Lu Site

	$\tilde{\theta}_s$	$\tilde{K}_{sh}$	$\tilde{K}_{sv}$	$\tilde{\alpha}$
$\tilde{K}_{sh}$	0.386			
$\tilde{K}_{sv}$	0.541	0.511		
$\tilde{\alpha}$	0.045	0.634	-0.037	
$\tilde{n}$	0.134	0.005	-0.330	0.107

Table 5.5. The Effective Parameters of Individual Layers After an Inverse Scaling of the Inversely-Determined Parameters of the Reference Soil Material

Material Type	θ_s ($m^3\ m^{-3}$)	K_{sh} ($m\ s^{-1}$)	K_{sv} ($m\ s^{-1}$)	α (m^{-1})	n (-)
T1	0.398	70.675	20.747	0.272	1.860
T2	0.376	23.558	6.916	0.052	1.981
T3	0.355	14.135	4.149	0.192	1.776
T4	0.333	6.544	1.921	0.089	2.328
T5	0.311	0.349	0.103	0.015	3.359
T6	0.290	0.349	0.103	0.015	3.359
T7	0.258	0.151	0.044	0.030	1.860

Using the field-scale parameter values in Table 5.5 and the values of θ_s and θ_r in Table 5.2, the flow was simulated. As a comparison, the flow was also simulated using the local-scale parameter values in Table 5.2. Comparisons between the simulated and observed water contents for each of the seven textures are shown in Figure 5.8. The results show that the simulated water content in all the textures were significantly improved after applying parameter scaling and inverse modeling. When the local-scale parameter values were used, the overall standard error (σ) of water content was 0.038 $m^3\ m^{-3}$, and the coefficient of determination (R^2) was 0.34. When the field-scale parameter values were used, the value of

σ decreased by 34% to 0.025 $m^3\ m^{-3}$ and $R^2 = 0.57$. The results indicate that the combination of parameter scaling and the inverse procedure is a very effective approach to estimate field-scale hydraulic parameters since only four parameters were inversely estimated with a significant reduction in simulation time.

However, some of the θ observations were not simulated well. Possible causes include error in local-scale parameters, the determination of soil texture and their distribution, and the saturation-dependent soil anisotropy. The errors in the local-scale parameters will lead to errors in the calculated scaling factors. Alternative methods, e.g., using the particle-size-distribution information, may be used to estimate the local-scale values of the hydraulic parameters. Another cause may be the error in determining the soil-texture distribution since we used soil porosity as a criterion for texture classification. There is a possibility that a small portion of the soil texture was not classified well. Thus, some of the seven texture types may be further divided into sub-groups according to other criteria, e.g., steady-state water content, for a more detailed description of texture distribution. In the simulation, soil anisotropy was assumed to be independent of soil saturation, and hence the lateral movement of water might be underestimated. The works for more accurate scaling factors and a model to describe saturation-dependent anisotropy are in progress.

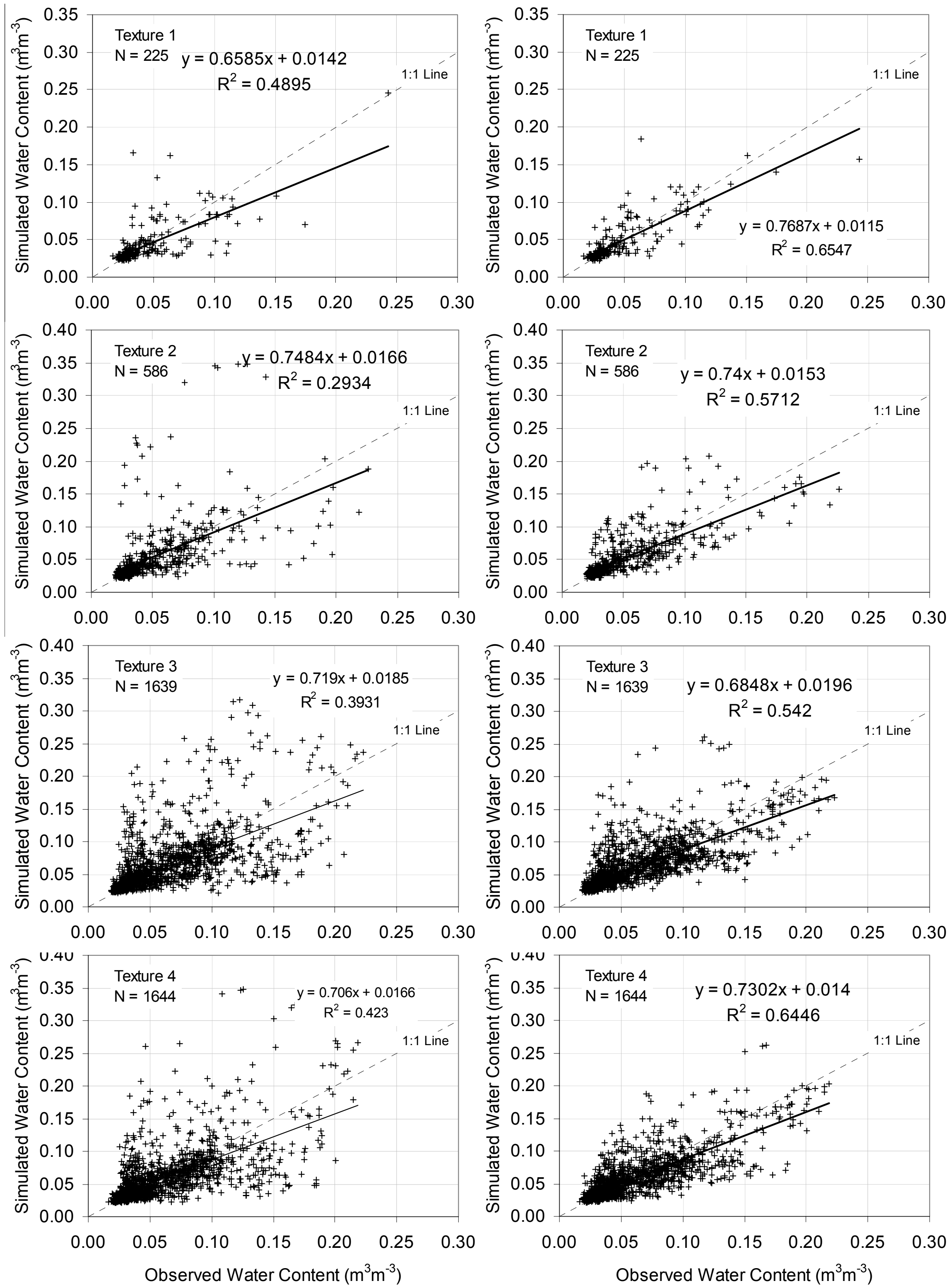

Figure 5.8. Comparisons of the Simulates and Observed Water Contents of the Sisson and Lu Experiment Using the Local-Scale (Left Column) and Field-Scale (Right Column) Values of the Hydraulic Parameters

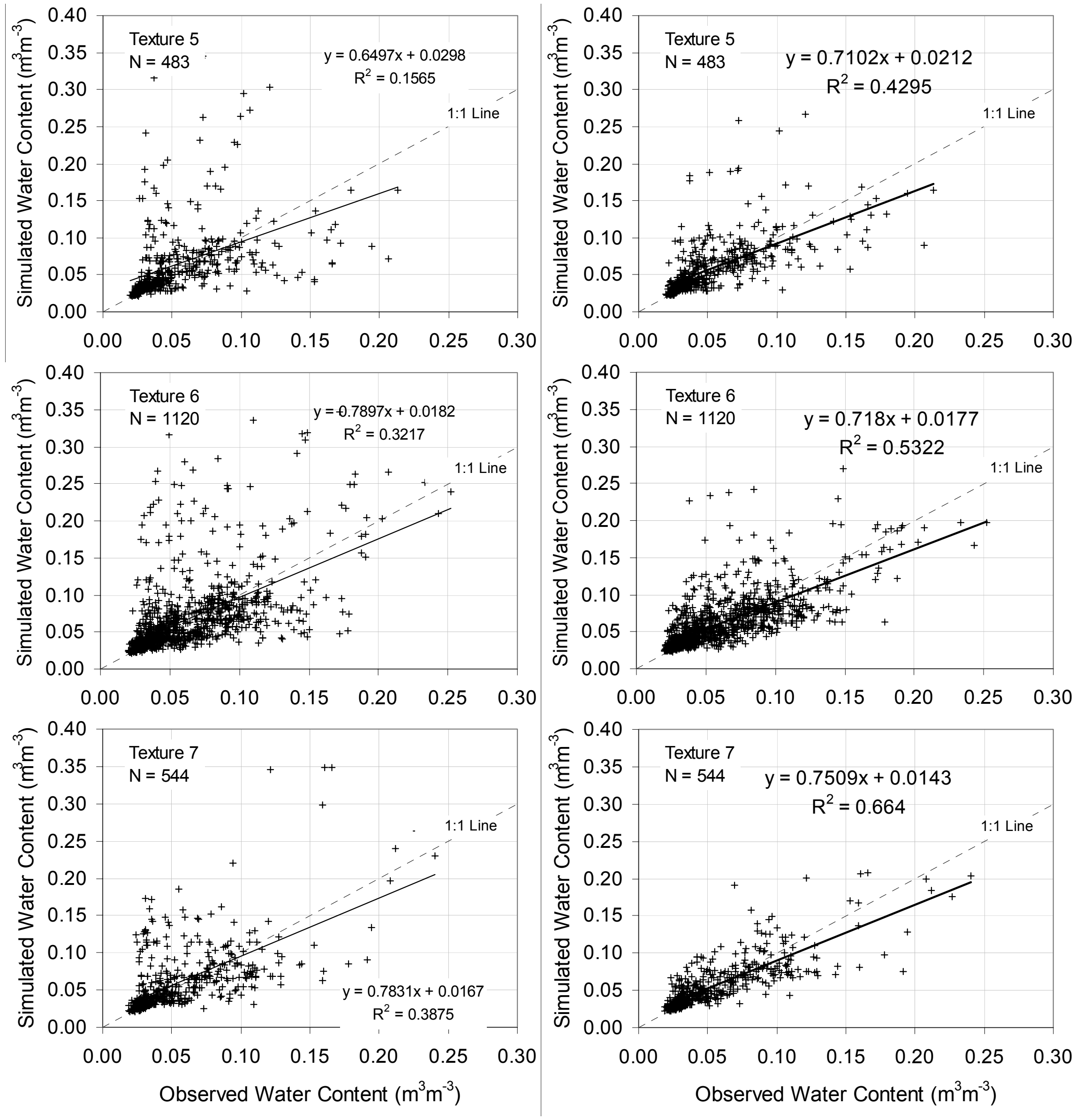

Figure 5.8 (Cont)

6.0 Conclusions

The field-scale values of soil hydraulic parameters were estimated inversely using the parameter-scaling method and inverse procedures. Parameter scaling factors link the hydraulic-parameter values measured at different spatial scales for different soil textures. Parameter-scaling factors relevant to a reference texture of field soils are determined using these local-scale parameter values, e.g., those measured in the lab using small soil cores. After parameter scaling is applied, the total number of unknown variables of hydraulic parameters is reduced by a factor equal to the number of soil textures. The field-scale values of the unknown variables can then be estimated using inverse techniques and a well-designed field experiment. Finally, parameters for individual textures are obtained through inverse scaling of the reference values using an *a priori* relationship between reference parameter values and the specific values for each texture.

The inverse modeling was carried out using two computer models, one for forward flow modeling and the other for nonlinear regression. The forward model used to simulate water flow was the STOMP numerical simulator (White and Oostrom 2000). STOMP was designed to solve a variety of nonlinear, multiple-phase, flow-and-transport problems for unsaturated porous media. The UCODE model (Poeter and Hill 1998) was used to perform inverse modeling posed as a parameter-estimation problem using nonlinear regression. The inverse techniques were applied to two cases of 1-D flow in layered soils and one case of 3-D flow in a heterogeneous soil. The results show that the simulation errors were significantly reduced after applying parameter scaling and inverse modeling. When compared to the use of local-scale parameters, parameter scaling reduced the sum of the squared weighted residual by 93 to 96% for the relatively smaller scale (~2 m [~6.56 ft]) 1-D flow example (Hanford Grass Site) and 57% for the much more complex Sisson and Lu site, which has the spatial scale of about 18 m (59 ft).

Since only the hydraulic parameters of the reference soil material were estimated during inverse modeling, the time used for inverse modeling was greatly shortened. These parameter estimation methods will be applied to analyze data from the more recent field tests at the Sisson and Lu site described in Gee and Ward (2001), at the clastic dike site described in Ward and Gee (2002), and in FY02 field tests.

7.0 References

Abbaspour KC, MT van Genuchten, R Schulin, and E Schlappi. 1997. "A sequential uncertainty domain inverse procedure for estimating subsurface flow and transport parameters" *Water Resour. Res.* 33:1879-1892.

Abbaspour KC, R Kasteel, and R Schulin. 2000. "Inverse parameter estimation in a layered unsaturated field soil," *Soil Sci.* 165(2):109-123.

Brooks RH, and AT Corey. 1964. "Hydraulic properties of porous media affecting fluid flow," *Proc. ASCE J. Irrig. Drain. Div.* 92:61-88.

Fayer MJ, RE Lewis, RE Engleman, AL Pearson, CJ Murray, JL Smoot, RR Randall, WH Wegener, and AH Lu. 1995. *Re-evaluation of a subsurface injection experiment for testing flow and transport models,* PNL-10860, Pacific Northwest National Laboratory, Richland, WA.

Gee, G. W., and A. L. Ward. 2001. *Vadose Zone Transport Field Study: Status Report.* PNNL-13679, Pacific Northwest National Laboratory, Richland, Washington.

Inoue M, J Simunek, S Shiozawa, and JW Hopmans. 2000. "Simultaneous estimation of soil hydraulic and solute transport parameters from transient infiltration experiments," *Adv. Water Res.* 23:677-688.

Last, G. V., and TG Caldwell. 2001. Core sampling in support of the vadose zone transport field study. PNNL-13454, Pacific Northwest National Laboratory, Richland, WA.

Lehmann F, and P Ackerer. 1997. "Determining soil hydraulic properties by inverse method in one-dimensional unsaturated flow," *J. Environ. Qual.* 26:76-81.

Lu AH, and R Khaleel. 1993. "Calibration/validation of VAM3D model using injection test data at Hanford." In: *Vadose zone modeling workshop proceedings*, March 29-30, 1993. R. Khaleel (ed.), WHC-MR-0420, Westinghouse Hanford Company, Richland, WA.

Pachepsky YA, DJ Timlin, and LR Ahuja. 1999. Estimating saturated hydraulic conductivity using water retention data and neural networks. *Soil Sci.* 164:552-560.

Parkin GW, RG Kachanoski, DE Elrick, and RG Gibson. 1995. "Unsaturated hydraulic conductivity measured by time domain reflectometry under a rainfall simulator," *Water Resour. Res.* 31:447-454.

Poeter EP, and MC Hill. 1998. *Documentation of UCODE, a computer code for universal inverse modeling.* U.S. Geological survey, water-resources investigations report 98-4080.

River Protection Project (RPP). 2002. *Field Investigation Report for Waste Management Area S-SX.* RPP-7884, Rev. 0, Prepared for the Office of River Protection by CH2M Hill Hanford Group, Richland, Washington.

Rockhold ML, MJ Fayer, and GW Gee. 1988. *Characterization of unsaturated hydraulic conductivity at the Hanford site.* PNL-6488, Pacific Northwest Laboratory, Richland, WA.

Rockhold ML, CJ Murray, and MJ Fayer. 1999. "Conditional simulation and upscaling of soil hydraulic properties." In: *Characterization and measurement of the hydraulic properties of unsaturated porous media* by M.Th. van Genuchten, F.J. Leij, and L. Wu (editors). Published by the University of California, Riverside.

Simunek J, and MT van Genuchten. 1996. "Estimating unsaturated soil hydraulic properties from tension disc infiltrometer data by numerical inversion," *Water Resour. Res.* 32:2683-2696.

Sisson JB, and A Lu. 1984. *Field calibration of computer models for application to buried liquid discharges: A status report,* RHO-ST-46 P, Rockwell Hanford Operations, Richland, WA.

Smoot JL, and AH Lu. 1994. *Interpretation and Modeling of a subsurface injection test, 200 East Area, Hanford, Washington. Pasco, Washington*, Battelle Press, Columbus, OH.

Smoot JL. 1995. *Development of a geostatistical accuracy assessment approach for modeling water content in unsaturated lithologic units.* Ph.D. Dissertation, University of Idaho.

van Dam JC, JNM Stricker, and P Droogers. 1992. "Inverse method for determining soil hydraulic functions from one-step outflow experiments," *Soil Sci. Soc. Am. J.* 56:1042-1050.

van Genuchten M Th. 1980. "A closed form equation for predicting the hydraulic conductivity of unsaturated soils," *Soil Sci. Soc. Am. J.* 44: 892-898.

Ward, A. L., and G. W. Gee. 2001. *Vadose Zone Transport Field Study: FY 2001 Test Plan*. PNNL-13451, Rev. 1., Pacific Northwest National Laboratory, Richland, Washington.

Ward, A. L., and G. W. Gee. 2002. *Vadose Zone Transport Field Study: FY 2002 Test Plan*. PNNL-13857, Pacific Northwest National Laboratory, Richland, Washington.

Wierenga PJ, RG Hills, and DB Hudson. 1991. "The Las Cruces trench site: Characterization, experimental results, and one-dimensional flow predictions." *Water Resour. Res.* 27:2695-2705.

White MD, and M Oostrom. 2000. *User's guide of STOMP - Subsurface transport over multiple phases,* PNNL-12034 UC-2010, Pacific Northwest National Laboratory, Richland, WA.

Zhang ZF, RG Kachanoski, GW Parkin, and B Si. 2000. "Measuring hydraulic properties using a line source: II. Field test," *Soil Sci. Soc. Am. J.* 64:1563-4569.

Zhang ZF, AL Ward, and GW Gee. 2002. "A parameter scaling concept for estimating field-scale hydraulic functions of layered soils." In: *Findikakis A.N. (ed.), "Bridging the Gap between Measurement and Modeling in Heterogeneous Media", Proceedings of the International Groundwater Symposium*, March 25-28, Berkeley, CA, pp. 103-107, published by IAHR, Madrid, Spain.

Appendix A

Input Files

Appendix A: Input Files

Infiltration and Drainage in Layered Soil

Case 1: Hanford Grass Site

STOMP Input File: *input*

```
~Simulation Title Card
1,
Scaling Method,
Zhang,
PNNL,
22 June 2001,
13:40,
2,
Rockhold et al.(1988)
Drainage in the Grass Site

~Solution Control Card
Normal w/ Scaling w/ Inverse,
Water,
1,
0,s,1980000,s,0.1,s,1800,s,1.25,8,1.e-06,
10000000,
0,

~Grid Card
uniform cartesian,
1,1,166,
1.,cm,
1.,cm,
1.,cm,

~Rock/Soil Zonation Card
4,
L1,1,1,1,1,158,166,R1,
L2,1,1,1,1,143,157,R1,
L3,1,1,1,1,128,142,R1,
L4,1,1,1,1,1,127,R1,

~Mechanical Properties Card
R1,,,0.258,0.258,,,Millington and Quirk,

~Hydraulic Properties Card
R1,2.799e-003,hc:m/s,2.799e-003,hc:m/s,2.799e-003,hc:m/s,

~Saturation Function Card
R1,van Genuchten,0.1128,1/cm, 1.2147,0.212,,

~Aqueous Relative Permeability Card
R1,Mualem,,

~Scaling Card
Linear,Linear,Linear,Linear,Linear,
L1,1.0000,1.000,1.000,1.000,1.000,
L2,0.0429,0.754,0.933,1.003,0.681,
L3,0.0256,0.580,1.512,1.100,0.681,
L4,0.0105,0.553,1.561,1.667,1.301,

~Initial Conditions Card
Gas Pressure,Aqueous Pressure,
2,
Aqueous
Pressure,0.99561e+5,Pa,0.0,1/cm,0.0,1/cm,0.0,1/m,1,1,1,1,158,166
,
Aqueous
Pressure,1.01227e+5,Pa,0.0,1/cm,0.0,1/cm,0.0,1/m,1,1,1,1,1,157,

~Boundary Conditions Card
2,
top,Dirichlet,
1,1,1,1,166,166,21,
0,s,99561,Pa,
484,s,99365,Pa,
1080,s,99071,Pa,
1680,s,98777,Pa,
2880,s,98189,Pa,
4080,s,97503,Pa,
5280,s,97013,Pa,
7080,s,96915,Pa,
8880,s,96817,Pa,
13100,s,96229,Pa,
16700,s,96033,Pa,
19700,s,95935,Pa,
68900,s,94955,Pa,
99300,s,94465,Pa,
187000,s,92799,Pa,
427000,s,88977,Pa,
618000,s,86821,Pa,
767000,s,85057,Pa,
1030000,s,82803,Pa,
1380000,s,82411,Pa,
1980000,s,78197,Pa,
Bottom,Dirichlet,
1,1,1,1,1,1,21,
0,s,101227,Pa,
484,s,101227,Pa,
1080,s,101129,Pa,
1680,s,101031,Pa,
2880,s,100835,Pa,
4080,s,100737,Pa,
5280,s,100639,Pa,
7080,s,100443,Pa,
8880,s,100345,Pa,
13100,s,100149,Pa,
16700,s,100149,Pa,
19700,s,100149,Pa,
68900,s,99659,Pa,
99300,s,99659,Pa,
187000,s,99659,Pa,
427000,s,99561,Pa,
618000,s,99463,Pa,
767000,s,99365,Pa,
1030000,s,99365,Pa,
1380000,s,99267,Pa,
```

1980000,s,99267,Pa,

~Output Options Card
1,
1,1,31,
1,1,s,cm,6,6,6,
2,
aqueous moisture content,,
matric potential,cm,
2,
1,day,
5,day,
2,
aqueous moisture content,,
matric potential,cm,

~UCode Control Card
1,1,0.01,0.01,0,20,1.0,
..\bin\MRDRIVE,
1,
batch,
3,0,1,1,

~Observed Data Card
14,
field,aqueous moisture
content,,0.5,cm,0.5,cm,165.5,cm,1,0.01,0.8,0.95,
21,
0,s,0.218,,
484,s,0.213,,
1080,s,0.213,,
1680,s,0.204,,
2880,s,0.204,,
4080,s,0.205,,
5280,s,0.207,,
7080,s,0.204,,
8880,s,0.209,,
13100,s,0.201,,
16700,s,0.201,,
19700,s,0.205,,
68900,s,0.2,,
99300,s,0.196,,
187000,s,0.191,,
427000,s,0.174,,
618000,s,0.164,,
767000,s,0.159,,
1030000,s,0.151,,
1380000,s,0.143,,
1980000,s,0.136,,
field,aqueous moisture
content,,0.5,cm,0.5,cm,150.5,cm,1,0.01,0.8,0.95,
21,
0,s,0.191,,
484,s,0.183,,
1080,s,0.177,,
1680,s,0.173,,
2880,s,0.17,,
4080,s,0.161,,
5280,s,0.159,,
7080,s,0.161,,
8880,s,0.158,,
13100,s,0.16,,
16700,s,0.154,,
19700,s,0.154,,
68900,s,0.146,,
99300,s,0.147,,
187000,s,0.138,,
427000,s,0.128,,
618000,s,0.122,,
767000,s,0.118,,
1030000,s,0.114,,
1380000,s,0.112,,
1980000,s,0.108,,
field,aqueous moisture
content,,0.5,cm,0.5,cm,135.5,cm,1,0.01,0.8,0.95,
21,
0,s,0.146,,
484,s,0.144,,
1080,s,0.14,,
1680,s,0.133,,
2880,s,0.124,,
4080,s,0.118,,
5280,s,0.116,,
7080,s,0.109,,
8880,s,0.11,,
13100,s,0.105,,
16700,s,0.104,,
19700,s,0.101,,
68900,s,0.094,,
99300,s,0.095,,
187000,s,0.083,,
427000,s,0.074,,
618000,s,0.074,,
767000,s,0.07,,
1030000,s,0.068,,
1380000,s,0.068,,
1980000,s,0.065,,
field,aqueous moisture
content,,0.5,cm,0.5,cm,120.5,cm,1,0.01,0.8,0.95,
21,
0,s,0.132,,
484,s,0.129,,
1080,s,0.121,,
1680,s,0.116,,
2880,s,0.108,,
4080,s,0.105,,
5280,s,0.102,,
7080,s,0.094,,
8880,s,0.089,,
13100,s,0.089,,
16700,s,0.087,,
19700,s,0.087,,
68900,s,0.079,,
99300,s,0.076,,
187000,s,0.069,,
427000,s,0.061,,
618000,s,0.057,,
767000,s,0.057,,
1030000,s,0.054,,
1380000,s,0.055,,
1980000,s,0.052,,
field,aqueous moisture
content,,0.5,cm,0.5,cm,90.5,cm,1,0.01,0.8,0.95,
21,
0,s,0.132,,
484,s,0.131,,
1080,s,0.125,,
1680,s,0.122,,
2880,s,0.114,,
4080,s,0.112,,
5280,s,0.105,,
7080,s,0.099,,

8880,s,0.1,,
13100,s,0.091,,
16700,s,0.086,,
19700,s,0.083,,
68900,s,0.077,,
99300,s,0.073,,
187000,s,0.07,,
427000,s,0.066,,
618000,s,0.066,,
767000,s,0.061,,
1030000,s,0.061,,
1380000,s,0.059,,
1980000,s,0.055,,
field,aqueous moisture content,,0.5,cm,0.5,cm,60.5,cm,1,0.01,0.8,0.95,
21,
0,s,0.128,,
484,s,0.131,,
1080,s,0.126,,
1680,s,0.117,,
2880,s,0.121,,
4080,s,0.11,,
5280,s,0.106,,
7080,s,0.1,,
8880,s,0.094,,
13100,s,0.087,,
16700,s,0.085,,
19700,s,0.082,,
68900,s,0.072,,
99300,s,0.07,,
187000,s,0.067,,
427000,s,0.065,,
618000,s,0.06,,
767000,s,0.057,,
1030000,s,0.055,,
1380000,s,0.055,,
1980000,s,0.052,,
field,aqueous moisture content,,0.5,cm,0.5,cm,30.5,cm,1,0.01,0.8,0.95,
21,
0,s,0.13,,
484,s,0.128,,
1080,s,0.13,,
1680,s,0.124,,
2880,s,0.121,,
4080,s,0.115,,
5280,s,0.111,,
7080,s,0.103,,
8880,s,0.101,,
13100,s,0.091,,
16700,s,0.083,,
19700,s,0.086,,
68900,s,0.073,,
99300,s,0.07,,
187000,s,0.066,,
427000,s,0.06,,
618000,s,0.058,,
767000,s,0.057,,
1030000,s,0.054,,
1380000,s,0.052,,
1980000,s,0.048,,
field,aqueous moisture content,,0.5,cm,0.5,cm,0.5,cm,1,0.01,0.8,0.95,
21,
0,s,0.142,,
484,s,0.141,,
1080,s,0.143,,
1680,s,0.136,,
2880,s,0.132,,
4080,s,0.129,,
5280,s,0.123,,
7080,s,0.116,,
8880,s,0.112,,
13100,s,0.101,,
16700,s,0.096,,
19700,s,0.09,,
68900,s,0.074,,
99300,s,0.07,,
187000,s,0.066,,
427000,s,0.061,,
618000,s,0.059,,
767000,s,0.058,,
1030000,s,0.056,,
1380000,s,0.054,,
1980000,s,0.052,,
field,matric potential,cm,0.5,cm,0.5,cm,150.5,cm,1,4.0,0.8,0.8,
21,
0,s,-1,cm,
484,s,-6,cm,
1080,s,-11,cm,
1680,s,-17,cm,
2880,s,-24,cm,
4080,s,-28,cm,
5280,s,-32,cm,
7080,s,-33,cm,
8880,s,-33,cm,
13100,s,-38,cm,
16700,s,-39,cm,
19700,s,-39,cm,
68900,s,-50,cm,
99300,s,-54,cm,
187000,s,-70,cm,
427000,s,-108,cm,
618000,s,-129,cm,
767000,s,-150,cm,
1030000,s,-171,cm,
1380000,s,-174,cm,
1980000,s,-216,cm,
field,matric potential,cm,0.5,cm,0.5,cm,135.5,cm,1,4.0,0.8,0.8,
21,
0,s,-1,cm,
484,s,-3,cm,
1080,s,-5,cm,
1680,s,-6,cm,
2880,s,-11,cm,
4080,s,-16,cm,
5280,s,-20,cm,
7080,s,-20,cm,
8880,s,-20,cm,
13100,s,-24,cm,
16700,s,-26,cm,
19700,s,-26,cm,
68900,s,-31,cm,
99300,s,-34,cm,
187000,s,-51,cm,
427000,s,-79,cm,
618000,s,-100,cm,
767000,s,-106,cm,
1030000,s,-131,cm,
1380000,s,-106,cm,
1980000,s,-123,cm,
field,matric potential,cm,0.5,cm,0.5,cm,120.5,cm,1,4.0,0.8,0.8,

21,
0,s,-1,cm,
484,s,-2,cm,
1080,s,-4,cm,
1680,s,-5,cm,
2880,s,-8,cm,
4080,s,-11,cm,
5280,s,-13,cm,
7080,s,-14,cm,
8880,s,-14,cm,
13100,s,-16,cm,
16700,s,-16,cm,
19700,s,-16,cm,
68900,s,-22,cm,
99300,s,-23,cm,
187000,s,-35,cm,
427000,s,-47,cm,
618000,s,-57,cm,
767000,s,-58,cm,
1030000,s,-72,cm,
1380000,s,-85,cm,
1980000,s,-86,cm,
field,matric potential,cm,0.5,cm,0.5,cm,90.5,cm,1,4.0,0.8,0.8,
21,
0,s,-1,cm,
484,s,-1,cm,
1080,s,-1,cm,
1680,s,-2,cm,
2880,s,-3,cm,
4080,s,-5,cm,
5280,s,-6,cm,
7080,s,-8,cm,
8880,s,-10,cm,
13100,s,-14,cm,
16700,s,-16,cm,
19700,s,-16,cm,
68900,s,-20,cm,
99300,s,-20,cm,
187000,s,-21,cm,
427000,s,-21,cm,
618000,s,-24,cm,
767000,s,-24,cm,
1030000,s,-25,cm,
1380000,s,-19,cm,
1980000,s,-30,cm,
field,matric potential,cm,0.5,cm,0.5,cm,60.5,cm,1,4.0,0.8,0.8,
21,
0,s,-1,cm,
484,s,-1,cm,
1080,s,-2,cm,
1680,s,-3,cm,
2880,s,-5,cm,
4080,s,-7,cm,
5280,s,-9,cm,
7080,s,-10,cm,
8880,s,-11,cm,
13100,s,-14,cm,
16700,s,-16,cm,
19700,s,-16,cm,
68900,s,-20,cm,
99300,s,-20,cm,
187000,s,-23,cm,
427000,s,-24,cm,
618000,s,-26,cm,
767000,s,-27,cm,
1030000,s,-28,cm,
1380000,s,-31,cm,
1980000,s,-33,cm,
field,matric potential,cm,0.5,cm,0.5,cm,30.5,cm,1,4.0,0.8,0.8,
21,
0,s,-1,cm,
484,s,-1,cm,
1080,s,-2,cm,
1680,s,-3,cm,
2880,s,-5,cm,
4080,s,-6,cm,
5280,s,-7,cm,
7080,s,-8,cm,
8880,s,-9,cm,
13100,s,-12,cm,
16700,s,-14,cm,
19700,s,-14,cm,
68900,s,-17,cm,
99300,s,-17,cm,
187000,s,-18,cm,
427000,s,-18,cm,
618000,s,-19,cm,
767000,s,-19,cm,
1030000,s,-20,cm,
1380000,s,-22,cm,
1980000,s,-23,cm,

UCODE Template File: *input.tpl*

Only the first part is shown. The rest is the same as the corresponding parts in the input file.

```
~Simulation Title Card
1,
Scaling Method,
Zhang,
PNNL,
22 June 2001,
13:40,
2,
Rockhold et al.(1988)
Drainage in the Grass Site

~Solution Control Card
Normal w/ Scaling w/ Inverse,
Water,
1,
0,s,1980000,s,0.1,s,1800,s,1.25,8,1.e-06,
10000000,
0,

~Grid Card
uniform cartesian,
1,1,166,
1.,cm,
1.,cm,
1.,cm,

~Rock/Soil Zonation Card
4,
L1,1,1,1,1,158,166,R1,
L2,1,1,1,1,143,157,R1,
L3,1,1,1,1,128,142,R1,
L4,1,1,1,1,1,127,R1,

~Mechanical Properties Card
R1,,,!thetas,,,,,!,!thetas,,,,,!,,,Millington and Quirk,

~Hydraulic Properties Card
R1,!ks,,,,,,,,!,hc:m/s,!ks,,,,,,,,!,hc:m/s,!ks,,,,,,,,!,hc:m/s,

~Saturation Function Card
R1,van Genuchten,!alpha,,,,,!,1/cm,!n,,,,,!,!sr,,,,,!,,

~Aqueous Relative Permeability Card
R1,Mualem,,

~Scaling Card
Linear,Linear,Linear,Linear,Linear,
L1,1.0000,1.000,1.000,1.000,1.000,
L2,0.0429,0.754,0.933,1.003,0.681,
L3,0.0256,0.580,1.512,1.100,0.681,
L4,0.0105,0.553,1.561,1.667,1.301,

~Initial Conditions Card
Gas Pressure,Aqueous Pressure,
2,
Aqueous
Pressure,0.99561e+5,Pa,0.0,1/cm,0.0,1/cm,0.0,1/m,1,1,1,1,158,166
,
Aqueous
Pressure,1.01227e+5,Pa,0.0,1/cm,0.0,1/cm,0.0,1/m,1,1,1,1,1,157,
… (the rest parts are the same as those in the input file)
```

UCODE Prepare File: *out_uc1.pre*

```
#
F no
#INPUT FILES
<input.tpl
>input
# Search-String Start-Val Min Max Perturbation Format Log-Transform? Estimate?
/!ks,,,,,,,,!  5.0e-4    1.0e-7    1.0e-2    0.05  %10.3e 1 1
/!thetas,,,,,!           0.264     0.3       0.5       0.05  %5.3f 0 1
/!alpha,,,,,! 0.0841    0.01      0.3600    0.05  %6.4f 1 1
/!n,,,,,!      1.232     1.1       10.000    0.05  %7.4f 1 1
/!sr,,,,,!     0.163     0.000     0.40      0.01  %5.3f 0 1
END
```

UCODE Universal File: *out_uc1.uni*

```
#STOMP.UNI FILE FOR UCODE
#
3                 #phase
1                 #differencing (1=forward [recommended],
2=central)
 0.0100           #tol (0.01 recommended)
 0.0100           #tolerance sosr (0.0 [recommended])
0                 #nopt (0=no quasi-Newton updating, 1=quasi-
Newton updating)
20                #maximum number of iterations
 1.0000           #maximum fractional parameter change
..\bin\MRDRIVE    #path and name of inverse code
1                 #number of application models
batch             #application model execution commands
3                 #scale-sensitivities ( 0=no scaling,
1=dimensionless, 2=1%, and 3=both 1 and 2)
0                 #print intermediate ( 0=no printing, 1=print )
1                 #graph ( 0=no printing, 1=print )
1                 #number-residual-sets
#
# Observations
# Stat-Flag (0=variance, 1=standard deviation, 2=coefficient of
variation)
# Obs-Name Obs-Value   Stat.      Stat-Flag   Plot-Symbol
#
mcl000001   2.1800E-01  1.0000E-02  1     1
mcl000002   1.9100E-01  1.0000E-02  1     2
mcl000003   1.4600E-01  1.0000E-02  1     3
mcl000004   1.3200E-01  1.0000E-02  1     4
mcl000005   1.3200E-01  1.0000E-02  1     5
mcl000006   1.2800E-01  1.0000E-02  1     6
mcl000007   1.3000E-01  1.0000E-02  1     7
mcl000008   1.4200E-01  1.0000E-02  1     8
mph000009  -1.0000E+00  4.0000E+00  1     9
mph000010  -1.0000E+00  4.0000E+00  1    10
mph000011  -1.0000E+00  4.0000E+00  1    11
mph000012  -1.0000E+00  4.0000E+00  1    12
mph000013  -1.0000E+00  4.0000E+00  1    13
mph000014  -1.0000E+00  4.0000E+00  1    14
mcl000015   2.1300E-01  1.0000E-02  1     1
mcl000016   1.8300E-01  1.0000E-02  1     2
mcl000017   1.4400E-01  1.0000E-02  1     3
mcl000018   1.2900E-01  1.0000E-02  1     4
mcl000019   1.3100E-01  1.0000E-02  1     5
mcl000020   1.3100E-01  1.0000E-02  1     6
mcl000021   1.2800E-01  1.0000E-02  1     7
mcl000022   1.4100E-01  1.0000E-02  1     8
mph000023  -6.0000E+00  4.0000E+00  1     9
mph000024  -3.0000E+00  4.0000E+00  1    10
mph000025  -2.0000E+00  4.0000E+00  1    11
mph000026  -1.0000E+00  4.0000E+00  1    12
mph000027  -1.0000E+00  4.0000E+00  1    13
mph000028  -1.0000E+00  4.0000E+00  1    14
mcl000029   2.1300E-01  1.0000E-02  1     1
mcl000030   1.7700E-01  1.0000E-02  1     2
mcl000031   1.4000E-01  1.0000E-02  1     3
mcl000032   1.2100E-01  1.0000E-02  1     4
mcl000033   1.2500E-01  1.0000E-02  1     5
mcl000034   1.2600E-01  1.0000E-02  1     6
mcl000035   1.3000E-01  1.0000E-02  1     7
mcl000036   1.4300E-01  1.0000E-02  1     8
mph000037  -1.1000E+01  4.0000E+00  1     9
mph000038  -5.0000E+00  4.0000E+00  1    10
mph000039  -4.0000E+00  4.0000E+00  1    11
mph000040  -1.0000E+00  4.0000E+00  1    12
mph000041  -2.0000E+00  4.0000E+00  1    13
mph000042  -2.0000E+00  4.0000E+00  1    14
mcl000043   2.0400E-01  1.0000E-02  1     1
mcl000044   1.7300E-01  1.0000E-02  1     2
mcl000045   1.3300E-01  1.0000E-02  1     3
mcl000046   1.1600E-01  1.0000E-02  1     4
mcl000047   1.2200E-01  1.0000E-02  1     5
mcl000048   1.1700E-01  1.0000E-02  1     6
mcl000049   1.2400E-01  1.0000E-02  1     7
mcl000050   1.3600E-01  1.0000E-02  1     8
mph000051  -1.7000E+01  4.0000E+00  1     9
mph000052  -6.0000E+00  4.0000E+00  1    10
mph000053  -5.0000E+00  4.0000E+00  1    11
mph000054  -2.0000E+00  4.0000E+00  1    12
mph000055  -3.0000E+00  4.0000E+00  1    13
mph000056  -3.0000E+00  4.0000E+00  1    14
mcl000057   2.0400E-01  1.0000E-02  1     1
mcl000058   1.7000E-01  1.0000E-02  1     2
mcl000059   1.2400E-01  1.0000E-02  1     3
mcl000060   1.0800E-01  1.0000E-02  1     4
mcl000061   1.1400E-01  1.0000E-02  1     5
mcl000062   1.2100E-01  1.0000E-02  1     6
mcl000063   1.2100E-01  1.0000E-02  1     7
mcl000064   1.3200E-01  1.0000E-02  1     8
mph000065  -2.4000E+01  4.0000E+00  1     9
mph000066  -1.1000E+01  4.0000E+00  1    10
mph000067  -8.0000E+00  4.0000E+00  1    11
mph000068  -3.0000E+00  4.0000E+00  1    12
mph000069  -5.0000E+00  4.0000E+00  1    13
mph000070  -5.0000E+00  4.0000E+00  1    14
mcl000071   2.0500E-01  1.0000E-02  1     1
mcl000072   1.6100E-01  1.0000E-02  1     2
mcl000073   1.1800E-01  1.0000E-02  1     3
mcl000074   1.0500E-01  1.0000E-02  1     4
mcl000075   1.1200E-01  1.0000E-02  1     5
mcl000076   1.1000E-01  1.0000E-02  1     6
mcl000077   1.1500E-01  1.0000E-02  1     7
mcl000078   1.2900E-01  1.0000E-02  1     8
mph000079  -2.8000E+01  4.0000E+00  1     9
mph000080  -1.6000E+01  4.0000E+00  1    10
mph000081  -1.1000E+01  4.0000E+00  1    11
mph000082  -5.0000E+00  4.0000E+00  1    12
mph000083  -7.0000E+00  4.0000E+00  1    13
mph000084  -6.0000E+00  4.0000E+00  1    14
mcl000085   2.0700E-01  1.0000E-02  1     1
mcl000086   1.5900E-01  1.0000E-02  1     2
mcl000087   1.1600E-01  1.0000E-02  1     3
mcl000088   1.0200E-01  1.0000E-02  1     4
mcl000089   1.0500E-01  1.0000E-02  1     5
mcl000090   1.0600E-01  1.0000E-02  1     6
mcl000091   1.1100E-01  1.0000E-02  1     7
mcl000092   1.2300E-01  1.0000E-02  1     8
mph000093  -3.2000E+01  4.0000E+00  1     9
mph000094  -2.0000E+01  4.0000E+00  1    10
mph000095  -1.3000E+01  4.0000E+00  1    11
mph000096  -6.0000E+00  4.0000E+00  1    12
mph000097  -9.0000E+00  4.0000E+00  1    13
```

mph000098	-7.0000E+00	4.0000E+00	1	14
mcl000099	2.0400E-01	1.0000E-02	1	1
mcl000100	1.6100E-01	1.0000E-02	1	2
mcl000101	1.0900E-01	1.0000E-02	1	3
mcl000102	9.4000E-02	1.0000E-02	1	4
mcl000103	9.9000E-02	1.0000E-02	1	5
mcl000104	1.0000E-01	1.0000E-02	1	6
mcl000105	1.0300E-01	1.0000E-02	1	7
mcl000106	1.1600E-01	1.0000E-02	1	8
mph000107	-3.3000E+01	4.0000E+00	1	9
mph000108	-2.0000E+01	4.0000E+00	1	10
mph000109	-1.4000E+01	4.0000E+00	1	11
mph000110	-8.0000E+00	4.0000E+00	1	12
mph000111	-1.0000E+01	4.0000E+00	1	13
mph000112	-8.0000E+00	4.0000E+00	1	14
mcl000113	2.0900E-01	1.0000E-02	1	1
mcl000114	1.5800E-01	1.0000E-02	1	2
mcl000115	1.1000E-01	1.0000E-02	1	3
mcl000116	8.9000E-02	1.0000E-02	1	4
mcl000117	1.0000E-01	1.0000E-02	1	5
mcl000118	9.4000E-02	1.0000E-02	1	6
mcl000119	1.0100E-01	1.0000E-02	1	7
mcl000120	1.1200E-01	1.0000E-02	1	8
mph000121	-3.3000E+01	4.0000E+00	1	9
mph000122	-2.0000E+01	4.0000E+00	1	10
mph000123	-1.4000E+01	4.0000E+00	1	11
mph000124	-1.0000E+01	4.0000E+00	1	12
mph000125	-1.1000E+01	4.0000E+00	1	13
mph000126	-9.0000E+00	4.0000E+00	1	14
mcl000127	2.0100E-01	1.0000E-02	1	1
mcl000128	1.6000E-01	1.0000E-02	1	2
mcl000129	1.0500E-01	1.0000E-02	1	3
mcl000130	8.9000E-02	1.0000E-02	1	4
mcl000131	9.1000E-02	1.0000E-02	1	5
mcl000132	8.7000E-02	1.0000E-02	1	6
mcl000133	9.1000E-02	1.0000E-02	1	7
mcl000134	1.0100E-01	1.0000E-02	1	8
mph000135	-3.8000E+01	4.0000E+00	1	9
mph000136	-2.4000E+01	4.0000E+00	1	10
mph000137	-1.6000E+01	4.0000E+00	1	11
mph000138	-1.4000E+01	4.0000E+00	1	12
mph000139	-1.4000E+01	4.0000E+00	1	13
mph000140	-1.2000E+01	4.0000E+00	1	14
mcl000141	2.0100E-01	1.0000E-02	1	1
mcl000142	1.5400E-01	1.0000E-02	1	2
mcl000143	1.0400E-01	1.0000E-02	1	3
mcl000144	8.7000E-02	1.0000E-02	1	4
mcl000145	8.6000E-02	1.0000E-02	1	5
mcl000146	8.5000E-02	1.0000E-02	1	6
mcl000147	8.3000E-02	1.0000E-02	1	7
mcl000148	9.6000E-02	1.0000E-02	1	8
mph000149	-3.9000E+01	4.0000E+00	1	9
mph000150	-2.6000E+01	4.0000E+00	1	10
mph000151	-1.6000E+01	4.0000E+00	1	11
mph000152	-1.6000E+01	4.0000E+00	1	12
mph000153	-1.6000E+01	4.0000E+00	1	13
mph000154	-1.4000E+01	4.0000E+00	1	14
mcl000155	2.0500E-01	1.0000E-02	1	1
mcl000156	1.5400E-01	1.0000E-02	1	2
mcl000157	1.0100E-01	1.0000E-02	1	3
mcl000158	8.7000E-02	1.0000E-02	1	4
mcl000159	8.3000E-02	1.0000E-02	1	5
mcl000160	8.2000E-02	1.0000E-02	1	6
mcl000161	8.6000E-02	1.0000E-02	1	7
mcl000162	9.0000E-02	1.0000E-02	1	8
mph000163	-3.9000E+01	4.0000E+00	1	9
mph000164	-2.6000E+01	4.0000E+00	1	10
mph000165	-1.6000E+01	4.0000E+00	1	11
mph000166	-1.6000E+01	4.0000E+00	1	12
mph000167	-1.6000E+01	4.0000E+00	1	13
mph000168	-1.4000E+01	4.0000E+00	1	14
mcl000169	2.0000E-01	1.0000E-02	1	1
mcl000170	1.4600E-01	1.0000E-02	1	2
mcl000171	9.4000E-02	1.0000E-02	1	3
mcl000172	7.9000E-02	1.0000E-02	1	4
mcl000173	7.7000E-02	1.0000E-02	1	5
mcl000174	7.2000E-02	1.0000E-02	1	6
mcl000175	7.3000E-02	1.0000E-02	1	7
mcl000176	7.4000E-02	1.0000E-02	1	8
mph000177	-5.0000E+01	4.0000E+00	1	9
mph000178	-3.1000E+01	4.0000E+00	1	10
mph000179	-2.2000E+01	4.0000E+00	1	11
mph000180	-2.0000E+01	4.0000E+00	1	12
mph000181	-2.0000E+01	4.0000E+00	1	13
mph000182	-1.7000E+01	4.0000E+00	1	14
mcl000183	1.9600E-01	1.0000E-02	1	1
mcl000184	1.4700E-01	1.0000E-02	1	2
mcl000185	9.5000E-02	1.0000E-02	1	3
mcl000186	7.6000E-02	1.0000E-02	1	4
mcl000187	7.3000E-02	1.0000E-02	1	5
mcl000188	7.0000E-02	1.0000E-02	1	6
mcl000189	7.0000E-02	1.0000E-02	1	7
mcl000190	7.0000E-02	1.0000E-02	1	8
mph000191	-5.4000E+01	4.0000E+00	1	9
mph000192	-3.4000E+01	4.0000E+00	1	10
mph000193	-2.3000E+01	4.0000E+00	1	11
mph000194	-2.0000E+01	4.0000E+00	1	12
mph000195	-2.0000E+01	4.0000E+00	1	13
mph000196	-1.7000E+01	4.0000E+00	1	14
mcl000197	1.9100E-01	1.0000E-02	1	1
mcl000198	1.3800E-01	1.0000E-02	1	2
mcl000199	8.3000E-02	1.0000E-02	1	3
mcl000200	6.9000E-02	1.0000E-02	1	4
mcl000201	7.0000E-02	1.0000E-02	1	5
mcl000202	6.7000E-02	1.0000E-02	1	6
mcl000203	6.6000E-02	1.0000E-02	1	7
mcl000204	6.6000E-02	1.0000E-02	1	8
mph000205	-7.0000E+01	4.0000E+00	1	9
mph000206	-5.1000E+01	4.0000E+00	1	10
mph000207	-3.5000E+01	4.0000E+00	1	11
mph000208	-2.1000E+01	4.0000E+00	1	12
mph000209	-2.3000E+01	4.0000E+00	1	13
mph000210	-1.8000E+01	4.0000E+00	1	14
mcl000211	1.7400E-01	1.0000E-02	1	1
mcl000212	1.2800E-01	1.0000E-02	1	2
mcl000213	7.4000E-02	1.0000E-02	1	3
mcl000214	6.1000E-02	1.0000E-02	1	4
mcl000215	6.6000E-02	1.0000E-02	1	5
mcl000216	6.5000E-02	1.0000E-02	1	6
mcl000217	6.0000E-02	1.0000E-02	1	7
mcl000218	6.1000E-02	1.0000E-02	1	8
mph000219	-1.0800E+02	4.0000E+00	1	9
mph000220	-7.9000E+01	4.0000E+00	1	10
mph000221	-4.7000E+01	4.0000E+00	1	11
mph000222	-2.1000E+01	4.0000E+00	1	12
mph000223	-2.4000E+01	4.0000E+00	1	13
mph000224	-1.8000E+01	4.0000E+00	1	14
mcl000225	1.6400E-01	1.0000E-02	1	1
mcl000226	1.2200E-01	1.0000E-02	1	2
mcl000227	7.4000E-02	1.0000E-02	1	3
mcl000228	5.7000E-02	1.0000E-02	1	4
mcl000229	6.6000E-02	1.0000E-02	1	5

mcl000230	6.0000E-02	1.0000E-02	1	6
mcl000231	5.8000E-02	1.0000E-02	1	7
mcl000232	5.9000E-02	1.0000E-02	1	8
mph000233	-1.2900E+02	4.0000E+00	1	9
mph000234	-1.0000E+02	4.0000E+00	1	10
mph000235	-5.7000E+01	4.0000E+00	1	11
mph000236	-2.4000E+01	4.0000E+00	1	12
mph000237	-2.6000E+01	4.0000E+00	1	13
mph000238	-1.9000E+01	4.0000E+00	1	14
mcl000239	1.5900E-01	1.0000E-02	1	1
mcl000240	1.1800E-01	1.0000E-02	1	2
mcl000241	7.0000E-02	1.0000E-02	1	3
mcl000242	5.7000E-02	1.0000E-02	1	4
mcl000243	6.1000E-02	1.0000E-02	1	5
mcl000244	5.7000E-02	1.0000E-02	1	6
mcl000245	5.7000E-02	1.0000E-02	1	7
mcl000246	5.8000E-02	1.0000E-02	1	8
mph000247	-1.5000E+02	4.0000E+00	1	9
mph000248	-1.0600E+02	4.0000E+00	1	10
mph000249	-5.8000E+01	4.0000E+00	1	11
mph000250	-2.4000E+01	4.0000E+00	1	12
mph000251	-2.7000E+01	4.0000E+00	1	13
mph000252	-1.9000E+01	4.0000E+00	1	14
mcl000253	1.5100E-01	1.0000E-02	1	1
mcl000254	1.1400E-01	1.0000E-02	1	2
mcl000255	6.8000E-02	1.0000E-02	1	3
mcl000256	5.4000E-02	1.0000E-02	1	4
mcl000257	6.1000E-02	1.0000E-02	1	5
mcl000258	5.5000E-02	1.0000E-02	1	6
mcl000259	5.4000E-02	1.0000E-02	1	7
mcl000260	5.6000E-02	1.0000E-02	1	8
mph000261	-1.7100E+02	4.0000E+00	1	9
mph000262	-1.3100E+02	4.0000E+00	1	10
mph000263	-7.2000E+01	4.0000E+00	1	11
mph000264	-2.5000E+01	4.0000E+00	1	12
mph000265	-2.8000E+01	4.0000E+00	1	13
mph000266	-2.0000E+01	4.0000E+00	1	14
mcl000267	1.4300E-01	1.0000E-02	1	1
mcl000268	1.1200E-01	1.0000E-02	1	2
mcl000269	6.8000E-02	1.0000E-02	1	3
mcl000270	5.5000E-02	1.0000E-02	1	4
mcl000271	5.9000E-02	1.0000E-02	1	5
mcl000272	5.5000E-02	1.0000E-02	1	6
mcl000273	5.2000E-02	1.0000E-02	1	7
mcl000274	5.4000E-02	1.0000E-02	1	8
mph000275	-1.7400E+02	4.0000E+00	1	9
mph000276	-1.0600E+02	4.0000E+00	1	10
mph000277	-8.5000E+01	4.0000E+00	1	11
mph000278	-1.9000E+01	4.0000E+00	1	12
mph000279	-3.1000E+01	4.0000E+00	1	13
mph000280	-2.2000E+01	4.0000E+00	1	14
mcl000281	1.3600E-01	1.0000E-02	1	1
mcl000282	1.0800E-01	1.0000E-02	1	2
mcl000283	6.5000E-02	1.0000E-02	1	3
mcl000284	5.2000E-02	1.0000E-02	1	4
mcl000285	5.5000E-02	1.0000E-02	1	5
mcl000286	5.2000E-02	1.0000E-02	1	6
mcl000287	4.8000E-02	1.0000E-02	1	7
mcl000288	5.2000E-02	1.0000E-02	1	8
mph000289	-2.1600E+02	4.0000E+00	1	9
mph000290	-1.2300E+02	4.0000E+00	1	10
mph000291	-8.6000E+01	4.0000E+00	1	11
mph000292	-3.0000E+01	4.0000E+00	1	12
mph000293	-3.3000E+01	4.0000E+00	1	13
mph000294	-2.3000E+01	4.0000E+00	1	14

END

UCODE Extract File: *out_uc1.ext*

<out_uc1.sto
#
o mcl000001
/mcl000001/
C12_23
#
o mcl000002
/mcl000002/
C12_23
#
o mcl000003
/mcl000003/
C12_23
#
o mcl000004
/mcl000004/
C12_23
#
o mcl000005
/mcl000005/
C12_23
#
o mcl000006
/mcl000006/
C12_23
#
o mcl000007
/mcl000007/
C12_23
#
o mcl000008
/mcl000008/
C12_23
#
o mph000009
/mph000009/
C12_23
#
o mph000010
/mph000010/
C12_23
#
o mph000011
/mph000011/
C12_23
#
o mph000012
/mph000012/
C12_23
#
o mph000013
/mph000013/
C12_23
#
o mph000014
/mph000014/
C12_23
#
o mcl000015
/mcl000015/
C12_23
#
o mcl000016
/mcl000016/
C12_23
#
o mcl000017
/mcl000017/
C12_23
#
o mcl000018
/mcl000018/
C12_23
#
o mcl000019
/mcl000019/
C12_23
#
o mcl000020
/mcl000020/
C12_23
#
o mcl000021
/mcl000021/
C12_23
#
o mcl000022
/mcl000022/
C12_23
#
o mph000023
/mph000023/
C12_23
#
o mph000024
/mph000024/
C12_23
#
o mph000025
/mph000025/
C12_23
#
o mph000026
/mph000026/
C12_23
#
o mph000027
/mph000027/
C12_23
#
o mph000028
/mph000028/
C12_23
#
o mcl000029
/mcl000029/
C12_23
#
o mcl000030
/mcl000030/
C12_23
#
o mcl000031
/mcl000031/
C12_23
#
o mcl000032
/mcl000032/
C12_23
#
o mcl000033
/mcl000033/
C12_23
#
o mcl000034
/mcl000034/
C12_23
#
o mcl000035
/mcl000035/
C12_23
#
o mcl000036
/mcl000036/
C12_23
#
o mph000037
/mph000037/
C12_23
#
o mph000038
/mph000038/
C12_23
#
o mph000039
/mph000039/
C12_23
#
o mph000040
/mph000040/
C12_23
#
o mph000041
/mph000041/
C12_23
#
o mph000042
/mph000042/
C12_23
#
o mcl000043
/mcl000043/
C12_23
#
o mcl000044
/mcl000044/
C12_23
#
o mcl000045
/mcl000045/
C12_23
#
o mcl000046
/mcl000046/
C12_23
#
o mcl000047
/mcl000047/
C12_23
#
o mcl000048
/mcl000048/
C12_23
#
o mcl000049
/mcl000049/
C12_23
#
o mcl000050
/mcl000050/
C12_23
#
o mph000051
/mph000051/
C12_23
#
o mph000052
/mph000052/
C12_23
#
o mph000053
/mph000053/
C12_23
#
o mph000054
/mph000054/
C12_23
#
o mph000055
/mph000055/
C12_23
#
o mph000056
/mph000056/
C12_23
#
o mcl000057
/mcl000057/
C12_23
#
o mcl000058
/mcl000058/
C12_23
#
o mcl000059
/mcl000059/
C12_23
#
o mcl000060
/mcl000060/
C12_23
#
o mcl000061
/mcl000061/

C12_23
#
o mcl000062
/mcl000062/
C12_23
#
o mcl000063
/mcl000063/
C12_23
#
o mcl000064
/mcl000064/
C12_23
#
o mph000065
/mph000065/
C12_23
#
o mph000066
/mph000066/
C12_23
#
o mph000067
/mph000067/
C12_23
#
o mph000068
/mph000068/
C12_23
#
o mph000069
/mph000069/
C12_23
#
o mph000070
/mph000070/
C12_23
#
o mcl000071
/mcl000071/
C12_23
#
o mcl000072
/mcl000072/
C12_23
#
o mcl000073
/mcl000073/
C12_23
#
o mcl000074
/mcl000074/
C12_23
#
o mcl000075
/mcl000075/
C12_23
#
o mcl000076
/mcl000076/
C12_23
#
o mcl000077
/mcl000077/
C12_23
#
o mcl000078
/mcl000078/
C12_23
#
o mph000079
/mph000079/
C12_23
#
o mph000080
/mph000080/
C12_23
#
o mph000081
/mph000081/
C12_23
#
o mph000082
/mph000082/
C12_23
#
o mph000083
/mph000083/
C12_23
#
o mph000084
/mph000084/
C12_23
#
o mcl000085
/mcl000085/
C12_23
#
o mcl000086
/mcl000086/
C12_23
#
o mcl000087
/mcl000087/
C12_23
#
o mcl000088
/mcl000088/
C12_23
#
o mcl000089
/mcl000089/
C12_23
#
o mcl000090
/mcl000090/
C12_23
#
o mcl000091
/mcl000091/
C12_23
#
o mcl000092
/mcl000092/
C12_23
#
o mph000093
/mph000093/
C12_23
#
o mph000094
/mph000094/
C12_23
#
o mph000095
/mph000095/
C12_23
#
o mph000096
/mph000096/
C12_23
#
o mph000097
/mph000097/
C12_23
#
o mph000098
/mph000098/
C12_23
#
o mcl000099
/mcl000099/
C12_23
#
o mcl000100
/mcl000100/
C12_23
#
o mcl000101
/mcl000101/
C12_23
#
o mcl000102
/mcl000102/
C12_23
#
o mcl000103
/mcl000103/
C12_23
#
o mcl000104
/mcl000104/
C12_23
#
o mcl000105
/mcl000105/
C12_23
#
o mcl000106
/mcl000106/
C12_23
#
o mph000107
/mph000107/
C12_23
#
o mph000108
/mph000108/
C12_23
#
o mph000109
/mph000109/
C12_23
#
o mph000110
/mph000110/
C12_23
#
o mph000111
/mph000111/
C12_23
#
o mph000112
/mph000112/
C12_23
#
o mcl000113
/mcl000113/
C12_23
#
o mcl000114
/mcl000114/
C12_23
#
o mcl000115
/mcl000115/
C12_23
#
o mcl000116
/mcl000116/
C12_23
#
o mcl000117
/mcl000117/
C12_23
#
o mcl000118
/mcl000118/
C12_23
#
o mcl000119
/mcl000119/
C12_23
#
o mcl000120
/mcl000120/
C12_23
#
o mph000121
/mph000121/
C12_23
#
o mph000122
/mph000122/
C12_23
#
o mph000123
/mph000123/
C12_23
#
o mph000124
/mph000124/
C12_23
#
o mph000125
/mph000125/
C12_23
#
o mph000126
/mph000126/
C12_23
#
o mcl000127
/mcl000127/

C12_23
#
o mcl000128
/mcl000128/
C12_23
#
o mcl000129
/mcl000129/
C12_23
#
o mcl000130
/mcl000130/
C12_23
#
o mcl000131
/mcl000131/
C12_23
#
o mcl000132
/mcl000132/
C12_23
#
o mcl000133
/mcl000133/
C12_23
#
o mcl000134
/mcl000134/
C12_23
#
o mph000135
/mph000135/
C12_23
#
o mph000136
/mph000136/
C12_23
#
o mph000137
/mph000137/
C12_23
#
o mph000138
/mph000138/
C12_23
#
o mph000139
/mph000139/
C12_23
#
o mph000140
/mph000140/
C12_23
#
o mcl000141
/mcl000141/
C12_23
#
o mcl000142
/mcl000142/
C12_23
#
o mcl000143
/mcl000143/
C12_23
#
o mcl000144
/mcl000144/
C12_23
#
o mcl000145
/mcl000145/
C12_23
#
o mcl000146
/mcl000146/
C12_23
#
o mcl000147
/mcl000147/
C12_23
#
o mcl000148
/mcl000148/
C12_23
#
o mph000149
/mph000149/
C12_23
#
o mph000150
/mph000150/
C12_23
#
o mph000151
/mph000151/
C12_23
#
o mph000152
/mph000152/
C12_23
#
o mph000153
/mph000153/
C12_23
#
o mph000154
/mph000154/
C12_23
#
o mcl000155
/mcl000155/
C12_23
#
o mcl000156
/mcl000156/
C12_23
#
o mcl000157
/mcl000157/
C12_23
#
o mcl000158
/mcl000158/
C12_23
#
o mcl000159
/mcl000159/
C12_23
#
o mcl000160
/mcl000160/
C12_23
#
o mcl000161
/mcl000161/
C12_23
#
o mcl000162
/mcl000162/
C12_23
#
o mph000163
/mph000163/
C12_23
#
o mph000164
/mph000164/
C12_23
#
o mph000165
/mph000165/
C12_23
#
o mph000166
/mph000166/
C12_23
#
o mph000167
/mph000167/
C12_23
#
o mph000168
/mph000168/
C12_23
#
o mcl000169
/mcl000169/
C12_23
#
o mcl000170
/mcl000170/
C12_23
#
o mcl000171
/mcl000171/
C12_23
#
o mcl000172
/mcl000172/
C12_23
#
o mcl000173
/mcl000173/
C12_23
#
o mcl000174
/mcl000174/
C12_23
#
o mcl000175
/mcl000175/
C12_23
#
o mcl000176
/mcl000176/
C12_23
#
o mph000177
/mph000177/
C12_23
#
o mph000178
/mph000178/
C12_23
#
o mph000179
/mph000179/
C12_23
#
o mph000180
/mph000180/
C12_23
#
o mph000181
/mph000181/
C12_23
#
o mph000182
/mph000182/
C12_23
#
o mcl000183
/mcl000183/
C12_23
#
o mcl000184
/mcl000184/
C12_23
#
o mcl000185
/mcl000185/
C12_23
#
o mcl000186
/mcl000186/
C12_23
#
o mcl000187
/mcl000187/
C12_23
#
o mcl000188
/mcl000188/
C12_23
#
o mcl000189
/mcl000189/
C12_23
#
o mcl000190
/mcl000190/
C12_23
#
o mph000191
/mph000191/
C12_23
#
o mph000192
/mph000192/
C12_23
#
o mph000193
/mph000193/

C12_23
#
o mph000194
/mph000194/
C12_23
#
o mph000195
/mph000195/
C12_23
#
o mph000196
/mph000196/
C12_23
#
o mcl000197
/mcl000197/
C12_23
#
o mcl000198
/mcl000198/
C12_23
#
o mcl000199
/mcl000199/
C12_23
#
o mcl000200
/mcl000200/
C12_23
#
o mcl000201
/mcl000201/
C12_23
#
o mcl000202
/mcl000202/
C12_23
#
o mcl000203
/mcl000203/
C12_23
#
o mcl000204
/mcl000204/
C12_23
#
o mph000205
/mph000205/
C12_23
#
o mph000206
/mph000206/
C12_23
#
o mph000207
/mph000207/
C12_23
#
o mph000208
/mph000208/
C12_23
#
o mph000209
/mph000209/
C12_23
#
o mph000210
/mph000210/
C12_23
#
o mcl000211
/mcl000211/
C12_23
#
o mcl000212
/mcl000212/
C12_23
#
o mcl000213
/mcl000213/
C12_23
#
o mcl000214
/mcl000214/
C12_23
#
o mcl000215
/mcl000215/
C12_23
#
o mcl000216
/mcl000216/
C12_23
#
o mcl000217
/mcl000217/
C12_23
#
o mcl000218
/mcl000218/
C12_23
#
o mph000219
/mph000219/
C12_23
#
o mph000220
/mph000220/
C12_23
#
o mph000221
/mph000221/
C12_23
#
o mph000222
/mph000222/
C12_23
#
o mph000223
/mph000223/
C12_23
#
o mph000224
/mph000224/
C12_23
#
o mcl000225
/mcl000225/
C12_23
#
o mcl000226
/mcl000226/
C12_23
#
o mcl000227
/mcl000227/
C12_23
#
o mcl000228
/mcl000228/
C12_23
#
o mcl000229
/mcl000229/
C12_23
#
o mcl000230
/mcl000230/
C12_23
#
o mcl000231
/mcl000231/
C12_23
#
o mcl000232
/mcl000232/
C12_23
#
o mph000233
/mph000233/
C12_23
#
o mph000234
/mph000234/
C12_23
#
o mph000235
/mph000235/
C12_23
#
o mph000236
/mph000236/
C12_23
#
o mph000237
/mph000237/
C12_23
#
o mph000238
/mph000238/
C12_23
#
o mcl000239
/mcl000239/
C12_23
#
o mcl000240
/mcl000240/
C12_23
#
o mcl000241
/mcl000241/
C12_23
#
o mcl000242
/mcl000242/
C12_23
#
o mcl000243
/mcl000243/
C12_23
#
o mcl000244
/mcl000244/
C12_23
#
o mcl000245
/mcl000245/
C12_23
#
o mcl000246
/mcl000246/
C12_23
#
o mph000247
/mph000247/
C12_23
#
o mph000248
/mph000248/
C12_23
#
o mph000249
/mph000249/
C12_23
#
o mph000250
/mph000250/
C12_23
#
o mph000251
/mph000251/
C12_23
#
o mph000252
/mph000252/
C12_23
#
o mcl000253
/mcl000253/
C12_23
#
o mcl000254
/mcl000254/
C12_23
#
o mcl000255
/mcl000255/
C12_23
#
o mcl000256
/mcl000256/
C12_23
#
o mcl000257
/mcl000257/
C12_23
#
o mcl000258
/mcl000258/
C12_23
#
o mcl000259
/mcl000259/

C12_23
#
o mcl000260
/mcl000260/
C12_23
#
o mph000261
/mph000261/
C12_23
#
o mph000262
/mph000262/
C12_23
#
o mph000263
/mph000263/
C12_23
#
o mph000264
/mph000264/
C12_23
#
o mph000265
/mph000265/
C12_23
#
o mph000266
/mph000266/
C12_23
#
o mcl000267
/mcl000267/
C12_23
#
o mcl000268
/mcl000268/
C12_23
#
o mcl000269
/mcl000269/
C12_23
#
o mcl000270
/mcl000270/
C12_23
#
o mcl000271
/mcl000271/
C12_23
#
o mcl000272
/mcl000272/
C12_23
#
o mcl000273
/mcl000273/
C12_23
#
o mcl000274
/mcl000274/
C12_23
#
o mph000275
/mph000275/
C12_23
#
o mph000276
/mph000276/
C12_23
#
o mph000277
/mph000277/
C12_23
#
o mph000278
/mph000278/
C12_23
#
o mph000279
/mph000279/
C12_23
#
o mph000280
/mph000280/
C12_23
#
o mcl000281
/mcl000281/
C12_23
#
o mcl000282
/mcl000282/
C12_23
#
o mcl000283
/mcl000283/
C12_23
#
o mcl000284
/mcl000284/
C12_23
#
o mcl000285
/mcl000285/
C12_23
#
o mcl000286
/mcl000286/
C12_23
#
o mcl000287
/mcl000287/
C12_23
#
o mcl000288
/mcl000288/
C12_23
#
o mph000289
/mph000289/
C12_23
#
o mph000290
/mph000290/
C12_23
#
o mph000291
/mph000291/
C12_23
#
o mph000292
/mph000292/
C12_23
#
o mph000293
/mph000293/
C12_23
#
o mph000294
/mph000294/
C12_23
#
END

Case 2 Andelfingen Site

STOMP Input File: *input*

```
~Simulation Title Card
1,
Scaling Factor Test,
Zhang,
PNNL,
July 13, 2001,
14:39,
2,
Abbaspour (2000):Irrigation and Drainage Phase - Scaling method
Reference to L1,

~Solution Control Card
Normal w/ Scaling w/ Inverse,
Water,
1,
0,day,51,day,0.001,day,0.1,day,1.25,8,1.e-06,
10000,
0,

~Grid Card
uniform cartesian,
1,1,76,
1.,cm,
1.,cm,
1.,cm,

~Rock/Soil Zonation Card
4,
L1,1,1,1,1,68,76,R1,
L2,1,1,1,1,46,67,R1,
L3,1,1,1,1,6,45,R1,
L4,1,1,1,1,1,5,R1,

~Mechanical Properties Card
R1,,,0.3622,0.3622,,,Millington and Quirk,

~Hydraulic Properties Card
R1,3.586e-008,hc:m/s,3.586e-008,hc:m/s,3.586e-008,hc:m/s,

~Saturation Function Card
R1,van Genuchten,2.526e-003,1/cm,1.425e+000,0.2490,,

~Aqueous Relative Permeability Card
R1,Mualem,,

~Scaling Card
Linear,Linear,Linear,Linear,Linear,
L1,1,1,1,1,1,
L2,10.053,0.789,4.073,1.078,0.845,
L3,587.9,1.115,17.28,1.198,0,
L4,11.87,1.053,1.914,1.028,0.919,

~Initial Conditions Card
Gas Pressure,Aqueous Pressure,
3,
Aqueous Pressure,8.71444e+4,Pa,0.0,1/cm,0.0,1/cm,-
231.5,1/cm,1,1,1,1,56,76,
Aqueous Pressure,8.94572e+4,Pa,0.0,1/cm,0.0,1/cm,-
92.5,1/cm,1,1,1,1,31,55,
Aqueous
Pressure,8.94572e+4,Pa,0.0,1/cm,0.0,1/cm,0.0,1/m,1,1,1,1,1,30,

~Boundary Conditions Card
2,
top,Dirichlet,
1,1,1,1,76,76,31,
0.0,day,82509,Pa,
1.2,day,99388,Pa,
2.1,day,101463,Pa,
2.9,day,101187,Pa,
4.1,day,101187,Pa,
5.3,day,101187,Pa,
6.1,day,101187,Pa,
6.2,day,100218,Pa,
7.0,day,101463,Pa,
10.2,day,100633,Pa,
10.9,day,101463,Pa,
11.9,day,101463,Pa,
14.0,day,100910,Pa,
15.1,day,100910,Pa,
16.0,day,101325,Pa,
19.1,day,101325,Pa,
19.8,day,101187,Pa,
20.9,day,101048,Pa,
22.1,day,101048,Pa,
22.9,day,101187,Pa,
25.7,day,100772,Pa,
26.9,day,100495,Pa,
28.1,day,97174,Pa,
29.1,day,95929,Pa,
30.0,day,94131,Pa,
31.9,day,93577,Pa,
36.3,day,90395,Pa,
42.0,day,80157,Pa,
45.2,day,71579,Pa,
46.8,day,65077,Pa,
51.0,day,43217,Pa,
Bottom,Dirichlet,
1,1,1,1,1,1,31,
0.0,day,93233,Pa,
1.2,day,91979,Pa,
2.1,day,91530,Pa,
2.9,day,92020,Pa,
4.1,day,92643,Pa,
5.3,day,93446,Pa,
6.1,day,93309,Pa,
6.2,day,92683,Pa,
7,day,93128,Pa,
10.2,day,93882,Pa,
10.9,day,94192,Pa,
11.9,day,94369,Pa,
14,day,93336,Pa,
15.1,day,93334,Pa,
16,day,92885,Pa,
19.1,day,91760,Pa,
19.8,day,91848,Pa,
20.9,day,92516,Pa,
22.1,day,91888,Pa,
22.9,day,92467,Pa,
25.7,day,91253,Pa,
26.9,day,91206,Pa,
28.1,day,89773,Pa,
```

29.1,day,89771,Pa,
30,day,89634,Pa,
31.9,day,90256,Pa,
36.3,day,88056,Pa,
42,day,87864,Pa,
45.2,day,87455,Pa,
46.8,day,87049,Pa,
51,day,85116,Pa,

~Output Options Card
3,
1,1,1,
1,1,31,
1,1,56,
1,1,day,cm,6,6,6,
2,
aqueous moisture content,,
matric potential,cm,
2,
1,day,
27,day,
2,
aqueous moisture content,,
matric potential,cm,
~UCode Control Card
1,1,0.01,0.01,0,20,1.0,
..\bin\MRDRIVE,
1,
batch,
3,0,1,1,

~Observed Data Card
6,
field,aqueous moisture
content,,0.5,cm,0.5,cm,0.5,cm,1,0.01,0.8,0.95,
31,
0.1,day,0.352,,
1.2,day,0.353,,
2.1,day,0.351,,
2.9,day,0.348,,
4.1,day,0.354,,
5.3,day,0.354,,
6.1,day,0.357,,
6.2,day,0.356,,
7.0,day,0.355,,
10.2,day,0.363,,
10.9,day,0.364,,
11.9,day,0.365,,
14.0,day,0.365,,
15.1,day,0.364,,
16.0,day,0.363,,
19.1,day,0.361,,
19.8,day,0.364,,
20.9,day,0.363,,
22.1,day,0.363,,
22.9,day,0.363,,
25.7,day,0.360,,
26.9,day,0.357,,
28.1,day,0.353,,
29.1,day,0.351,,
30.0,day,0.348,,
31.9,day,0.352,,
36.3,day,0.342,,
42.0,day,0.338,,
45.2,day,0.336,,
46.8,day,0.334,,
51.0,day,0.329,,
field,aqueous moisture
content,,0.5,cm,0.5,cm,30.5,cm,1,0.01,0.8,0.95,
31,
0.1,day,0.124,,
1.2,day,0.121,,
2.1,day,0.123,,
2.9,day,0.154,,
4.1,day,0.176,,
5.3,day,0.177,,
6.1,day,0.180,,
6.2,day,0.181,,
7.0,day,0.181,,
10.2,day,0.188,,
10.9,day,0.191,,
11.9,day,0.189,,
14.0,day,0.187,,
15.1,day,0.189,,
16.0,day,0.187,,
19.1,day,0.175,,
19.8,day,0.182,,
20.9,day,0.185,,
22.1,day,0.186,,
22.9,day,0.187,,
25.7,day,0.176,,
26.9,day,0.173,,
28.1,day,0.154,,
29.1,day,0.141,,
30.0,day,0.134,,
31.9,day,0.133,,
36.3,day,0.118,,
42.0,day,0.111,,
45.2,day,0.108,,
46.8,day,0.107,,
51.0,day,0.102,,
field,aqueous moisture
content,,0.5,cm,0.5,cm,55.5,cm,1,0.01,0.8,0.95,
31,
0.1,day,0.205,,
1.2,day,0.205,,
2.1,day,0.245,,
2.9,day,0.258,,
4.1,day,0.259,,
5.3,day,0.255,,
6.1,day,0.263,,
6.2,day,0.259,,
7.0,day,0.263,,
10.2,day,0.263,,
10.9,day,0.266,,
11.9,day,0.265,,
14.0,day,0.268,,
15.1,day,0.269,,
16.0,day,0.267,,
19.1,day,0.271,,
19.8,day,0.275,,
20.9,day,0.272,,
22.1,day,0.275,,
22.9,day,0.275,,
25.7,day,0.274,,
26.9,day,0.271,,
28.1,day,0.257,,
29.1,day,0.253,,
30.0,day,0.247,,
31.9,day,0.242,,
36.3,day,0.232,,
42.0,day,0.217,,

45.2,day,0.208,,
46.8,day,0.203,,
51.0,day,0.190,,
field,aqueous moisture
content,,0.5,cm,0.5,cm,75.5,cm,1,0.01,0.8,0.95,
31,
0.1,day,0.315,,
1.2,day,0.345,,
2.1,day,0.360,,
2.9,day,0.372,,
4.1,day,0.367,,
5.3,day,0.365,,
6.1,day,0.372,,
6.2,day,0.367,,
7.0,day,0.371,,
10.2,day,0.373,,
10.9,day,0.376,,
11.9,day,0.371,,
14.0,day,0.374,,
15.1,day,0.371,,
16.0,day,0.370,,
19.1,day,0.378,,
19.8,day,0.387,,
20.9,day,0.388,,
22.1,day,0.388,,
22.9,day,0.384,,
25.7,day,0.384,,
26.9,day,0.385,,
28.1,day,0.373,,
29.1,day,0.362,,
30.0,day,0.369,,
31.9,day,0.364,,
36.3,day,0.358,,
42.0,day,0.341,,
45.2,day,0.329,,
46.8,day,0.319,,
51.0,day,0.295,,
field,matric potential,cm,0.5,cm,0.5,cm,30.5,cm,1,4.0,0.8,0.8,
30,
1.2,day,-94,cm,
2.1,day,-118,cm,
2.9,day,-70,cm,
4.1,day,-63,cm,
5.3,day,-54,cm,
6.1,day,-54,cm,
6.2,day,-65,cm,
7.0,day,-60,cm,
10.2,day,-60,cm,
10.9,day,-51,cm,
11.9,day,-52,cm,
14.0,day,-55,cm,
15.1,day,-58,cm,
16.0,day,-61,cm,
19.1,day,-64,cm,
19.8,day,-62,cm,
20.9,day,-53,cm,
22.1,day,-61,cm,
22.9,day,-51,cm,
25.7,day,-61,cm,
26.9,day,-59,cm,
28.1,day,-82,cm,
29.1,day,-80,cm,
30.0,day,-78,cm,
31.9,day,-109,cm,
36.3,day,-109,cm,
42.0,day,-133,cm,
45.2,day,-135,cm,
46.8,day,-153,cm,
51.0,day,-184,cm,
field,matric potential,cm,0.5,cm,0.5,cm,55.5,cm,1,4.0,0.8,0.8,
30,
1.2,day,-125,cm,
2.1,day,-60,cm,
2.9,day,-47,cm,
4.1,day,-48,cm,
5.3,day,-36,cm,
6.1,day,-53,cm,
6.2,day,-36,cm,
7.0,day,-44,cm,
10.2,day,-45,cm,
10.9,day,-35,cm,
11.9,day,-29,cm,
14.0,day,-38,cm,
15.1,day,-42,cm,
16.0,day,-44,cm,
19.1,day,-38,cm,
19.8,day,-39,cm,
20.9,day,-35,cm,
22.1,day,-43,cm,
22.9,day,-33,cm,
25.7,day,-52,cm,
26.9,day,-51,cm,
28.1,day,-75,cm,
29.1,day,-76,cm,
30.0,day,-81,cm,
31.9,day,-99,cm,
36.3,day,-112,cm,
42.0,day,-122,cm,
45.2,day,-145,cm,
46.8,day,-156,cm,
51.0,day,-213,cm,

UCODE Template File: *input.tpl*

```
~Simulation Title Card
1,
Scaling Factor Test,
Zhang,
PNNL,
July 13, 2001,
14:39,
2,
Abbaspour (2000):Irrigation and Drainage Phase - Scaling method
Reference to L1,

~Solution Control Card
Normal w/ Scaling w/ Inverse,
Water,
1,
0,day,51,day,0.001,day,0.1,day,1.25,8,1.e-06,
10000,
0,

~Grid Card
uniform cartesian,
1,1,76,
1.,cm,
1.,cm,
1.,cm,

~Rock/Soil Zonation Card
4,
L1,1,1,1,1,68,76,R1,
L2,1,1,1,1,46,67,R1,
L3,1,1,1,1,6,45,R1,
L4,1,1,1,1,1,5,R1,

~Mechanical Properties Card
R1,,,!thetas,,,,!,!thetas,,,,!,,,Millington and Quirk,

~Hydraulic Properties Card
R1,!ks,,,,,,,,!,hc:m/s,!ks,,,,,,,,!,hc:m/s,!ks,,,,,,,,!,hc:m/s,

~Saturation Function Card
R1,van Genuchten,!alpha,,,,,!,1/cm,!n,,,,,,,,,!,!sr,,,,,,,,!,,

~Aqueous Relative Permeability Card
R1,Mualem,,

~Scaling Card
Linear,Linear,Linear,Linear,Linear,
L1,1,1,1,1,1,
L2,10.053,0.789,4.073,1.078,0.845,
L3,587.9,1.115,17.28,1.198,0,
L4,11.87,1.053,1.914,1.028,0.919,

~Initial Conditions Card
Gas Pressure,Aqueous Pressure,
3,
Aqueous Pressure,8.71444e+4,Pa,0.0,1/cm,0.0,1/cm,-
231.5,1/cm,1,1,1,1,56,76,
Aqueous Pressure,8.94572e+4,Pa,0.0,1/cm,0.0,1/cm,-
92.5,1/cm,1,1,1,1,31,55,
Aqueous
Pressure,8.94572e+4,Pa,0.0,1/cm,0.0,1/cm,0.0,1/m,1,1,1,1,1,30,

…
```

UCODE Prepare File: *out_uc1.pre*

```
#
F no
#INPUT FILES
<input.tpl
>input
# Search-String Start-Val Min Max Perturbation Format Log-Transform? Estimate?
/!ks,,,,,,,,!         3.858e-7   1.0e-9     1.0e-5    0.05  %10.3e 1 1
/!thetas,,,,!         0.374                 0.3       0.5       0.05  %6.4f  0 1
/!alpha,,,,,!         0.00383               0.01      0.3600    0.05  %10.3e 1 1
/!n,,,,,,,,,!         1.331                 1.1       10.000    0.05  %10.3e 1 1
/!sr,,,,,,,,!         0.249                 0.000     0.40      0.01  %6.4f  0 0
END
```

UCODE Universal File: *out_uc1.uni*

```
#STOMP.UNI FILE FOR UCODE
#
3                  #phase
1                  #differencing (1=forward [recommended], 2=central)
 0.0100            #tol (0.01 recommended)
 0.0100            #tolerance sosr (0.0 [recommended])
0                  #nopt (0=no quasi-Newton updating, 1=quasi-Newton updating)
20                 #maximum number of iterations
 1.0000            #maximum fractional parameter change
..\bin\MRDRIVE     #path and name of inverse code
1                  #number of application models
batch              #application model execution commands
3                  #scale-sensitivities ( 0=no scaling, 1=dimensionless, 2=1%, and 3=both 1 and 2)
0                  #print intermediate ( 0=no printing, 1=print )
1                  #graph ( 0=no printing, 1=print )
1                  #number-residual-sets
#
# Observations
# Stat-Flag (0=variance, 1=standard deviation, 2=coefficient of variation)
# Obs-Name Obs-Value   Stat.       Stat-Flag   Plot-Symbol
#
mcl000001   3.5200E-01  1.0000E-02  1   1
mcl000002   1.2400E-01  1.0000E-02  1   2
mcl000003   2.0500E-01  1.0000E-02  1   3
mcl000004   3.1500E-01  1.0000E-02  1   4
mcl000005   3.5300E-01  1.0000E-02  1   1
mcl000006   1.2100E-01  1.0000E-02  1   2
mcl000007   2.0500E-01  1.0000E-02  1   3
mcl000008   3.4500E-01  1.0000E-02  1   4
mph000009  -9.4000E+01  4.0000E+00  1   5
mph000010  -1.2500E+02  4.0000E+00  1   6
mcl000011   3.5100E-01  1.0000E-02  1   1
mcl000012   1.2300E-01  1.0000E-02  1   2
mcl000013   2.4500E-01  1.0000E-02  1   3
mcl000014   3.6000E-01  1.0000E-02  1   4
mph000015  -1.1800E+02  4.0000E+00  1   5
mph000016  -6.0000E+01  4.0000E+00  1   6
mcl000017   3.4800E-01  1.0000E-02  1   1
mcl000018   1.5400E-01  1.0000E-02  1   2
mcl000019   2.5800E-01  1.0000E-02  1   3
mcl000020   3.7200E-01  1.0000E-02  1   4
mph000021  -7.0000E+01  4.0000E+00  1   5
mph000022  -4.7000E+01  4.0000E+00  1   6
mcl000023   3.5400E-01  1.0000E-02  1   1
mcl000024   1.7600E-01  1.0000E-02  1   2
mcl000025   2.5900E-01  1.0000E-02  1   3
mcl000026   3.6700E-01  1.0000E-02  1   4
mph000027  -6.3000E+01  4.0000E+00  1   5
mph000028  -4.8000E+01  4.0000E+00  1   6
mcl000029   3.5400E-01  1.0000E-02  1   1
mcl000030   1.7700E-01  1.0000E-02  1   2
mcl000031   2.5500E-01  1.0000E-02  1   3
mcl000032   3.6500E-01  1.0000E-02  1   4
mph000033  -5.4000E+01  4.0000E+00  1   5
mph000034  -3.6000E+01  4.0000E+00  1   6
mcl000035   3.5700E-01  1.0000E-02  1   1
mcl000036   1.8000E-01  1.0000E-02  1   2
mcl000037   2.6300E-01  1.0000E-02  1   3
mcl000038   3.7200E-01  1.0000E-02  1   4
mph000039  -5.4000E+01  4.0000E+00  1   5
mph000040  -5.3000E+01  4.0000E+00  1   6
mcl000041   3.5600E-01  1.0000E-02  1   1
mcl000042   1.8100E-01  1.0000E-02  1   2
mcl000043   2.5900E-01  1.0000E-02  1   3
mcl000044   3.6700E-01  1.0000E-02  1   4
mph000045  -6.5000E+01  4.0000E+00  1   5
mph000046  -3.6000E+01  4.0000E+00  1   6
mcl000047   3.5500E-01  1.0000E-02  1   1
mcl000048   1.8100E-01  1.0000E-02  1   2
mcl000049   2.6300E-01  1.0000E-02  1   3
mcl000050   3.7100E-01  1.0000E-02  1   4
mph000051  -6.0000E+01  4.0000E+00  1   5
mph000052  -4.4000E+01  4.0000E+00  1   6
mcl000053   3.6300E-01  1.0000E-02  1   1
mcl000054   1.8800E-01  1.0000E-02  1   2
mcl000055   2.6300E-01  1.0000E-02  1   3
mcl000056   3.7300E-01  1.0000E-02  1   4
mph000057  -6.0000E+01  4.0000E+00  1   5
mph000058  -4.5000E+01  4.0000E+00  1   6
mcl000059   3.6400E-01  1.0000E-02  1   1
mcl000060   1.9100E-01  1.0000E-02  1   2
mcl000061   2.6600E-01  1.0000E-02  1   3
mcl000062   3.7600E-01  1.0000E-02  1   4
mph000063  -5.1000E+01  4.0000E+00  1   5
mph000064  -3.5000E+01  4.0000E+00  1   6
mcl000065   3.6500E-01  1.0000E-02  1   1
mcl000066   1.8900E-01  1.0000E-02  1   2
mcl000067   2.6500E-01  1.0000E-02  1   3
mcl000068   3.7100E-01  1.0000E-02  1   4
mph000069  -5.2000E+01  4.0000E+00  1   5
mph000070  -2.9000E+01  4.0000E+00  1   6
mcl000071   3.6500E-01  1.0000E-02  1   1
mcl000072   1.8700E-01  1.0000E-02  1   2
mcl000073   2.6800E-01  1.0000E-02  1   3
mcl000074   3.7400E-01  1.0000E-02  1   4
mph000075  -5.5000E+01  4.0000E+00  1   5
mph000076  -3.8000E+01  4.0000E+00  1   6
mcl000077   3.6400E-01  1.0000E-02  1   1
mcl000078   1.8900E-01  1.0000E-02  1   2
mcl000079   2.6900E-01  1.0000E-02  1   3
mcl000080   3.7100E-01  1.0000E-02  1   4
mph000081  -5.8000E+01  4.0000E+00  1   5
mph000082  -4.2000E+01  4.0000E+00  1   6
mcl000083   3.6300E-01  1.0000E-02  1   1
mcl000084   1.8700E-01  1.0000E-02  1   2
mcl000085   2.6700E-01  1.0000E-02  1   3
mcl000086   3.7000E-01  1.0000E-02  1   4
mph000087  -6.1000E+01  4.0000E+00  1   5
mph000088  -4.4000E+01  4.0000E+00  1   6
mcl000089   3.6100E-01  1.0000E-02  1   1
mcl000090   1.7500E-01  1.0000E-02  1   2
mcl000091   2.7100E-01  1.0000E-02  1   3
mcl000092   3.7800E-01  1.0000E-02  1   4
mph000093  -6.4000E+01  4.0000E+00  1   5
mph000094  -3.8000E+01  4.0000E+00  1   6
mcl000095   3.6400E-01  1.0000E-02  1   1
mcl000096   1.8200E-01  1.0000E-02  1   2
mcl000097   2.7500E-01  1.0000E-02  1   3
mcl000098   3.8700E-01  1.0000E-02  1   4
mph000099  -6.2000E+01  4.0000E+00  1   5
```

mph000100	-3.9000E+01	4.0000E+00	1	6
mcl000101	3.6300E-01	1.0000E-02	1	1
mcl000102	1.8500E-01	1.0000E-02	1	2
mcl000103	2.7200E-01	1.0000E-02	1	3
mcl000104	3.8800E-01	1.0000E-02	1	4
mph000105	-5.3000E+01	4.0000E+00	1	5
mph000106	-3.5000E+01	4.0000E+00	1	6
mcl000107	3.6300E-01	1.0000E-02	1	1
mcl000108	1.8600E-01	1.0000E-02	1	2
mcl000109	2.7500E-01	1.0000E-02	1	3
mcl000110	3.8800E-01	1.0000E-02	1	4
mph000111	-6.1000E+01	4.0000E+00	1	5
mph000112	-4.3000E+01	4.0000E+00	1	6
mcl000113	3.6300E-01	1.0000E-02	1	1
mcl000114	1.8700E-01	1.0000E-02	1	2
mcl000115	2.7500E-01	1.0000E-02	1	3
mcl000116	3.8400E-01	1.0000E-02	1	4
mph000117	-5.1000E+01	4.0000E+00	1	5
mph000118	-3.3000E+01	4.0000E+00	1	6
mcl000119	3.6000E-01	1.0000E-02	1	1
mcl000120	1.7600E-01	1.0000E-02	1	2
mcl000121	2.7400E-01	1.0000E-02	1	3
mcl000122	3.8400E-01	1.0000E-02	1	4
mph000123	-6.1000E+01	4.0000E+00	1	5
mph000124	-5.2000E+01	4.0000E+00	1	6
mcl000125	3.5700E-01	1.0000E-02	1	1
mcl000126	1.7300E-01	1.0000E-02	1	2
mcl000127	2.7100E-01	1.0000E-02	1	3
mcl000128	3.8500E-01	1.0000E-02	1	4
mph000129	-5.9000E+01	4.0000E+00	1	5
mph000130	-5.1000E+01	4.0000E+00	1	6
mcl000131	3.5300E-01	1.0000E-02	1	1
mcl000132	1.5400E-01	1.0000E-02	1	2
mcl000133	2.5700E-01	1.0000E-02	1	3
mcl000134	3.7300E-01	1.0000E-02	1	4
mph000135	-8.2000E+01	4.0000E+00	1	5
mph000136	-7.5000E+01	4.0000E+00	1	6
mcl000137	3.5100E-01	1.0000E-02	1	1
mcl000138	1.4100E-01	1.0000E-02	1	2
mcl000139	2.5300E-01	1.0000E-02	1	3
mcl000140	3.6200E-01	1.0000E-02	1	4
mph000141	-8.0000E+01	4.0000E+00	1	5
mph000142	-7.6000E+01	4.0000E+00	1	6
mcl000143	3.4800E-01	1.0000E-02	1	1
mcl000144	1.3400E-01	1.0000E-02	1	2
mcl000145	2.4700E-01	1.0000E-02	1	3
mcl000146	3.6900E-01	1.0000E-02	1	4
mph000147	-7.8000E+01	4.0000E+00	1	5
mph000148	-8.1000E+01	4.0000E+00	1	6
mcl000149	3.5200E-01	1.0000E-02	1	1
mcl000150	1.3300E-01	1.0000E-02	1	2
mcl000151	2.4200E-01	1.0000E-02	1	3
mcl000152	3.6400E-01	1.0000E-02	1	4
mph000153	-1.0900E+02	4.0000E+00	1	5
mph000154	-9.9000E+01	4.0000E+00	1	6
mcl000155	3.4200E-01	1.0000E-02	1	1
mcl000156	1.1800E-01	1.0000E-02	1	2
mcl000157	2.3200E-01	1.0000E-02	1	3
mcl000158	3.5800E-01	1.0000E-02	1	4
mph000159	-1.0900E+02	4.0000E+00	1	5
mph000160	-1.1200E+02	4.0000E+00	1	6
mcl000161	3.3800E-01	1.0000E-02	1	1
mcl000162	1.1100E-01	1.0000E-02	1	2
mcl000163	2.1700E-01	1.0000E-02	1	3
mcl000164	3.4100E-01	1.0000E-02	1	4
mph000165	-1.3300E+02	4.0000E+00	1	5
mph000166	-1.2200E+02	4.0000E+00	1	6
mcl000167	3.3600E-01	1.0000E-02	1	1
mcl000168	1.0800E-01	1.0000E-02	1	2
mcl000169	2.0800E-01	1.0000E-02	1	3
mcl000170	3.2900E-01	1.0000E-02	1	4
mph000171	-1.3500E+02	4.0000E+00	1	5
mph000172	-1.4500E+02	4.0000E+00	1	6
mcl000173	3.3400E-01	1.0000E-02	1	1
mcl000174	1.0700E-01	1.0000E-02	1	2
mcl000175	2.0300E-01	1.0000E-02	1	3
mcl000176	3.1900E-01	1.0000E-02	1	4
mph000177	-1.5300E+02	4.0000E+00	1	5
mph000178	-1.5600E+02	4.0000E+00	1	6
mcl000179	3.2900E-01	1.0000E-02	1	1
mcl000180	1.0200E-01	1.0000E-02	1	2
mcl000181	1.9000E-01	1.0000E-02	1	3
mcl000182	2.9500E-01	1.0000E-02	1	4
mph000183	-1.8400E+02	4.0000E+00	1	5
mph000184	-2.1300E+02	4.0000E+00	1	6

END

UCODE Extract File: *out_uc1.ext*

```
<out_uc1.sto
#
o  mcl000001
/mcl000001/
C12_23
#
o  mcl000002
/mcl000002/
C12_23
#
o  mcl000003
/mcl000003/
C12_23
#
o  mcl000004
/mcl000004/
C12_23
#
o  mcl000005
/mcl000005/
C12_23
#
o  mcl000006
/mcl000006/
C12_23
#
o  mcl000007
/mcl000007/
C12_23
#
o  mcl000008
/mcl000008/
C12_23
#
o  mph000009
/mph000009/
C12_23
#
o  mph000010
/mph000010/
C12_23
#
o  mcl000011
/mcl000011/
C12_23
#
o  mcl000012
/mcl000012/
C12_23
#
o  mcl000013
/mcl000013/
C12_23
#
o  mcl000014
/mcl000014/
C12_23
#
o  mph000015
/mph000015/
C12_23
#
o  mph000016
/mph000016/
C12_23
#
o  mcl000017
/mcl000017/
C12_23
#
o  mcl000018
/mcl000018/
C12_23
#
o  mcl000019
/mcl000019/
C12_23
#
o  mcl000020
/mcl000020/
C12_23
#
o  mph000021
/mph000021/
C12_23
#
o  mph000022
/mph000022/
C12_23
#
o  mcl000023
/mcl000023/
C12_23
#
o  mcl000024
/mcl000024/
C12_23
#
o  mcl000025
/mcl000025/
C12_23
#
o  mcl000026
/mcl000026/
C12_23
#
o  mph000027
/mph000027/
C12_23
#
o  mph000028
/mph000028/
C12_23
#
o  mcl000029
/mcl000029/
C12_23
#
o  mcl000030
/mcl000030/
C12_23
#
o  mcl000031
/mcl000031/
C12_23
#
o  mcl000032
/mcl000032/
C12_23
#
o  mph000033
/mph000033/
C12_23
#
o  mph000034
/mph000034/
C12_23
#
o  mcl000035
/mcl000035/
C12_23
#
o  mcl000036
/mcl000036/
C12_23
#
o  mcl000037
/mcl000037/
C12_23
#
o  mcl000038
/mcl000038/
C12_23
#
o  mph000039
/mph000039/
C12_23
#
o  mph000040
/mph000040/
C12_23
#
o  mcl000041
/mcl000041/
C12_23
#
o  mcl000042
/mcl000042/
C12_23
#
o  mcl000043
/mcl000043/
C12_23
#
o  mcl000044
/mcl000044/
C12_23
#
o  mph000045
/mph000045/
C12_23
#
o  mph000046
/mph000046/
C12_23
#
o  mcl000047
/mcl000047/
C12_23
#
o  mcl000048
/mcl000048/
C12_23
#
o  mcl000049
/mcl000049/
C12_23
#
o  mcl000050
/mcl000050/
C12_23
#
o  mph000051
/mph000051/
C12_23
#
o  mph000052
/mph000052/
C12_23
#
o  mcl000053
/mcl000053/
C12_23
#
o  mcl000054
/mcl000054/
C12_23
#
o  mcl000055
/mcl000055/
C12_23
#
o  mcl000056
/mcl000056/
C12_23
#
o  mph000057
/mph000057/
C12_23
#
o  mph000058
/mph000058/
C12_23
#
o  mcl000059
/mcl000059/
C12_23
#
o  mcl000060
/mcl000060/
C12_23
#
o  mcl000061
/mcl000061/
C12_23
#
o  mcl000062
/mcl000062/
```

C12_23
#
o mph000063
/mph000063/
C12_23
#
o mph000064
/mph000064/
C12_23
#
o mcl000065
/mcl000065/
C12_23
#
o mcl000066
/mcl000066/
C12_23
#
o mcl000067
/mcl000067/
C12_23
#
o mcl000068
/mcl000068/
C12_23
#
o mph000069
/mph000069/
C12_23
#
o mph000070
/mph000070/
C12_23
#
o mcl000071
/mcl000071/
C12_23
#
o mcl000072
/mcl000072/
C12_23
#
o mcl000073
/mcl000073/
C12_23
#
o mcl000074
/mcl000074/
C12_23
#
o mph000075
/mph000075/
C12_23
#
o mph000076
/mph000076/
C12_23
#
o mcl000077
/mcl000077/
C12_23
#
o mcl000078
/mcl000078/
C12_23
#
o mcl000079
/mcl000079/
C12_23
#
o mcl000080
/mcl000080/
C12_23
#
o mph000081
/mph000081/
C12_23
#
o mph000082
/mph000082/
C12_23
#
o mcl000083
/mcl000083/
C12_23
#
o mcl000084
/mcl000084/
C12_23
#
o mcl000085
/mcl000085/
C12_23
#
o mcl000086
/mcl000086/
C12_23
#
o mph000087
/mph000087/
C12_23
#
o mph000088
/mph000088/
C12_23
#
o mcl000089
/mcl000089/
C12_23
#
o mcl000090
/mcl000090/
C12_23
#
o mcl000091
/mcl000091/
C12_23
#
o mcl000092
/mcl000092/
C12_23
#
o mph000093
/mph000093/
C12_23
#
o mph000094
/mph000094/
C12_23
#
o mcl000095
/mcl000095/
C12_23
#
o mcl000096
/mcl000096/
C12_23
#
o mcl000097
/mcl000097/
C12_23
#
o mcl000098
/mcl000098/
C12_23
#
o mph000099
/mph000099/
C12_23
#
o mph000100
/mph000100/
C12_23
#
o mcl000101
/mcl000101/
C12_23
#
o mcl000102
/mcl000102/
C12_23
#
o mcl000103
/mcl000103/
C12_23
#
o mcl000104
/mcl000104/
C12_23
#
o mph000105
/mph000105/
C12_23
#
o mph000106
/mph000106/
C12_23
#
o mcl000107
/mcl000107/
C12_23
#
o mcl000108
/mcl000108/
C12_23
#
o mcl000109
/mcl000109/
C12_23
#
o mcl000110
/mcl000110/
C12_23
#
o mph000111
/mph000111/
C12_23
#
o mph000112
/mph000112/
C12_23
#
o mcl000113
/mcl000113/
C12_23
#
o mcl000114
/mcl000114/
C12_23
#
o mcl000115
/mcl000115/
C12_23
#
o mcl000116
/mcl000116/
C12_23
#
o mph000117
/mph000117/
C12_23
#
o mph000118
/mph000118/
C12_23
#
o mcl000119
/mcl000119/
C12_23
#
o mcl000120
/mcl000120/
C12_23
#
o mcl000121
/mcl000121/
C12_23
#
o mcl000122
/mcl000122/
C12_23
#
o mph000123
/mph000123/
C12_23
#
o mph000124
/mph000124/
C12_23
#
o mcl000125
/mcl000125/
C12_23
#
o mcl000126
/mcl000126/
C12_23
#
o mcl000127
/mcl000127/
C12_23
#
o mcl000128
/mcl000128/

C12_23
#
o mph000129
/mph000129/
C12_23
#
o mph000130
/mph000130/
C12_23
#
o mcl000131
/mcl000131/
C12_23
#
o mcl000132
/mcl000132/
C12_23
#
o mcl000133
/mcl000133/
C12_23
#
o mcl000134
/mcl000134/
C12_23
#
o mph000135
/mph000135/
C12_23
#
o mph000136
/mph000136/
C12_23
#
o mcl000137
/mcl000137/
C12_23
#
o mcl000138
/mcl000138/
C12_23
#
o mcl000139
/mcl000139/
C12_23
#
o mcl000140
/mcl000140/
C12_23
#
o mph000141
/mph000141/
C12_23
#
o mph000142
/mph000142/
C12_23
#
o mcl000143
/mcl000143/
C12_23
#
o mcl000144
/mcl000144/
C12_23
#
o mcl000145
/mcl000145/
C12_23
#
o mcl000146
/mcl000146/
C12_23
#
o mph000147
/mph000147/
C12_23
#
o mph000148
/mph000148/
C12_23
#
o mcl000149
/mcl000149/
C12_23
#
o mcl000150
/mcl000150/
C12_23
#
o mcl000151
/mcl000151/
C12_23
#
o mcl000152
/mcl000152/
C12_23
#
o mph000153
/mph000153/
C12_23
#
o mph000154
/mph000154/
C12_23
#
o mcl000155
/mcl000155/
C12_23
#
o mcl000156
/mcl000156/
C12_23
#
o mcl000157
/mcl000157/
C12_23
#
o mcl000158
/mcl000158/
C12_23
#
o mph000159
/mph000159/
C12_23
#
o mph000160
/mph000160/
C12_23
#
o mcl000161
/mcl000161/
C12_23
#
o mcl000162
/mcl000162/
C12_23
#
o mcl000163
/mcl000163/
C12_23
#
o mcl000164
/mcl000164/
C12_23
#
o mph000165
/mph000165/
C12_23
#
o mph000166
/mph000166/
C12_23
#
o mcl000167
/mcl000167/
C12_23
#
o mcl000168
/mcl000168/
C12_23
#
o mcl000169
/mcl000169/
C12_23
#
o mcl000170
/mcl000170/
C12_23
#
o mph000171
/mph000171/
C12_23
#
o mph000172
/mph000172/
C12_23
#
o mcl000173
/mcl000173/
C12_23
#
o mcl000174
/mcl000174/
C12_23
#
o mcl000175
/mcl000175/
C12_23
#
o mcl000176
/mcl000176/
C12_23
#
o mph000177
/mph000177/
C12_23
#
o mph000178
/mph000178/
C12_23
#
o mcl000179
/mcl000179/
C12_23
#
o mcl000180
/mcl000180/
C12_23
#
o mcl000181
/mcl000181/
C12_23
#
o mcl000182
/mcl000182/
C12_23
#
o mph000183
/mph000183/
C12_23
#
o mph000184
/mph000184/
C12_23
#
END

Inverse Modeling of Flow from a Point Source

STOMP Input File: *input*

```
~Simulation Title Card
1,
Simulation of S&L 1980 experiment,
Fred Zhang,
PNL,
Sept 26, 2002,
9:00,
2,
Injection #1,
Textue classified according to porosity and steady-state water
content,

~Solution Control Card
Normal w/Inverse,
Water,
1,
0,day,5.5,day,0.001,day,0.3,day,1.2,8,1.E-06,
10000,
0,

~Grid Card
Cartesian,
 24, 24, 40,
0.0,m,
1@5.4288,m,1@4.0213,m,1@2.9787,m,1@2.2065,m,1@1.6344,m
,
1@1.2107,m,1@0.8968,m,1@0.6643,m,1@0.4921,m,1@0.3645,m
,
1@0.2700,m,1@0.2000,m,1@0.2000,m,1@0.2700,m,1@0.3645,m
,
1@0.4921,m,1@0.6643,m,1@0.8968,m,1@1.2107,m,1@1.6344,m
,
1@2.2065,m,1@2.9787,m,1@4.0213,m,1@5.4288,m,
0.0,m,
1@5.4288,m,1@4.0213,m,1@2.9787,m,1@2.2065,m,1@1.6344,m
,
1@1.2107,m,1@0.8968,m,1@0.6643,m,1@0.4921,m,1@0.3645,m
,
1@0.2700,m,1@0.2000,m,1@0.2000,m,1@0.2700,m,1@0.3645,m
,
1@0.4921,m,1@0.6643,m,1@0.8968,m,1@1.2107,m,1@1.6344,m
,
1@2.2065,m,1@2.9787,m,1@4.0213,m,1@5.4288,m,
0.0,m, 40@0.3048,m,

~Mechanical Properties Card
T1,,, 4.167e-01, 4.167e-01,,,Millington and Quirk,
T2,,, 3.940e-01, 3.940e-01,,,Millington and Quirk,
T3,,, 3.717e-01, 3.717e-01,,,Millington and Quirk,
T4,,, 3.490e-01, 3.490e-01,,,Millington and Quirk,
T5,,, 3.263e-01, 3.263e-01,,,Millington and Quirk,
T6,,, 3.040e-01, 3.040e-01,,,Millington and Quirk,
T7,,, 2.701e-01, 2.701e-01,,,Millington and Quirk,

~Hydraulic Properties Card
T1, 1.328e-02,hc:m/s, 1.328e-02,hc:m/s, 2.624e-03,hc:m/s,
T2, 4.428e-03,hc:m/s, 4.428e-03,hc:m/s, 8.748e-04,hc:m/s,
T3, 2.657e-03,hc:m/s, 2.657e-03,hc:m/s, 5.249e-04,hc:m/s,
T4, 1.230e-03,hc:m/s, 1.230e-03,hc:m/s, 2.430e-04,hc:m/s,
T5, 6.568e-05,hc:m/s, 6.568e-05,hc:m/s, 1.298e-05,hc:m/s,
T6, 6.568e-05,hc:m/s, 6.568e-05,hc:m/s, 1.298e-05,hc:m/s,
T7, 2.829e-05,hc:m/s, 2.829e-05,hc:m/s, 5.589e-06,hc:m/s,

~Saturation Function Card
T1,van genuchten, 4.026e-01,1/cm, 1.910e+00, 2.400e-02,,
T2,van genuchten, 7.663e-02,1/cm, 2.034e+00, 2.538e-02,,
T3,van genuchten, 9.394e-01,1/cm, 1.824e+00, 2.690e-02,,
T4,van genuchten, 1.310e-01,1/cm, 2.390e+00, 4.298e-02,,
T5,van genuchten, 2.240e-02,1/cm, 3.449e+00, 4.597e-02,,
T6,van genuchten, 2.240e-02,1/cm, 3.449e+00, 4.935e-02,,
T7,van genuchten, 4.454e-02,1/cm, 1.910e+00, 7.404e-02,,

~Aaqueous Relative Permeability Card
T1,Mualem,,
T2,Mualem,,
T3,Mualem,,
T4,Mualem,,
T5,Mualem,,
T6,Mualem,,
T7,Mualem,,

~Boundary Conditions Card
2,
Top,Neumann,
1,24,1,24,40,40,1,
0,day,0.0,mm/day,
Bottom,Unit Gradient,
1,24,1,24,1,1,1,
0,day,,,

~Source Card
1,
Aqueous Volumetric,13,13,12,12,34,34,3,
0.0,day,7882.6,L/day,
0.4014,day,7882.6,L/day,
0.4014,day,0.0,L/day,

~Output Options Card
1,
11,12,30,
1,2,day,m,5,5,5,
1,
Aqueous Moisture Content,,
5,
0,day,
0.4014,day,
1.4014,day,
3.0,day,
5.0,day,
1,
Aqueous Moisture Content,,

~UCode Control Card
1,1,0.02,0.02,0,10,2.0,
../bin/mrdrive,
1,
batch,
3,0,1,1,

~Rock/Soil Zonation Card
23040,
T1, 1, 1, 1, 1, 1, 1,
```

T1, 2, 2, 1, 1, 1, 1,
T1, 3, 3, 1, 1, 1, 1,
T1, 4, 4, 1, 1, 1, 1,
……

~Initial Condition Card
Gas Pressure,Moisture Content,
23041,
Gas Pressure,101325,Pa,,,,,,, 1,24, 1,24, 1,40,
Moisture Content, 2.53499E-02,,,,,,,, 1, 1, 1, 1, 1, 1,
Moisture Content, 2.53499E-02,,,,,,,, 2, 2, 1, 1, 1, 1,
Moisture Content, 2.53499E-02,,,,,,,, 3, 3, 1, 1, 1, 1,
……

~Observed Data Card
695,
field,aqueous moisture
content,,21.31,m,20.28,m,11.73,m,1,1.0,0.8,0.95,
10,
0.000000,day,0.0438,,
0.123047,day,0.0356,,
0.169922,day,0.0403,,
0.222656,day,0.0361,,
0.248047,day,0.0358,,
0.287109,day,0.0333,,
0.376953,day,0.0373,,
0.492188,day,0.0327,,
0.953125,day,0.0367,,
5.000000,day,0.0327,,
field,aqueous moisture
content,,21.31,m,20.28,m,11.43,m,1,1.0,0.8,0.95,
10,
0.000000,day,0.0332,,
0.123047,day,0.0327,,
…..

UCODE Template File: *input.tpl*

~Simulation Title Card
1,
Simulation of S&L 1980 experiment,
Fred Zhang,
PNL,
Sept 16, 2002,
16:30,
2,
Injection #1,
Textue classified according to porosity and steady-state water content,

~Solution Control Card
Normal w/Inverse,
Water,
1,
0,day,5.5,day,0.001,day,0.3,day,1.2,8,1.E-06,
10000,
0,

~Grid Card
Cartesian,
 24, 24, 40,
0.0,m,
1@5.4288,m,1@4.0213,m,1@2.9787,m,1@2.2065,m,1@1.6344,m
,
1@1.2107,m,1@0.8968,m,1@0.6643,m,1@0.4921,m,1@0.3645,m
,
1@0.2700,m,1@0.2000,m,1@0.2000,m,1@0.2700,m,1@0.3645,m
,
1@0.4921,m,1@0.6643,m,1@0.8968,m,1@1.2107,m,1@1.6344,m
,
1@2.2065,m,1@2.9787,m,1@4.0213,m,1@5.4288,m,
0.0,m,
1@5.4288,m,1@4.0213,m,1@2.9787,m,1@2.2065,m,1@1.6344,m
,
1@1.2107,m,1@0.8968,m,1@0.6643,m,1@0.4921,m,1@0.3645,m
,
1@0.2700,m,1@0.2000,m,1@0.2000,m,1@0.2700,m,1@0.3645,m
,
1@0.4921,m,1@0.6643,m,1@0.8968,m,1@1.2107,m,1@1.6344,m
,
1@2.2065,m,1@2.9787,m,1@4.0213,m,1@5.4288,m,
0.0,m, 40@0.3048,m,

~Mechanical Properties Card
T1,,,!qs,,,,,,,!,!qs,,,,,,,!,,,Millington and Quirk,
T2,,,!qs,,,,,,,!,!qs,,,,,,,!,,,Millington and Quirk,
T3,,,!qs,,,,,,,!,!qs,,,,,,,!,,,Millington and Quirk,
T4,,,!qs,,,,,,,!,!qs,,,,,,,!,,,Millington and Quirk,
T5,,,!qs,,,,,,,!,!qs,,,,,,,!,,,Millington and Quirk,
T6,,,!qs,,,,,,,!,!qs,,,,,,,!,,,Millington and Quirk,
T7,,,!qs,,,,,,,!,!qs,,,,,,,!,,,Millington and Quirk,

~Hydraulic Properties Card
T1,!ksh,,,,,,,!,hc:m/s,!ksh,,,,,,,!,hc:m/s,!ksv,,,,,,,!,hc:m/s,
T2,!ksh,,,,,,,!,hc:m/s,!ksh,,,,,,,!,hc:m/s,!ksv,,,,,,,!,hc:m/s,
T3,!ksh,,,,,,,!,hc:m/s,!ksh,,,,,,,!,hc:m/s,!ksv,,,,,,,!,hc:m/s,
T4,!ksh,,,,,,,!,hc:m/s,!ksh,,,,,,,!,hc:m/s,!ksv,,,,,,,!,hc:m/s,
T5,!ksh,,,,,,,!,hc:m/s,!ksh,,,,,,,!,hc:m/s,!ksv,,,,,,,!,hc:m/s,
T6,!ksh,,,,,,,!,hc:m/s,!ksh,,,,,,,!,hc:m/s,!ksv,,,,,,,!,hc:m/s,
T7,!ksh,,,,,,,!,hc:m/s,!ksh,,,,,,,!,hc:m/s,!ksv,,,,,,,!,hc:m/s,

~Saturation Function Card
T1,van genuchten,!alpha,,,,,!,1/cm,!n,,,,,,,,!,!qs,,,,,,,!,,
T2,van genuchten,!alpha,,,,,!,1/cm,!n,,,,,,,,!,!qs,,,,,,,!,,
T3,van genuchten,!alpha,,,,,!,1/cm,!n,,,,,,,,!,!qs,,,,,,,!,,
T4,van genuchten,!alpha,,,,,!,1/cm,!n,,,,,,,,!,!qs,,,,,,,!,,
T5,van genuchten,!alpha,,,,,!,1/cm,!n,,,,,,,,!,!qs,,,,,,,!,,
T6,van genuchten,!alpha,,,,,!,1/cm,!n,,,,,,,,!,!qs,,,,,,,!,,
T7,van genuchten,!alpha,,,,,!,1/cm,!n,,,,,,,,!,!qs,,,,,,,!,,

~Aaqueous Relative Permeability Card
T1,Mualem,,
T2,Mualem,,
T3,Mualem,,
T4,Mualem,,
T5,Mualem,,
T6,Mualem,,
T7,Mualem,,

~Boundary Conditions Card
2,
Top,Neumann,
1,24,1,24,40,40,1,
0,day,0.0,mm/day,
Bottom,Unit Gradient,
1,24,1,24,1,1,1,

```
0,day,,,                                    ……

~Source Card
```

UCODE Prepare File: *out_uc1.pre*

```
#
F yes
#INPUT FILES
<inputA.tpl
>inputA
<inputB.tpl
>inputB
<inputC.tpl
>inputC
# Search-String Start-Val Min Max Perturbation Format Log-Transform? Estimate?
/!qs,,,,,,,,!          0.3488    0.2        0.5       0.05  %10.3e 0 1
/!ksh,,,,,,,,!         3.025E-41.0E-3       1.0E-7    0.05  %10.3e 1 1
/!ksv,,,,,,,,!         6.050E-51.0E-2       1.0E-7    0.05  %10.3e 1 1
/!alpha,,,,,!          0.0410    0.01       1         0.05  %10.3e 1 1
/!n,,,,,,,,,!          1.9400    1.1        10        0.05  %10.3e 1 1
END
```

UCODE Universal File: *out_uc1.uni*

```
#STOMP.UNI FILE FOR UCODE
#
1               #phase
1               #differencing (1=forward [recommended], 2=central)
 0.0200            #tol (0.01 recommended)
 0.0200            #tolerance sosr (0.01 or 0.1 [recommended])
0               #nopt (0=no quasi-Newton updating, 1=quasi-Newton updating)
10               #maximum number of iterations
 2.0000            #maximum fractional parameter change
../bin/mrdrive       #path and name of inverse code
3               #number of application models
batchA            #application model A execution commands
batchB            #application model A execution commands
batchC            #application model A execution commands
3               #scale-sensitivities ( 0=no scaling, 1=dimensionless, 2=1%, and 3=both 1 and 2)
0               #print intermediate ( 0=no printing, 1=print )
1               #graph ( 0=no printing, 1=print )
1               #number-residual-sets
#
# Observations
# Stat-Flag (0=variance, 1=standard deviation, 2=coefficient of variation)
# Obs-Name Obs-Value   Stat.       Stat-Flag   Plot-Symbol
#
mcA000001   4.3800E-02  1.0000E+00  1          1
mcA000002   3.3200E-02  1.0000E+00  1          2
mcA000003   2.9300E-02  1.0000E+00  1          3
……
```

UCODE Extract File: *out_uc1.ext*

```
<out_uc1.stA
#
o   mcA000001
/mcA000001/
C12_23
#
o   mcA000002
/mcA000002/
C12_23
#
o   mcA000003
/mcA000003/
C12_23
#
o   mcA000004
/mcA000004/
C12_23
#
o   mcA000005
/mcA000005/
C12_23
#
o   mcA000006
/mcA000006/
C12_23
#
o   mcA000007
/mcA000007/
C12_23
……

END
```

UCODE Function File: *out_uc1.fnc*

```
:file inputA.tpl
:key      qs
1..2      $x*1.194
3..4      $x*1.129
5..6      $x*1.065
7..8      $x*1.000
9..10     $x*0.935
11..12    $x*0.871
13..14    $x*0.774
15        0.01/($x*1.194)
16        0.01/($x*1.129)
17        0.01/($x*1.065)
18        0.015/($x*1.000)
19        0.015/($x*0.935)
20        0.015/($x*0.871)
21        0.020/($x*0.774)
:key      ksh
1..2      $x*10.8
3..4      $x*3.60
5..6      $x*2.16
7..8      $x*1.00
9..10     $x*0.0534
11..12    $x*0.0534
13..14    $x*0.023
:key      ksv
1         $x*10.8
2         $x*3.60
3         $x*2.16
4         $x*1.00
5         $x*0.0534
6         $x*0.0534
7         $x*0.023
:key      alpha
1         $x*3.073
2         $x*0.585
3         $x*2.171
4         $x*1.00
5         $x*0.171
6         $x*0.171
7         $x*0.34
:key      n
1         $x*0.799
2         $x*0.851
3         $x*0.763
4         $x*1.00
5         $x*1.443
6         $x*1.443
7         $x*0.799
……
```

Distribution

No. of Copies

OFFSITE

Wesley L. Bratton
Vista Engineering
8203 W. Quinault Ave
Kennewick, WA., 99336

2 Lawrence Livermore National Laboratory
L-130
Livermore, California 94550
Attn: William D. Daily
Abe Ramirez

2 Lawrence Berkley National Laboratory
Department of Earth and Planetary Sciences
MS 4767
1 Cyclotron Road
Berkeley, California 94720-4767
Attn: Donald J. DePaolo
Mark Conrad

James B. Fink
HydroGEOPHYSICS, Inc.
5865 South Old Spanish Trail
Tucson, Arizona 85747

Sandra Lilligren
Nez Perce Tribe, ERWM
P.O. Box 365
Lapwai, Idaho 83450

Rosemary J. Knight
Stanford University Mitchell Bldg
Satnford, CA., 94305-2215

No. of Copies

OFFSITE

Jan W. Hopmans
Hydrology Program
Department of Land, Air and Water Resources
123 Veihmeyer Hall
University of California
Davis, CA 95616

Peter C. Lichtner
Los Alamos National Laboratory
Environmental Sciences Division (EES-5)
MS F-649
Los Alamos, New Mexico 87545

Brian J. Andraski
U.S. Geological Survey
333 W Nye Ln., Rm. 203
Carson City, NV, 89706

Ernest L. Majer
Lawrence Berkeley National Laboratory
1 Cyclotron Road (MS 90-116)
Berkeley, California 94720

Earl D. Mattson
Idaho National Engineering and Environmental Laboratory
P.O. Box 1625
2251 N. Boulevard
Idaho Falls, Idaho 83415-2107

Gregory A. Newman
Sandia National Laboratories
P.O. Box 5800
MS-0750
Albuquerque, New Mexico 87185-0750

Distribution (Contd)

No. of Copies

OFFSITE

Wade Riggsbee
Yakima Nation
1933 Jadwin
Richland, Washington 99352

James B. Sisson
Idaho National Engineering and Environmental Laboratory, BBWI
P.O. Box 1625, MS-2107
Idaho Falls, Idaho 83415-2107

John Baker
USDA-ARS
Department of Soil, Water, & Climate
439 Borlaug Hall
University of Minnesota
1991 Upper Buford Circle
St. Paul, MN 55108

Alan and Lorrie Flint
US Geological Survey
Placer Hall
6000 J Street
Sacramento CA, 95819-6129

Rien van Genuchten
U.S. Salinity Laboratory
450 West Big Springs Road
Riverside, CA 92507-4617

John Nimmo
U.S. Geological Survey
345 Middlefield Road, MS-421
Menlo Park, CA 94025

Michael H. Young
Div. of Hydrologic Sciences, Desert Research Institute
755 E. Flamingo Road, Las Vegas, NV 89119

No. of Copies

OFFSITE

2 Los Alamos National Laboratory
Environmental Science Group
MSJ495
Los Alamos, New Mexico 87545
Attn: Everett P. Springer
Brent Neuman

Carl. I. Steefel
Lawrence Livermore National Laboratory
L-204
P.O. Box 808
Livermore, California 94551

P. J. Wierenga
Soil, Water, and Environmental Science
University of Arizona
Tucson, Arizona 85721

Michael Wilt
EMI
1301 S. 46th St.
UCRFS Bldg. 300
Richmond, California 94804

Ivana Witt
Yakima Nation
1933 Jadwin
Richland, Washington 99352

T.C. Jim Yeh
University of Arizona
Department of Hydrology and Water Resources
The University of Arizona, Bldg. 11
Tucson, Arizona 85721

Distribution (Contd)

No. of Copies		
ONSITE		
2	**DOE Office of River Protection**	
	C. A. Babel	H6-60
	R. M. Yasek	H6-60
9	**DOE Richland Operations Office**	
	B. L. Foley	P7-62
	J. P. Hanson	K8-50
	R. D. Hildebrand	A5-13
	K. A. Kapsi	K8-50
	R. W. Lober	H6-60
	J. G. Morse	A5-13
	D. Tano	A7-75
	K. M. Thompson	A5-113
	R. M. Yasek	H6-60
8	**Bechtel Hanford Inc.**	
	R. L. Biggerstaff	H0-02
	L. R. Curry	H0-19
	A. G. Dada	H0-02
	R. J. Fabre	X5-50
	K. R. Fecht	H0-02
	B. H. Ford	H0-19
	M. J. Graham	H0-09
	R. L. Jackson	H0-19
8	**CH2M Hill Hanford Group**	
	J. W. Cammann	T4-08
	R. Khaleel	B4-43
	A. J. Knepp	H0-22
	F. M. Mann	H-022
	D. A. Myers	H0-22
	V. J. Rohay	H0-19
	L. C. Swanson	H9-02
	C. D. Wittreich	H9-03
2	**MACTER-ERS**	
	J. F. Bertsch	B1-42
	R. G. McCain	B1-42

No. of Copies		
ONSITE		
3	**Waste Management Technical Services**	
	M. G. Gardner	H1-11
	J. E. Meisner	H1-11
	R. K. Price	H1-11
6	**Washington Department of Ecology**	
	F. W. Bond	B5-18
	J. Caggiano	B5-18
	D. Goswami	B5-18
	A. Huckaby	B5-18
	S. Leja	B5-18
	N. H. Uziemblo	B5-18
1	**U.S. Environmental Protection Agency**	
	D. A. Faulk	B5-01
4	**Fluor Federal Services**	
	B. H. Ford	E6-35
	R. Jackson	E6-35
	R. Khaleel	E6-17
	R. T. Wilde	E6-35

Distribution (Contd)

No. of Copies		
ONSITE		
66	**Pacific Northwest National Laboratory**	
	B. Barnett	K6-81
	W. F. Bonner	K9-14
	R. W. Bryce	E6-35
	R. E. Clayton	P8-37
	P. W. Eslinger	K6-80
	M. J. Fayer	K3-33
	M. D. Freshley (2)	H0-21
	G. W. Gee (20)	K9-33
	J. O. Goreham	K9-33
	T. J. Gilmore	K6-81
	D. G. Horton	K6-81
	C. T. Kincaid	K9-33
	G. V. Last	K6-81
	P. E. Long	K9-33
	W. J. Martin	K3-54
	P. D. Meyer	BPO
	C. J. Murray	K6-81
	S. M. Narbutovskih	K6-96
	Mart Oostrom	K9-33
	W. E. Nichols	K9-33
	S. P. Reidel	K6-81
	M. L. Rockhold	K9-33
	R. J. Serne	K6-81
	C. E. Strickland	K9-36
	M. D. Sweeney	K6-81
	M. J. Truex	K2-10
	A. L. Ward (10)	K9-33
	K. Waters-Husted	K9-33
	M. White	K9-36
	B. A. Williams	K6-81
	M. D. Williams	K9-36
	S. B. Yabusaki	K9-36
	J. M. Zachara	K8-96
	F. Zhang (2)	K9-33
	Technical Report Files (2)	